# Metabolic flow at high temperatures and laboratory adaptation in thermotolerant yeast *Kluyveromyces marxianus* DMKU 3-1042

# (耐熱性酵母 *Kluyveromyces marxianus* DMKU 3-1042 の高温代謝フローと実験室適応)

**PhD Thesis**

**Pattanakittivorakul Sornsiri**

**A thesis submitted in partial fulfilment of the requirement for the degree of doctor of life science**

**Graduate School of Sciences and Technology for Innovation**

**Yamaguchi University**

**June 2022**

## CONTENTS

**CONTENTS**

**(Continued)**

**CONTENTS**

**(Continued)**

## LIST OF TABLES

**Tables** **Pages**

**CHAPTER 3**



**APPENDIX**

## LIST OF TABLES

## (Continued)

## LIST OF FIGURES

**Figures** **Pages**

**APPENDIX**

# CHAPTER 1

## General Introduction

Bioethanol is widely considered as an alternative to fossil fuels as it is one of clean renewable energy sources. Nowadays, lignocellulosic materials is one of the most interesting substrates because it is abundant without competing with food supplies and cheap cost (Hemansi *et al*. 2021). For economically bioethanol production, it is still costly than fossil fuels (Rozakis *et al*. 2013). High temperature fermentation (HTF) is one of technology that many industrial uses. It has several advantages including reduction of cooling cost, reduction the risk of contamination, reduction of enzymatic hydrolysis cost in saccharification and fermentation (SSF) and effective ethanol fermentation in tropical countries (Limtong *et al.* 2007; Murata *et al*. 2015).

*Saccharomyces cerevisiae* is widely used for industrial ethanol production due to this strain have capacity ethanol production, various stresses tolerance and utilize various sugar except five carbons (Lau *et al*. 2010; Lertwattanasakul *et al*. 2015). However, the temperature inside fermenters increases during the fermentation causes problem to this strain and cooling system that help to reduce temperature and cell survival increases production costs (Kosaka *et al*. 2018; Taweecheep *et al*. 2019). In recently, many researchers have been isolated thermotolerant ethanol fermenting yeast. *Kluyveromyces marxianus* is one of thermotolerant yeast that that has received interest. It has a good characteristic including high efficiency ethanol fermentation at high temperature, short doubling time, weak glucose repression, and ability to assimilate various sugar especially xylose that mostly found in lignocellulosic biomass (Limtong *et al.* 2007; Nitiyon *et al*. 2016; Techaparin *et al*. 2017).

*K. marxianus* DMKU 3-1042 is one the thermotolerant strain that have been widely study on phenotype, genotype, and complete genome sequence (Lertwattanasakul *et al*. 2015; Nitiyon *et al*. 2016; Nurcholis *et al*. 2019). This strain may have some mechanism for surviving at high temperature. Much evidence has been reported on thermotolerance. Inducing of heat shock proteins (HSPs) genes and

trehalose metabolism-related genes may support on thermotolerance (Satomura *et al*. 2013; Auesukaree 2017). Increasing nitric oxide (NO) levels provide tolerance to high temperature stress (Nasuno *et al*. 2014). High accumulation of glycogen and trehalose in mut 7 tolerated high temperature and ethanol concentration (Kumari *et al*. 2012).

During ethanol fermentation, yeast cells are exposed and respond to various stresses such as ethanol, acetic acid, osmotic stress, and oxidative stress from high concentrations of substrate sugar, all of which have effects on cell viability and ethanol production (Gibson *et al*. 2007; Auesukaree 2017; Zhang *et al*. 2015). Nowadays, ethanol production from lignocellulosic biomass become trendy because it is a renewable, abundant, inexpensive raw material and appropriate to use for the economic production (Sun and Cheng 2002; Cunha *et al*. 2019). However, conversion of biomass to sugar via pretreatment and hydolysi is released various by-products such as furfural, hydroxymethylfurfural (HMF) and phenolic compounds (Ibraheem and Ndimba 2013; Jönsson and Martín 2016). These compounds extend lag-phase, reduce cell growth, and reduce efficacy of ethanol production.

Improvement of ethanol production and characteristic of yeast strain can be achieved by strain development. Many strategies have been used to improve yeast strain (Bro *et al*. 2006; Hughes *et al*. 2012; Mobini-Dehkordi *et al*. 2008; Hemansi *et al*. 2021). Each strategies have different benefits and disadvantages. For example, sexual breeding and genetic engineering are difficult, take a time and high in cost while mutagenesis is a simple, take a short time and low in cost. In this study, adaptation was selected because it is a process that living cells adjusted their intracellular physiological conditions or some mechanisms to the surrounding environment for survival and growth (Dinh *et al*. 2008). This method seems to offer multiple advantages as an efficient way to select yeast populations, resistant to different stress conditions, and to expand their tolerance range (Zhang *et al*. 2014; Gurdo *et al*. 2018). In addition, this process is a simple, low in cost and giving a stable strain, but this process may take a time to perform.

In this study, there are two main objectives: 1) understanding strategy of thermotolerant yeast for survival at high temperature by growth and metabolic profiles,

determination of ROS, NADPH and GSH, observation of mitochondria morphology and transcriptome analysis and 2) improvement of ethanol production and stress resistance of thermotolerant yeast via adaption and study on adapted strain by characterization and genome analysis.

# CHAPTER 2

## Distinct metabolic flow in response to temperature in thermotolerant *Kluyveromyces marxianus*

### 2.1 Abstract

The intrinsic mechanism of the thermotolerance of *Kluyveromyces marxianus* was investigated by comparison of its physiological and metabolic properties at high and low temperatures. After glucose consumption, the conversion of ethanol to acetic acid became gradually prominent only at a high temperature (45°C) and eventually caused a decline in viability, which was prevented by exogenous glutathione. Distinct levels of reactive oxygen species (ROS), glutathione, and NADPH suggest a greater accumulation of ROS and enhanced ROS-scavenging activity at a high temperature. Fusion and fission forms of mitochondria were dominantly observed at 30°C and 45°C, respectively. Consistent results were obtained by temperature upshift experiments, including transcriptomic and enzymatic analyses, suggesting a change of metabolic flow from glycolysis to the pentose phosphate pathway. The results of this study suggest that *K. marxianus* survives at a high temperature by scavenging ROS via metabolic change for a period until a critical concentration of acetate is reached.

### 2.2 Introduction

*Kluyveromyces marxianus*, a thermotolerant yeast, can grow well at temperatures over 45°C, unlike *Kluyveromyces lactis*, which belongs to the same genus, or *Saccharomyces cerevisiae*, which is a closely related yeast in hemiascomycetous yeasts. *K. marxianus* may thus have an intrinsic mechanism to survive at high temperatures in addition to its efficient fermentation ability with various sugars and its short doubling time (Lertwattanasakul *et al*. 2011; Rodrussamee *et al*. 2011; Nurcholis *et al*. 2020). The thermotolerance of *K. marxianus* enables high-temperature fermentation (HTF), which can provide benefits, including reductions of cooling costs and the prevention of contamination by other microbes (Banat *et al*.

1998; Murata *et al*. 2015; Nitiyon *et al*. 2016), and attention has therefore been given to *K. marxianus* for industrial applications (Nurcholis *et al*. 2020).

Reactive oxygen species (ROS), which can induce oxidative stress, are mainly generated by the leakage of electrons from the respiratory chain in mitochondria (Pan 2011). In *S. cerevisiae*, electron leakage is enhanced at high temperatures due to the structural instability of the mitochondrial membrane (Tarrío *et al*. 2008) or by an increase in the respiration rate (Abbott *et al*. 2009). Low levels of ROS are scavenged by nonenzymatic and enzymatic antioxidizing agents such as glutathione (GSH), thioredoxin (TRX), superoxide dismutase, catalase, and peroxidases, but high levels of ROS cause the oxidation of intracellular components such as DNA, protein, and lipid and induce apoptosis (Madeo *et al*. 1999; Scherz-Shouval *et al*. 2007). Oxidative stress is a trigger of mitophagy (Frank *et al.* 2012; Kanki *et al.* 2015) and is also involved in heat-induced cell death (Davidson *et al*. 1996). Under oxidative stress conditions, cells activate the production of nicotinamide adenine dinucleotide phosphate (NADPH) that is required for the regeneration of GSH or a reduced form of TRX (López-Mirabal and Winther 2008), which is mainly produced by the pentose phosphate pathway (PPP) (Kruger and von Schaewen 2003). NADP1/NADPH is thus used as an indicator of oxidative stress and cell death (Xia *et al.* 2009; Itsumi *et al*. 2015).

The mitochondrion, which is an organelle that is responsible for various important tasks, including oxidative phosphorylation in eukaryotes, exhibits two types of morphology, fusion and fission, which are regulated by several vital genes (Shaw and Nunnari 2002) in response to nutrient depletion or stress (Youle and van der Bliek 2012). Damaged mitochondria are segregated in fission and degraded by mitophagy, by which mitochondrial homeostasis is maintained (Youle and van der Bliek 2012; Kotiadis *et al*. 2014; Palikaras and Tavernarakis 2014).

In *S. cerevisiae*, high temperature causes the accumulation of acetic acid and trehalose (Thevelein 1984; Woo *et al*. 2014). The former induces mitochondrion-dependent apoptosis (Ludovico *et al*. 2001; Ludovico *et al.* 2002), and the latter contributes to protein stabilization and inhibits apoptosis (Singer and Lindquist 1998; Petitjean *et al*. 2017). In *K. marxianus*, several genes for enzymes in the tricarboxylic

acid (TCA) cycle are downregulated and oxidative stress response genes are upregulated at a high temperature (Lertwattanasakul *et al*. 2015), indicating the possibility that mitochondrial metabolism is adapted to high-temperature conditions to avoid suffering from oxidative stress. However, the physiological and metabolic differences between low and high temperatures remain to be elucidated.

To understand the strategy of *K. marxianus* for survival at high temperatures, we first investigated cell growth, metabolites, and intracellular antioxidants in detail under long-term and short-term cultivation conditions. Under the former conditions, acetate that accumulated above a critical concentration caused a decline in cell survival, and the trigger of the drastic event was investigated by focusing on ROS, GSH, and NADPH levels. Under the latter conditions, changes in the dissolved oxygen (DO) concentration (DOC) and mitochondrial morphology were focused on. Temperature upshift experiments were also carried out, and the results revealed that the accumulation of ROS within a short time after the temperature shift caused a remarkable increase in the ratio of the fission form to the fusion form of mitochondria. On the basis of these findings and transcriptomic and enzymatic data, the metabolic change after a temperature upshift is discussed.

## 2.3 Materials and Methods

### 2.3.1 Strain, medium and cultivation

The yeast strain used in this study was *K. marxianus* DMKU 3-1042 (Limtong *et al*. 2007), which has been deposited in the NITE Biological Resource Center (NBRC) under deposit numbers NITE BP-283 and NBRC 104275. Cells were precultured in YP (1% yeast extract and 2% peptone) medium containing 2% glucose (YPD) at 30°C for about 12 h under reciprocally shaking conditions at 160 rpm. The preculture was inoculated at 1% into YPD medium, and culture was carried out under reciprocally shaking conditions at 160 rpm.

### 2.3.2 Analytical methods

Cells were pre-cultured in YPD at 30°C for about 12 h, and 1% of the pre-culture was inoculated into YPD medium for cultivation at 30°C or 45°C. Cell growth and pH were determined by measuring the optical density at 660 nm ($OD_{660}$) using a UV-visible (UV-VIS) spectrophotometer (Shimazu, Japan) and a pH meter (Horiba, Japan), respectively. Cell viability was determined as CFU by counting the number of colonies on YPD agar plates. During cultivation, samples were taken, diluted, spread onto plates, and subjected to incubation at 30°C, and the colonies that formed on the plates were enumerated after 48 h. Concentrations of glucose, ethanol, and acetate in the culture were determined on a high-performance liquid chromatography (HPLC) system (Hitachi, Japan) consisting of a Hitachi model D-2000 Elite HPLC system manager, column oven L-2130, pump L-2130, autosampler L-2200, and refractive index (RI) detector L-2490 equipped with a GL-C610H-S Gelpack column (Hitachi Chemical, Japan) or UV detector L-2400 equipped with a GL-C610-H Gelpack column (Hitachi Chemical, Japan). The dissolved oxygen concentration (DOC) was measured by using a DO sensor of Fibox 3 (PreSens Precision Sensing GmbH), and its sensor chip was set up at the center of the bottom of a 100-mL flask. NADH oxidase activity was measured as described previously (Sootsuwan *et al*. 2008; Lertwattanasakul *et al*. 2009).

### 2.3.3 Determination of cellular and mitochondrial levels of ROS

Cellular and mitochondrial levels of ROS were determined with the cell-permeant fluorescent probe 29,79-dichlorodihydrofluorescein diacetate ($H_2$DCFDA) (Funakoshi, Japan) and dihydrorhodamine 123 (Wako, Japan), respectively (Pérez-Gallardo *et al*. 2013). During cultivation, samples were taken and incubated with 10 μM $H_2$DCFDA or 10 μM dihydrorhodamine 123/1 × $10^7$ cells for 1 h before collecting cells. The collected cells were washed twice with phosphate-buffered saline (PBS) and resuspended in 4 mL of the same buffer containing protease inhibitor cocktail set IV (Wako, Japan). The cells were then disrupted by passage through a French pressure cell press (16,000 lb/$in^2$) and centrifuged at 6,000 × *g* for 10 min, and the fluorescence of the supernatant was measured by a Powerscan HT microplate reader (BioTek

Instruments Inc., Winooski, VT, USA). The protein concentration was determined by the Lowry method (Dulley and Grieve 1975).

### 2.3.4 Determination of levels of GSH and glutathione disulfide

Glutathione levels were determined by a modified method described previously (Gajendra *et al*. 2014). During cultivation, cells were harvested, washed twice with PBS, and resuspended in 4 mL of 1% 5-sulfosalicylic acid containing protease inhibitor cocktail set IV. The cells were disrupted by a French pressure cell press (16,000 lb/in$^2$) and centrifuged at 6,000 × *g* for 10 min. The supernatant was used for the determination of glutathione levels. Total glutathione was determined by the addition of 30 μL of the lysate to 450 mL of the assay mixture [0.1 M potassium phosphate (pH 7.0), 1 mM EDTA, 0.03 mg/ml 5, 5'-dithiobis (2-nitrobenzoic acid), and 0.12 U of glutathione reductase]. The samples were mixed and incubated for 5 min at room temperature, and 150 μL of NADPH (0.16 mg/mL) was added to the mixture. The formation of thiobis(2 - nitrobenzoic acid) was measured spectrophotometrically at 420 nm over a 5-min period. A standard curve was generated for each experiment using 0 to 0.5 nmol of GSH in 1% 5-sulfosalicylic acid. To measure glutathione disulfide (GSSG) levels, 200 μL of a lysate sample was derivatized by the addition of 4 μL of 97% 2-vinylpyridine, and the pH was adjusted by the addition of 4 μL of 25% triethanolamine. The samples were incubated at room temperature for 1 h. After incubation, the treated lysate was added to 300 μL of the assay mixture and incubated for 5 min at room temperature. Next, 100 μL of NADPH (0.16 mg/mL) was added, and the amount of thiobis formed was measured. GSSG standards (0 to 0.5 nmol) were also treated with 2-vinylpyridine in a manner identical to that for the samples. The amount of GSH in each sample was determined by subtracting the amount of GSSG in the lysate from the total amount of glutathione.

### 2.3.5 Determination of NADPH and NADP$^+$ levels

NADPH and NADP$^+$ levels were determined by an EnzyChrom$^{TM}$ NADP$^+$/NADPH assay Kit (BioAssay Systems). During cultivation, cells were harvested, washed twice with PBS, and resuspended in a NADPH or NADP$^+$ extraction buffer included in the kit. The sample was then incubated at 65 ˚C for 30

min. The amounts of NADPH and $NADP^+$ were determined by following the manufacturer's protocol.

### 2.3.6 Observation of mitochondrial morphology

The shape of the mitochondrial network in live cells was observed by microscopy. One hundred microliters of culture was collected and mixed with MitoTracker Red CMXRos (Molecular Probes) at the final concentration of 0.4 μM. The mixture was incubated at 30ºC for 10 min to 20 min and subjected to observation by the fluorescence microscope BX53 (OLYMPUS, Japan) with its green excitation light. Approximately 250 cells were observed to determine the ratio of fusion to fission forms of mitochondria. The fission or fusion form as a mitochondrial form was decided by the number of mitochondria; mitochondria in a cell that contains more than 4 mitochondria are of the fission form and mitochondria in a cell that contains 4 or less than 4 mitochondria are of the fusion form.

### 2.3.7 RNA-Seq analysis

For RNA preparation, cell growth was performed under three different conditions. Cells were grown in YPD medium at 30ºC for 4 h, the temperature was then increased to 45ºC, and the cells were further incubated for 30 min or 2 h or continuously incubated at 30ºC for 6 h. Total RNA was then isolated as described previously (Nurcholis *et al*. 2019) and purified by using the RNeasy mini plus kit (Qiagen) according to the instructions supplied by the company. All conditions were duplicated. The purified RNA was subjected to RNA-Seq analysis by Illumina NextSeq system. For RNA-Seq analysis, the *K. marxianus* genome sequence (GenBank accession numbers AP012213-AP012221) was used. Reads per kilobase of exon per million (RPKM) values were estimated using the CLC genomic workbench (Qiagen). Extraction of DEGs was based on unique exon read values from CLC genomics workbench outputs using the DESeq2 R package. The resulting *P* values were adjusted using Benjamin-Hochberg's method for controlling the false discovery rate. Genes with adjusted *P* values of less than 0.01 ($P_{adj} < 0.05$) and $\log_2$ fold change values of greater than 1 or lower than -1 were assigned as significant DEGs. Gene ontology (GO) enrichment analysis of significant DEGs was performed

using the topGO R package. GO terms with *P* values less than 0.01 were considered significantly enriched. Kyoto Encyclopedia of Genes and Genomes (KEGG) pathway mapping with these significant DEGs was performed by KEGG web tools (http://www.genome.jp/keg/tool/map_pathway1.html).

### 2.3.8 Enzyme assay

Cells were grown in YPD medium at 30ºC for 4 h, the temperature was then increased to 45°C, and the cells were further incubated for 30 min and 2 h or continuously incubated at 30ºC for 6 h or at 45ºC for 6 h. Cells were then harvested by centrifugation at 9,000 x *g* and 4ºC, washed with saline and resuspended in 10 mM potassium phosphate buffer (KPB) (pH 7.0). The resuspended cells were subjected to French pressure cell press (catalog number IL61801; SLM Aminco SLM Instruments, Inc.) at 24,000 lb/in$^2$ four times, followed by centrifugation at 9,000 x *g* and 4ºC for 10 min. The resultant supernatant was further subjected to centrifugation at 100,000 x *g* and 4ºC for 1 h. The supernatant was used as an ultracentrifugation supernatant for enzyme assay. Activities of glucose-6-phosphate dehydrogenase, 6-phosphogluconate dehydrogenase, phosphoglucose isomerase, glyceraldehyde-3-phosphate dehydrogenase and fructose-1,6-diphosphatase were determined spectrophotometrically (U-2000A spectrophotometer; Hitachi) by the methods reported previously (Amelunxen and Carr 1975; Kuby and Noltmann 1966; Noltmann 1966; Rosen 1975; Scott and Abramsky 1975). Glucose 6-phosphate, 6-phosphogluconate, fructose-6-phosphate, glyceraldehyde 3-phosphate, sodium arsenate, fructose 1,6-diphosphate, NADP and NAD were purchased from Oriental yeast co., LTD (Japan), Oriental yeast co., LTD, Nacalai tesque (Japan), CAYMAN (Japan), Nacalai tesque, CAYMAN, Oriental yeast co., LTD and Oriental yeast co., LTD, respectively. For the assay of phosphoglucose isomerase, glucose-6-phosphate dehydrogenase from Oriental yeast co., LTD was used. For the assay of fructose-1,6-diphosphatase, phosphoglucose isomerase and glucose-6-phosphate dehydrogenase from Nacalai tesque and Oriental yeast co., LTD, respectively, were used.

### 2.3.9 Quantification and statistical analyses

All experiments were performed independently at least three times, except for fluorescence microscopy and RNA-Seq analysis. For morphology observation by a fluorescence microscope, we chose a typical image from at least 10 random images. RNA-Seq analysis and its data analysis are described above. All of the data obtained by determination of ROS, GSH, GSSG, NADPH, $NADP^+$, NADH oxidase activity, and fission and fusion mitochondria were used to conduct an *F* test together with Turkey's honestly significant difference (HSD) test. All statistical analyses were performed using SPSS statistics software version 19.0 (IBM, New York, USA). A *P* value of $<0.05$ was considered statistically significant.

### 2.3.10 Data availability

All of the data were deposited in the DDBJ Sequence Read Archive (https://www.ddbj.nig.ac.jp/dra/index-e.html) under accession number DRA010932.

## 2.4 Results

### 2.4.1 HTF and effect of acetic acid on *K. marxianus*

*K. marxianus* bears capabilities for growth and fermentation at a high temperature as well as at a low temperature. To understand the fermentation ability of *K. marxianus* under different temperature conditions, the cell growth and metabolites of *K. marxianus* DMKU 3-1042 were compared in yeast extract-peptone-dextrose (YPD) medium at 30ºC and 45ºC for 72 h as a long-term cultivation (Fig. 2.1A to D). The cell turbidity, consumption of glucose, and ethanol production at 45 ºC were less than those at 30ºC. The concentration of ethanol peaked at 10 to12 h and then gradually decreased under both temperature conditions, and the decrease was faster at 45ºC until 36 h and then slowed down. Concomitantly, the concentration of acetate increased at 45ºC until 48 h, and the concentration was then maintained at 0.5% (w/v). In agreement with the accumulation of acetate, the pH of the culture medium greatly dropped (Fig. 2.1E). At 30ºC, the level of ethanol continuously decreased, but the level of acetate

was not as high as that at 45ºC. Notably, the number of CFU sharply decreased at 45ºC after the accumulation of acetate became about 0.4% (w/v) but did not decrease at 30ºC (Fig. 2.1F).

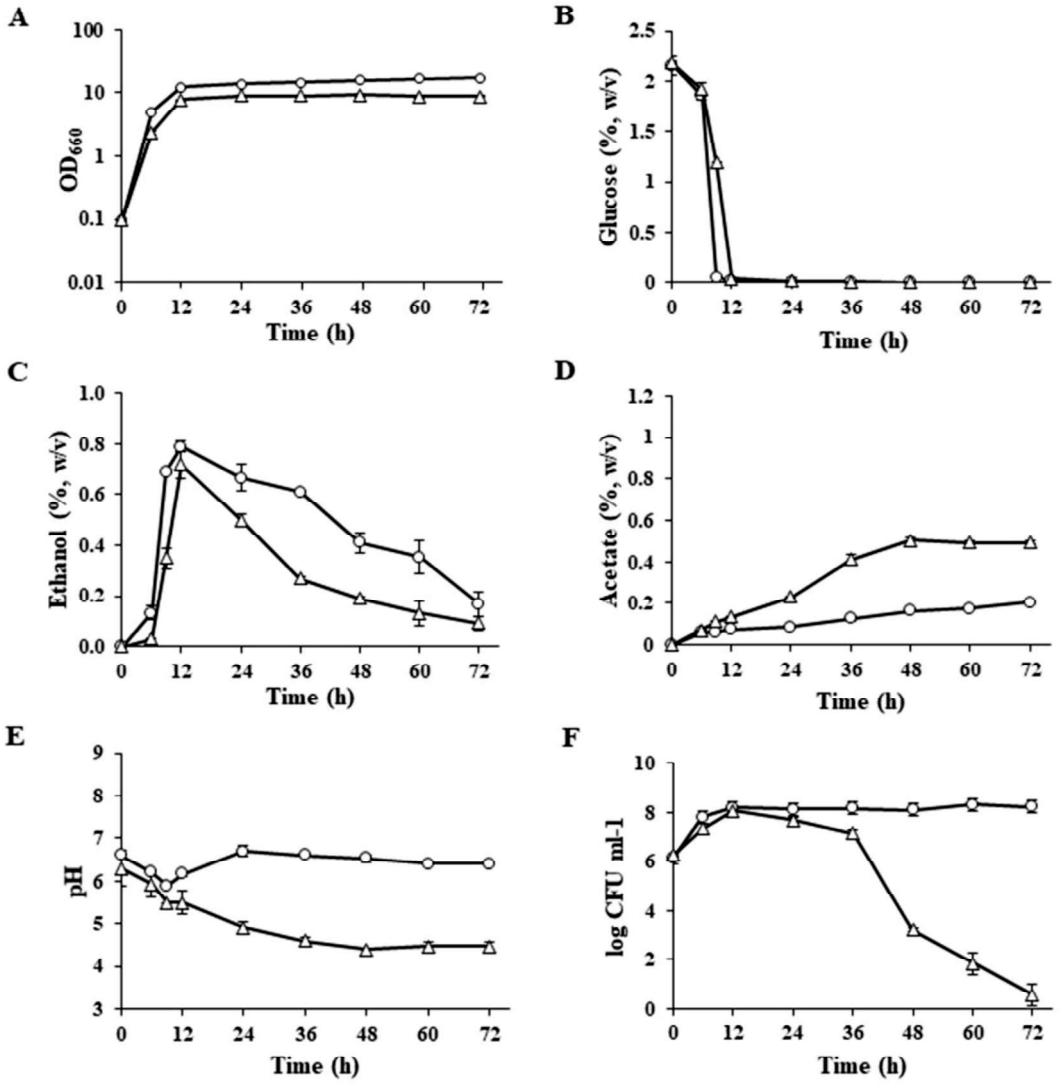


**Fig. 2.1** Ethanol fermentation of *K. marxianus* in long-term cultivation at 30ºC and 45ºC. Cells were cultivated in 2% YPD medium at 30ºC (open circles) and 45ºC (open triangles) under shaking conditions. (A) The cell density was estimated by measuring the turbidity at $OD_{660}$. (B to D) Concentrations of glucose (B), ethanol (C), and acetate (D) were determined by HPLC. (E and F) pH (E) and CFU (F) were also determined as described in Materials and Methods. Error bars represent standard deviations (SD) for triplicate experiments.

The decrease in the number of CFU suggested that the accumulation of acetate over a critical concentration caused cell death. To investigate this possibility, acetic acid and HCl were exogenously added to the culture medium at 45ºC (Fig. 2.2). The number of CFU was greatly decreased and the level of ROS was increased by the addition of 0.2% or 0.4% (w/v) of acetic acid but was not changed by the addition of HCl, which decreased pH to 4.2, being pH equivalent to 0.4% (w/v) of acetic acid. Therefore, the results suggested that exogenous acetic acid enhances the elevation of the level of ROS and the decrease in the number of CFU and that cell death is caused by the accumulation of acetate but not by pH reduction of the culture medium.

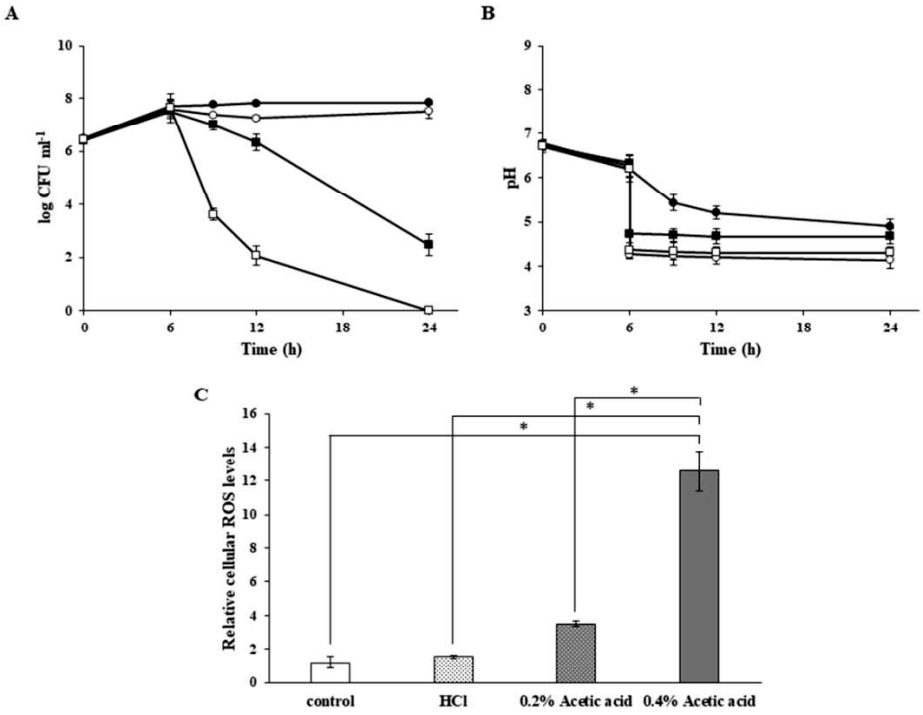


**Fig. 2.2** Effects of acetic acid on cell viability and cellular level of ROS of *K. marxianus* at 45ºC. Cells were cultivated in 2% YPD medium supplemented with acids at 45ºC under shaking conditions at 160 rpm. Six hours after inoculation, acids, including 0.118% (w/v) HCl (open circles), 0.2% (w/v) acetic acid (closed squares), and 0.4% (w/v) acetic acid (open squares) were added or not added (closed circles). (A and B) CFU (A) and pH (B) were determined as described in the legend of Fig. 2.1. (C) Relative cellular level of ROS was measured at a log phase (6 h) as described in Materials and Methods. Error bars represent SD for triplicate experiments. *, *P* value of <0.05.

### 2.4.2 Levels of ROS, GSH, and NADPH under a high-temperature condition

Since it was previously shown that levels of ROS remarkably increase under high-temperature conditions in *S. cerevisiae* (Zhang *et al*. 2015), cellular and mitochondrial levels of ROS were determined in the log phase (6 h) and in the acetate-accumulation phase (36 h) at 30ºC and 45ºC (Fig. 2.3A and B). At 6 h, cellular and mitochondrial levels of ROS at 45ºC were 4.0-fold and 10.9-fold higher than those at 30ºC, respectively. At 36 h, the cellular and mitochondrial levels of ROS at 45ºC were 5.9-fold and 3.1-fold higher than those at 30ºC, respectively. The levels of ROS were significantly higher in the acetate accumulation phase, during which the number of CFU was decreasing. These results suggest that heat stress increases cellular and mitochondrial levels of ROS. On the other hand, the cellular GSH and GSSG levels in the log phase at 45ºC were lower than those at 30ºC and the levels in the acetate accumulation phase at 45ºC were much lower (Fig. 2.3C to E), athough the ratios of GSH to GSSG at 45ºC in both phases were almost the same as those at 30ºC, indicating that the sum of GSH and GSSG values at 45ºC is low compared to that at 30ºC. Therefore, it is likely that either low synthesis or high degradation of GSH occurs at a high temperature in comparison to that at a low temperature, though the ratio of GSH/GSSG is maintained.

Since the enzymatic conversion of ethanol to acetic acid generates NADPH as a source of reducing equivalents for regeneration of GSH, it is assumed that acetic acid is produced to generate NADPH for the removal of ROS. To examine this assumption, NADPH and $NADP^+$ levels of the cells were determined in the log and acetate accumulation phases at 30ºC and 45ºC (Fig. 2.3F to H). In both phases, the NADPH levels at 45ºC were higher than those at 30ºC. Notably, at 45ºC, the ratio of NADPH/$NADP^+$ in the acetate accumulation phase was lower than that in the log phase, presumably indicating the requirement of a larger amount of NADPH in the acetate accumulation phase for removal of ROS. However, considering the report by Zhang *et al*. (2015), the ratio of NADPH/NADP could be low, so it cannot be denied that the method used in this study underestimated the amount of NADPH.

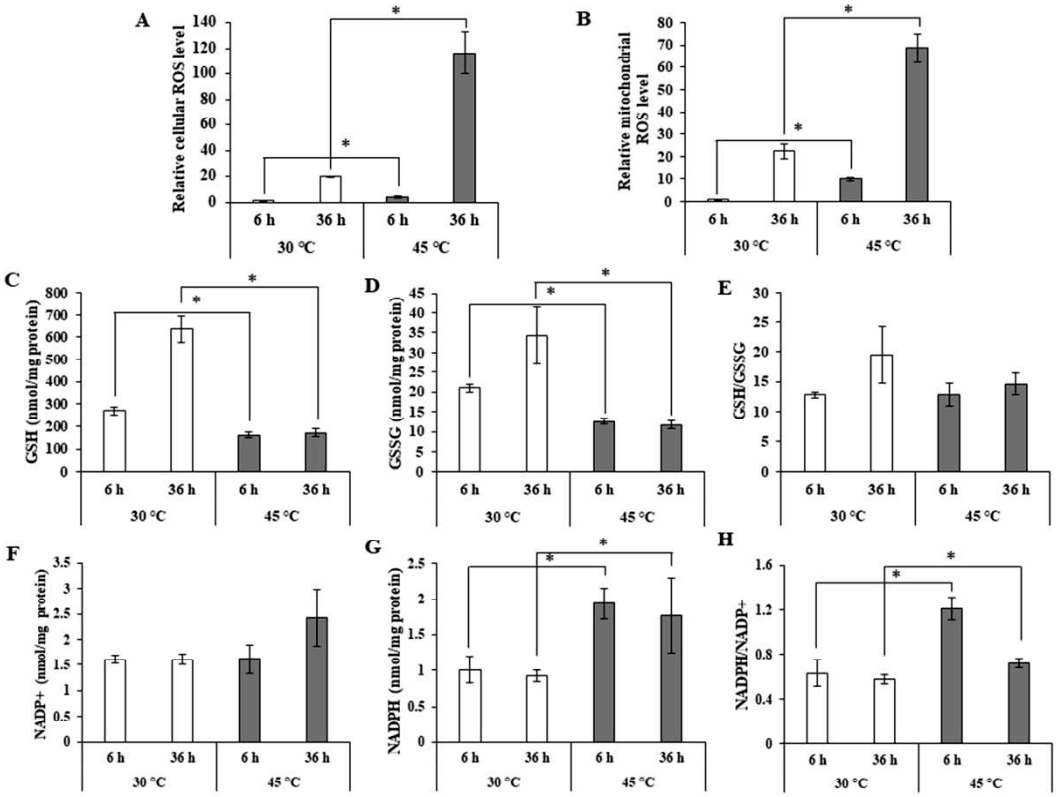


**Fig. 2.3** Cellular and mitochondrial levels of ROS and levels of glutathione and NADPH of *K. marxianus* at 30ºC and 45ºC. Cells were cultivated in 2% YPD medium at 30ºC and 45ºC under shaking conditions for 6 h or 36 h. (A and B) Cellular (A) and mitochondrial (B) levels of ROS at 6 h or 36 h were estimated as described in the legend of Fig. 2.2. White and grey columns represent levels of ROS at 30ºC and 45ºC, respectively. (C to H) GSH (C), GSSG (D), the GSH/GSSG ratio (E), $NADP^+$ (F), NADPH (G), and the NADPH/$NADP^+$ ratio (H) were determined as described in Materials and Methods. Error bars represent SD for triplicate experiments. *, *P* value of <0.05.

### 2.4.3 Effects of exogenous GSH on acetate accumulation and cell viability under a high-temperature condition

To reduce the oxidative stress level in cells, GSH was added to the culture medium, and ethanol consumption, acetate accumulation, and cell viability were examined (see Fig. S1 in appendix). The maximum concentration of acetate in the

presence of 4 mM GSH was 0.16% (w/v), which was much lower than that in the presence of 0 or 1 mM GSH. The addition of 4 mM GSH kept CFU at a high level and reduced the ethanol consumption speed compared to those with the addition of 0 or 1 mM GSH. These results indicate that exogenous GSH slows ethanol consumption, limits acetate accumulation, and prevents cell death at 45ºC. Taken together, the results of the experiments with long-term cultivation suggest that the high temperature of 45ºC causes the accumulation of ROS, which leads to the oxidation of ethanol to provide NADPH, resulting in the accumulation of acetate, which in turn leads to damage and death of cells. The provision of NADPH via ethanol oxidation may contribute to the prevention of ROS-induced cell death until the concentration of acetate reaches a critical level.

### 2.4.4 Analysis of fermentation at the early phase and mitochondrial morphology

To further understand metabolic differences at high and low temperatures, short-term cultivation was also performed (Fig. 2.4, Fig. 2.5 and Fig. S2). At 30ºC, the dissolved oxygen concentration (DOC) decreased to the minimum level within 4 h, with almost no consumption of glucose added, followed by an increasing and decreasing waves with a peak at around 17 h (Fig. 2.4A). The DOC goes to zero before glucose starts to be consumed, which could be due to respiration of intracellular reserves, including glycogen or trehalose. Glucose consumption continued until 10 h with the maximum ethanol concentration at 10 h (Fig. 2.5B and C). The increase in the DOC at 30ºC at about 14 h presumably represents the diauxic lag when the cells have ceased respirofermentative catabolism of glucose (at 10 h) but do not start to respire ethanol until after 12 h and then only slowly. At 45ºC, the decrease in the DOC was much slower than that at 30ºC, and no wave was observed (Fig. 2.4A and Fig. 2.5E). Ethanol fermentation appeared to be different at low and high temperatures in response to DOCs (Fig. 2.5C and E). Obvious glucose consumption and ethanol accumulation were observed after the DOC decreased to a minimum level at 30ºC, while glucose was fermented at a relatively high DOC at 45ºC (Fig 2.5B, C and E). The former could be due to respiration of intracellular glycogen or trehalose.

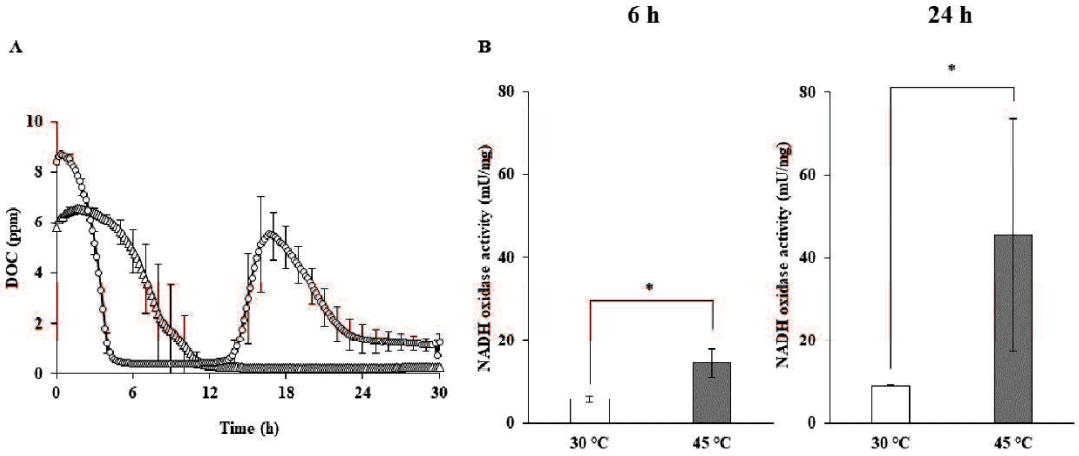


**Fig. 2.4** Distinct characteristics of *K. marxianus* at 30ºC and 45ºC. Cells were cultivated in 2% YPD medium at 30ºC and 45ºC under shaking conditions. (A) The DOC was measured by a DO sensor (open circles, 30ºC; open triangles, 45ºC). (B) NADH oxidase activity was determined with samples taken at 6 h and 24 h. Error bars represent SD for triplicate experiments. *, *P* value of <0.05.

Surprisingly, the distinct mitochondrial morphologies at 30ºC and 45ºC were observed at 3 h, 6 h, and 24 h (Fig. S2), but mitochondria were not clearly visible at 48 h under the condition at 45ºC (data not shown), at which time the number of CFU declined. NADH oxidase activities at 6 h and 24 h at 45 ˚C were found to be higher than those at 30ºC (Fig. 2.4, B), possibly being related to morphological change of mitochondoria and/or a greater accumulation of ROS at 45ºC. Notably, there was almost no difference in the concentrations of acetate until 8 h at 30ºC and 45ºC, athough the glucose and ethanol levels were different (Fig. 2.5), indicating the possibility that the acetate level in the culture media may not be responsible for the accumulation of ROS or for the generation of the mitochondrial fission form.

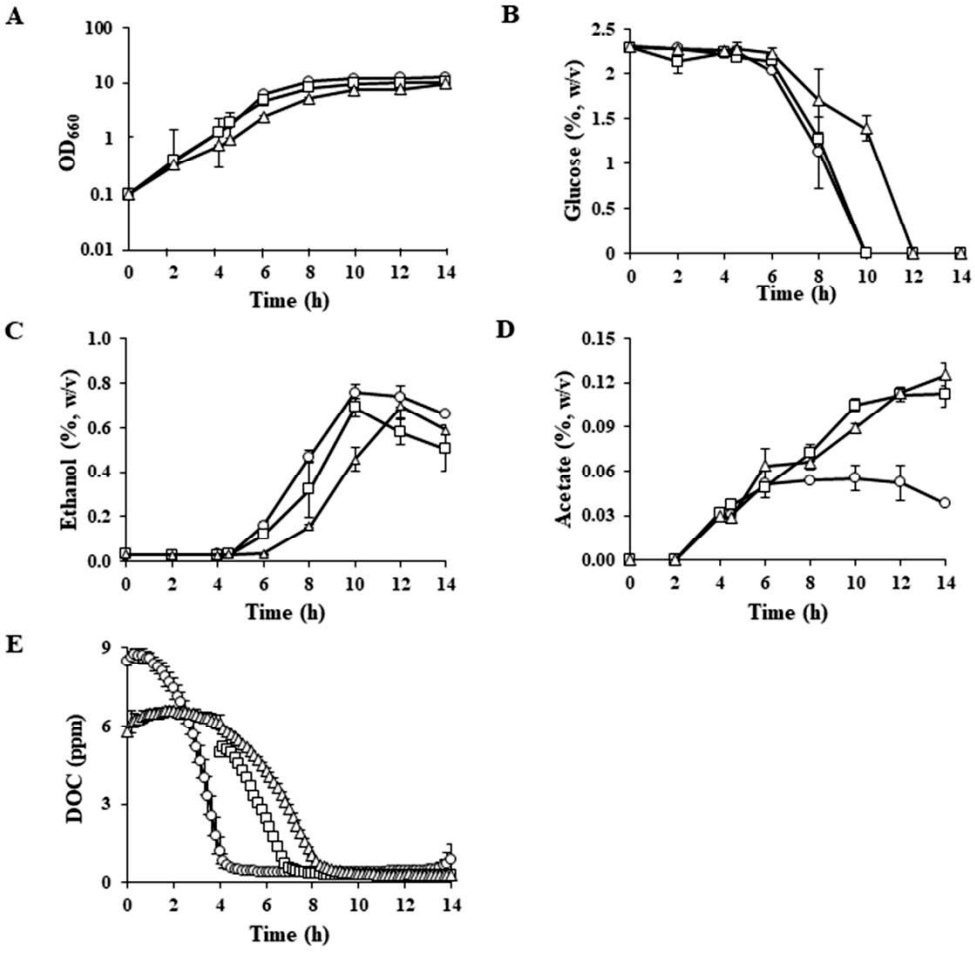


**Fig. 2.5** Ethanol fermentation of *K. marxianus* during short-term cultivation at 30°C and 45°C and effects of temperature upshift on *K. marxianus.* Cells were cultivated in 2% YPD medium at 30°C (open circles), 45°C (open triangles), or 30°C to 45°C (temperature upshift) (open squares) under shaking conditions. The temperature upshift was performed by transferring flasks from a 30°C incubator to a 45°C incubator 4 h after incubation at 30°C. Cell density (A) and concentrations of glucose (B), ethanol (C), and acetate (D) (%, w/v) were determined as described in the legend of Fig. 2.1. (E) The DOC was measured by a DO sensor. Error bars represent SD for triplicate experiments. *, *P* value of <0.05.

### 2.4.5 Effects of temperature upshift on cell growth and metabolism

To further understand the metabolic differences at 30ºC and 45ºC, cell growth and metabolites were examined when the cultivation temperature was increased to 45ºC after 4-h cultivation at 30ºC and compared with those under constant temperature conditions at 30ºC and 45ºC (Fig. 2.5). This temperature upshift or the transfer of cells pre-grown at 30ºC to medium at 45ºC may cause a heat shock response, which triggers changes in transcription and metabolism. Oxygen consumption was delayed almost immediately after the temperature upshift, and the profile was closer to that under the 45ºC constant conditions, but the profiles of cell turbidity, glucose consumption and ethanol accumulation were almost the same as those under the 30ºC constant conditions. Therefore, the temperature upshift may affect oxygen consumption without having negative effects on cell growth, glucose uptake, and ethanol production. The high DOC immediately after the temperature upshift may be due to a brief pause in shaking during the transfer of flasks from a 30ºC incubator to a 45ºC incubator.

On the other hand, no significant effect of temperature upshift on acetate accumulation was observed until 4 h after the upshift and its profile was similar to the profiles under the 30ºC and 45ºC constant conditions, but an increase in ROS occurred until 2 h after the upshift, and the level of ROS at 2 h was 11-fold higher than that under the 45ºC constant conditions (Fig. 2.6A). Therefore, it is assumed that ROS generated by the upshift are removed by means other than the process of conversion ethanol to acetic acid.

Observation of mitochondrial morphology in addition to the measurements of ROS were carried out at 2 h or 3 h after the temperature up-shift following a 4-h cultivation at 30ºC (Fig. 2.6B and Fig. S3). Surprisingly, the temperature upshift caused an increase in fission mitochondria, and fusion and fission forms of mitochondria in cells were 47% and 53%, respectively. The ratio of fission to fusion forms remarkably increased compared to that under the 30ºC constant conditions and was close to that under the 45ºC constant conditions (Fig. 2.6B).

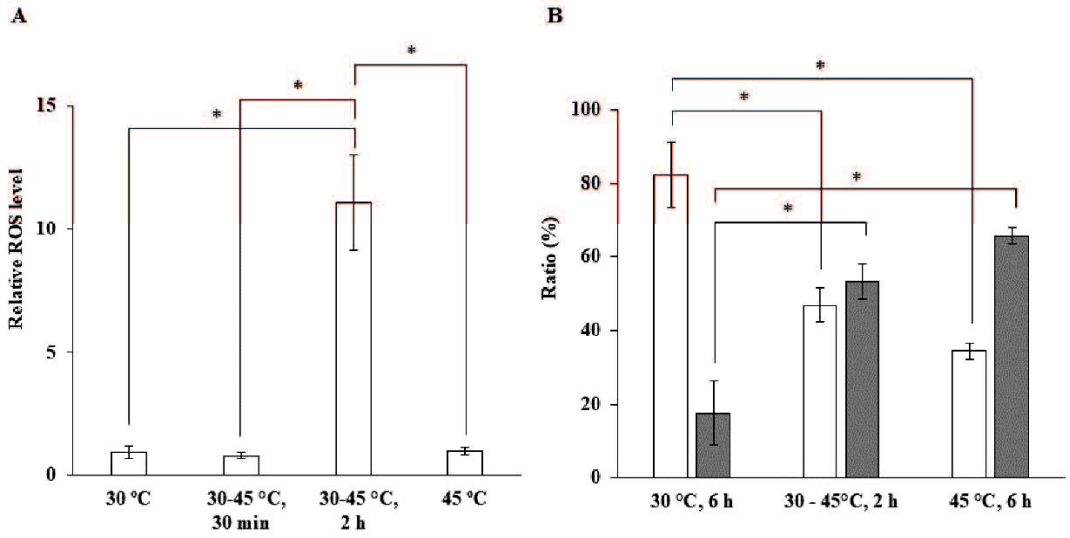


**Fig. 2.6** Effects of temperature upshift on cellular levels of ROS and mitochondrial morphology. Cells were cultivated in 2 % YPD medium at 30ºC, 45ºC or 30ºC to 45ºC under shaking conditions. The temperature upshift was performed as described in the legend of Fig. 2.5. (A) Relative levels of ROS were determined 30 min (30-45ºC, 30 min) or 2 h (30-45ºC, 2 h) after the temperature up-shift. (B) Mitochondrial morphology was observed 2 h (30-45ºC, 2 h) after the temperature upshift, and the ratios were determined by observation of 250 cells. White and gray columns represent fusion and fission forms of mitochondria, respectively. Determination of the cellular levels of ROS and observation of mitochondrial morphology were performed as described in Materials and Methods. Error bars represent SD for triplicate experiments. *, *P* value of <0.05.

### 2.4.6 Transcriptome analysis at the transition phase from a low temperature to a high temperature

The greatly altered profiles of ROS and DOCs and the change in mitochondrial morphology at the transition phase of temperature (Figs. 2.5 and 2.6) motivated us to perform genome-wide gene expression analysis (RNA sequencing [RNA-Seq]) under two different conditions. Under one condition, cells were grown in YPD medium at 30 °C for 4 h and further grown at 45°C for 30 min (4H30-30M45) or 2 h (4H30-2H45). In the other condition, cells were grown in YPD medium at 30 ºC for 6 h (6H30). The RPKM (reads per kilobase of exon per million) value of each gene was estimated as

transcript abundance. The difference in the expression of each gene in 4H30-30M45 or 4H30-2H45 from that in 6H30 was reflected as the ratio of the RPKM value in 4H30-30M45 or 4H30-2H45 to that in 6H30. To further explore the transcriptional changes, analysis of differentially expressed genes (DEGs) was conducted on the basis of the RNA-Seq data. DEGs showed significant changes at the transcription level with a $\log_2$ fold change of greater than 1 and a $\log_2$ fold change of less than -1 and an adjusted *P* value ($P_{adj}$) of less than 0.05 (Fig. S4). DEGs in 4H30-30M45 consisted of 2,069 genes, including 1,076 up-regulated and 993 down-regulated genes. DEGs in 4H30-2H45 consisted of 2,119 genes, including 1,054 up-regulated and 1,065 down-regulated genes. In the up- and downregulated DEGs, 817 genes and 773 genes, respectively, were shared between the 4H30-30M45 and 4H30-2H45 conditions (Fig. S5). These data for DEGs were used for gene ontology (GO) enrichment analysis and Kyoto Encyclopedia of Genes and Genomes (KEGG) pathway analysis (Tables S1 to S12).

In 4H30-30M45, 62 DEGs were highly significantly upregulated (> 4 $\log_2$). They included genes for heat shock proteins, cochaperone proteins, and many hypothetical or uncharacterized proteins (Table S1). GO enrichment analysis of DEGs (> 2 $\log_2$) showed that genes for ribonucleoprotein complex biogenesis, ribosome biogenesis, rRNA processing, the rRNA metabolic process, and maturation of single-subunit (SSU) rRNA as the top five were significantly enriched in the biological process (Table S2). KEGG pathway analysis revealed that pathways for protein processing in the endoplasmic reticulum, the spliceosome, the biosynthesis of secondary metabolism, the biosynthesis of antibiotics, the meiosis and MAPK signaling pathway, and the peroxisome were in the top ranks (Table S3). Moreover, pathways for lipid metabolism (glycerolipid, sphingolipid, glycerophospholipid, and fatty acid), GSH metabolism, and mitophagy were also listed. On the other hand, 89 DEGs were highly significantly downregulated (less than -4 $\log_2$), including genes for ribosomal proteins and transporters (Table S4). GO enrichment analysis revealed that many terms were related to biosynthetic processes and metabolic processes (Table S5). In KEGG pathway analysis, pathways for ribosome, the biosynthesis of secondary metabolites, the biosynthesis of antibiotics, the biosynthesis of amino acids, and

carbon metabolism were highlighted (Table S6). In addition, pathways for glycolysis/gluconeogenesis, steroid biosynthesis, the cell cycle, oxidative phosphorylation, fatty acid metabolism, and autophagy were listed.

In 4H30-2H45, 60 DEGs were highly significantly upregulated (> 4 $\log_2$). They included genes for heat shock proteins, cochaperone proteins, and many hypothetical proteins (Table S7), and 47 of these genes were included in the list of 4H30-30M45 (Table S1). Seven out of eight genes for heat shock proteins and cochaperone proteins in 4H30-30M45 were shared with those in 4H30-2H45. GO enrichment analysis showed that the top 20 terms were nearly the same as those of upregulated DEGs in 4H30-30M45 (Table S8). In KEGG pathway analysis, all pathways except for one pathway (one-carbon pool by folate) were listed in those of upregulated DEGs in 4H30-30M45 (Table S9). On the other hand, 31 DEGs were highly significantly downregulated (less than -4 $\log_2$). They included genes for carbon metabolism (Table S10), and 15 of these genes were also listed as downregulated DEGs in 4H30-30M45 (Table S4). Only 1 of the 50 genes for ribosomal proteins that were listed as downregulated DEGs in 4H30-30M45 (Table S4) was found in the list of 4H30-2H45. GO enrichment analysis showed that the top 18 terms except for 1 term were included in the top 34 of downregulated DEGs in 4H30-30M45 (Table S11). In the KEGG pathway analysis (Table S12), 32 pathways in the table were also listed as downregulated DEGs in 4H30-30M45 (Table S6). Therefore, upregulated and downregulated DEGs in 4H30-30M45 overlapped those of 4H30-2H45 well, except for many downregulated genes for ribosomal proteins in 4H30-30M45.

To understand the metabolic change around the central metabolic pathway caused by a temperature upshift, transcriptomic data related to glycolysis, the PPP, the TCA cycle, and cellular and mitochondrial oxidative stress responses were focused on (Fig. 2.7A and B and Fig. S6A and B). *RAG2*, *RAG5*, *PFK1*, *PFK2*, *FBA1*, *TPI1*, *GAP1*, *GAP3*, *PGK*, *GPM1*, *ENO,* and *PYK1* for glycolysis and *CIT1*, *ACO2b*, *LSC1*, *LSC2*, *FUM1,* and *MDH1* for the TCA cycle were downregulated in 4H30-30M45 and/or 4H30-2H45. In contrast, *GLK1*, *FBP1,* and *GPM3* for glycolysis; *SOL1* and *RKI1* for the PPP; *ADH1*, *KLMA_40624 (ADH)*, and *ADH6* for catalysis between ethanol and acetaldehyde in the cytosol; *ADH4a*, *ALD4,* and *ACS1* for catalysis

between ethanol and acetyl-CoA in mitochondria; and *CIT3*, *IDP1,* and *SDH4* for the TCA cycle were upregulated in 4H30-30M45 and/or 4H30-2H45. On the other hand, genes for oxidative stress response were upregulated (Fig. S6A and B) as expected, probably reflecting the accumulation of ROS under the conditions tested.

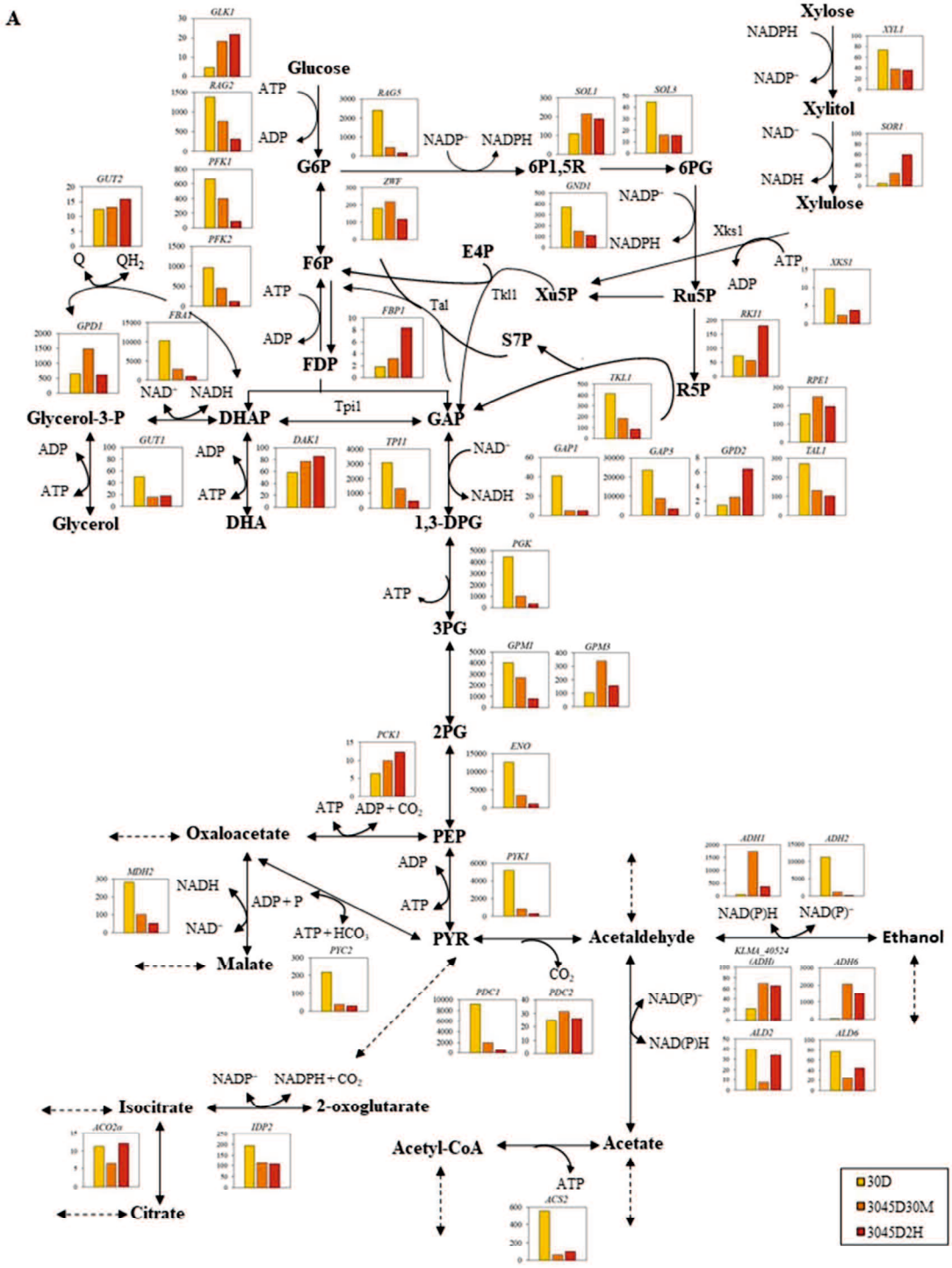

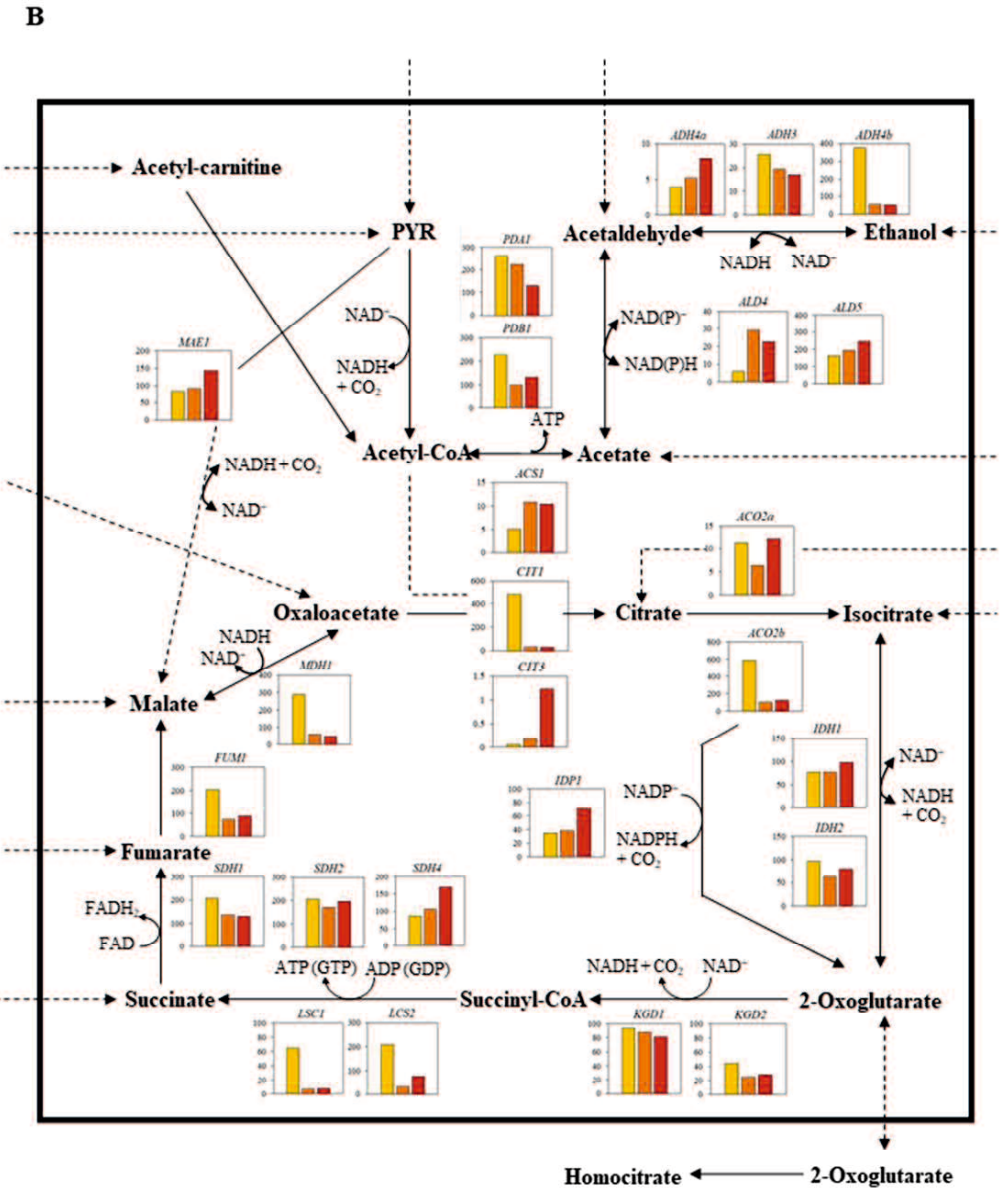


**Fig. 2.7** Transcriptome analysis of the effect of temperature upshift in *K. marxianus.* Cells were cultivated in YPD medium at 30ºC for 4 h under shaking conditions, and flasks were transferred from a 30ºC incubator to a 45ºC incubator for further culture for 30 min (4H30-30M45, orange) or 2 h (4H30-2H45, red). The control was the culture at 30ºC for 6 h under shaking conditions (6H30, yellow). Total RNA was then isolated, purified, and subjected to RNA-Seq analysis. The Y axis of each graph represents the reads per kilobase of exon per million (RPKM) of each gene under the conditions. Data for central metabolism (A) and TCA cycle (B) are shown. The

RPKM value of each gene represents the average value of two independent experiments. G6P, glucose-6-phosphate; F6P, fructose-6-phosphate; FDP, fructose 1,6 bisphosphate; DHAP, dihydroxyacetone phosphate; DHA, dihydroxyacetone; GAP, glyceraldehyde-3-phosphate; 1,3-DPG, 1,3-bisphosphoglycerate; 3PG, 3-phosphoglycerate; 2PG, 2-phosphoglycerate; PEP, phosphoenolpyruvate; PYR, pyruvate; 6P1,5R, 6-phospho-D-glucono-1,5-lactone; 6PG, 6-phosphogluconate; Ru5P, ribulose-5-phosphate; R5P, ribose-5-phosphate; Xu5P, xylulose-5-phosphate; E4P, erythrose-4-phosphate; S7P, sedoheptulose-7-phosphate; NAD, nicotinamide adenine dinucleotide; NADP, nicotinamide adenine dinucleotide phosphate; Q, quinone; ATP, adenosine triphosphate; ADP, adenosine diphosphate.

Since mitochondrial morphological change that is crucial for maintenance of functional mitochondria under stress conditions (Youle and van der Bliek 2012) was observed following the temperature upshift, genes for mitophagy and autophagy were focused on. As mitophagy-related genes, *ATG32* and *FIS1* were upregulated in both 4H30-30M45 and 4H30-2H45, and *SSK1*, *WSC3,* and *SLG1* were downregulated in 4H30-2H45 (Tables S13, S14). As autophagy-related genes, *RAS2*, *GCN4,* and *PCL5* were downregulated in 4H30-30M45 (Table S14). Gcn4 regulates nonselective autophagy activity through *ATG* transcription; for example, Gcn4 activates the expression of *ATG1*, *ATG13,* and *ATG14* during amino acid starvation (Delorme-Axford and Klionsky 2018; Natarajan *et al*. 2001). Such uncoordinated expression of genes for mitophagy and downregulation of genes for autophagy may contribute to the endurance of *K. marxianus* at a high temperature, which is discussed below. In addition, the longevity-regulating pathway in both 4H30-30M45 and 4H30-2H45 (Tables S3, S9) was listed. This pathway commonly consists of 5 genes, *SSA3*, *HSP78,* and *HSP104* for heat shock proteins and *SOD1* and *SOD2* for superoxide dismutase, reflecting the requirement of protection from heat shock and oxidative stress at high temperatures.

### 2.4.7 Activity of several enzymes at the transition from a low temperature to a high temperature

As several lines of evidence described above have shown, higher NADPH levels at 45°C than those at 30°C, the downregulation of most genes for glycolysis by a temperature upshift, and the upregulation of some genes for gluconeogenesis and the PPP imply metabolic changes. To confirm these metabolic changes, the activity of several enzymes in glycolysis and the PPP was determined using supernatants after the ultracentrifugation of cell extracts (Fig. 2.8). The change in activity of glyceraldehyde-3-phosphate dehydrogenase after the temperature upshift was almost consistent with the change in transcription of its gene, although the decrease in activity was delayed compared to that of transcription. The activity patterns of glucose-6-phosphate dehydrogenase and 6-phosphogluconate dehydrogenase were also in good agreement with their transcription patterns. Notably, the activities of fructose-1,6-diphosphatase in 4H30-2H45 and 6H45 were higher than that in 6H30, and the activity level of glucose-6-phosphate dehydrogenase was constant even after the temperature upshift. These findings suggest a metabolic flow to the PPP under elevated-temperature conditions. On the other hand, the activity of phosphoglucose isomerase was slightly decreased after the temperature upshift or at 45°C, although its transcription sharply declined, indicating the possibility that the enzyme is relatively stable, which may contribute gluconeogenesis.

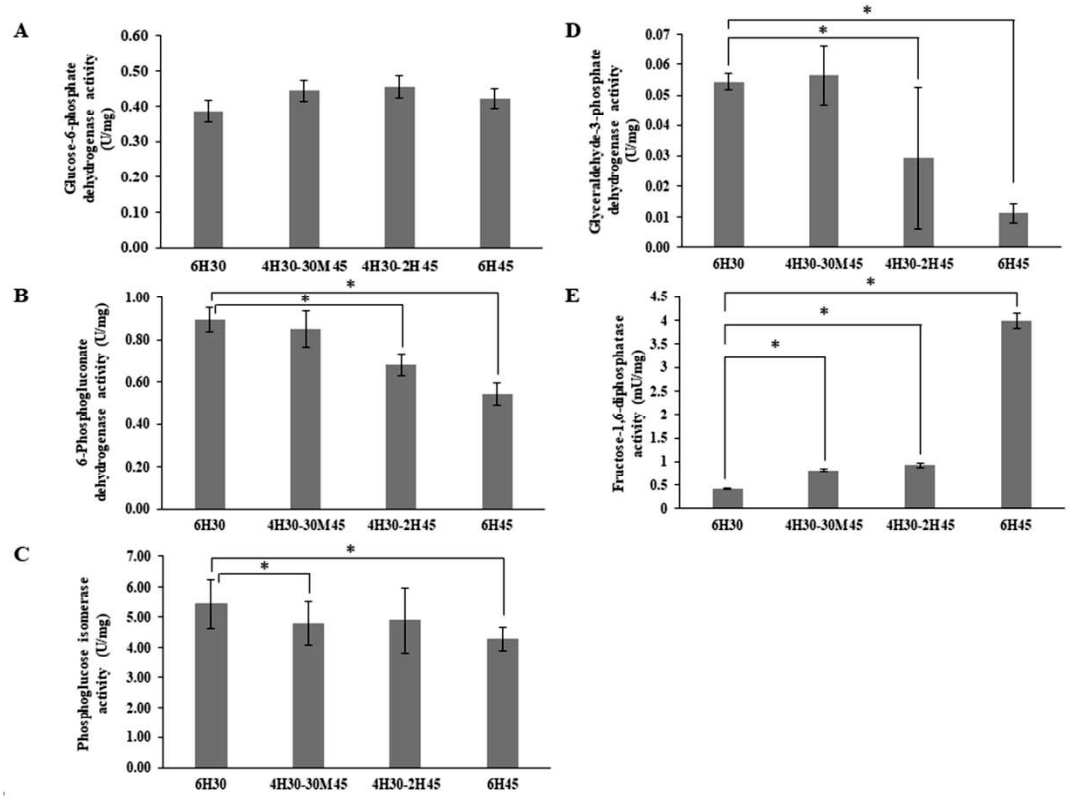


**Fig. 2.8** Enzyme activity analysis of the effect of temperature upshift on *K. marxianus.* Cells were cultivated in YPD medium at 30ºC for 4 h under shaking conditions, and flasks were transferred from a 30ºC incubator to a 45ºC incubator for further culture for 30 min (4H30-30M45) or 2 h (4H30-2H45). Cells were also cultivated in YPD medium at 30ºC for 6 h (6H30) or at 45ºC for 6 h (6H45) under shaking conditions. Cells were then harvested, and ultracentrifugation supernatants were prepared for enzyme assay as described in Materials and Methods. The activities of glucose-6-phosphate dehydrogenase (A) and 6-phosphogluconate dehydrogenase (B) in the PPP, of phosphoglucose isomerase (C) and glyceraldehyde-3-phosphate dehydrogenase (D) in glycolysis and of fructose-1,6-diphosphatase in gluconeogenesis (E) were determined spectrophotometrically. Error bars represent SD for triplicate experiments. *, *P* value of <0.05.

## 2.5 Discussion

In contrast to the physiological properties at 30ºC, the acetate concentration at 45ºC increased in long-term cultivation and exceeded a critical concentration of around

0.4% (w/v), which eventually resulted in a large reduction in the number of CFU (Fig. 2.1). Acetic acid, which is permeable to the cytoplasmic membrane as an undissociated acid, dissociates to protons and acetate anions inside cells, and the accumulation of protons lowers the intracellular pH, thereby leading to a great reduction of metabolic activity and, eventually, cell death (Russell 1991; Axe and Bailey 1995). The finding that exogenous GSH prevented the emergence of distinct properties of acetate accumulation and the reduction in the number of CFU (see Fig. S1 in appendix) suggests that the accumulation of ROS is the cause of the properties. Considering the evidence that acetic acid induces programmed cell death depending on ROS (Guaragnella *et al*. 2010), acetate accumulation may be a crucial factor responsible for the CFU reduction (Fig. 2.1). On the other hand, acetic acid production from ethanol by enzymatic reactions provides NADPH, which is involved in protection against the toxicity of ROS (López-Mirabal and Winther 2008). Therefore, it is assumed that *K. marxianus* produces acetic acid from ethanol after glucose depletion in response to the accumulation of ROS at high temperatures, keeping the levels of ROS below toxic levels (Fig. 2.9A and B).

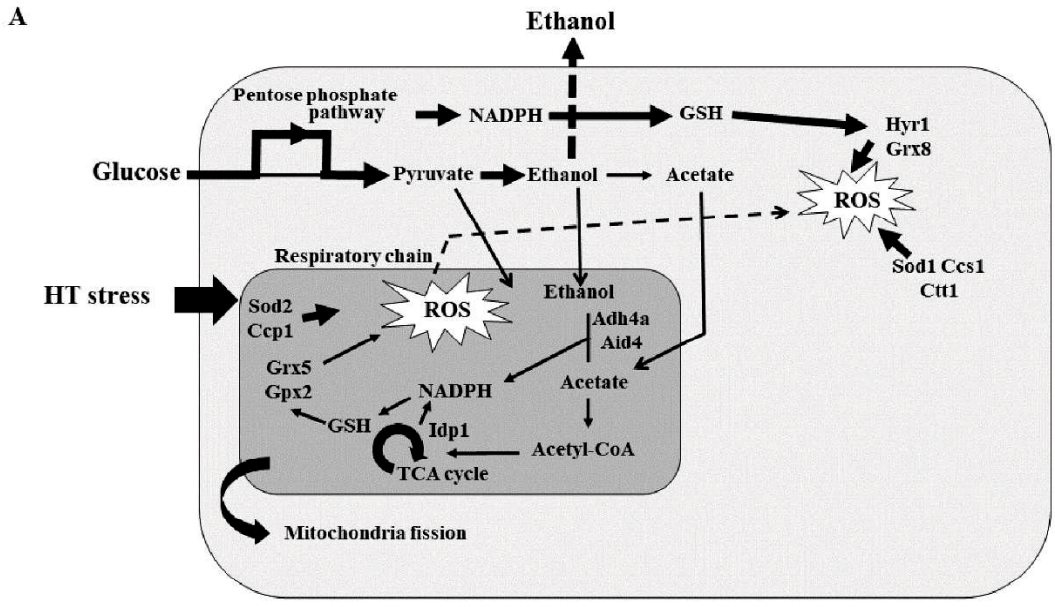

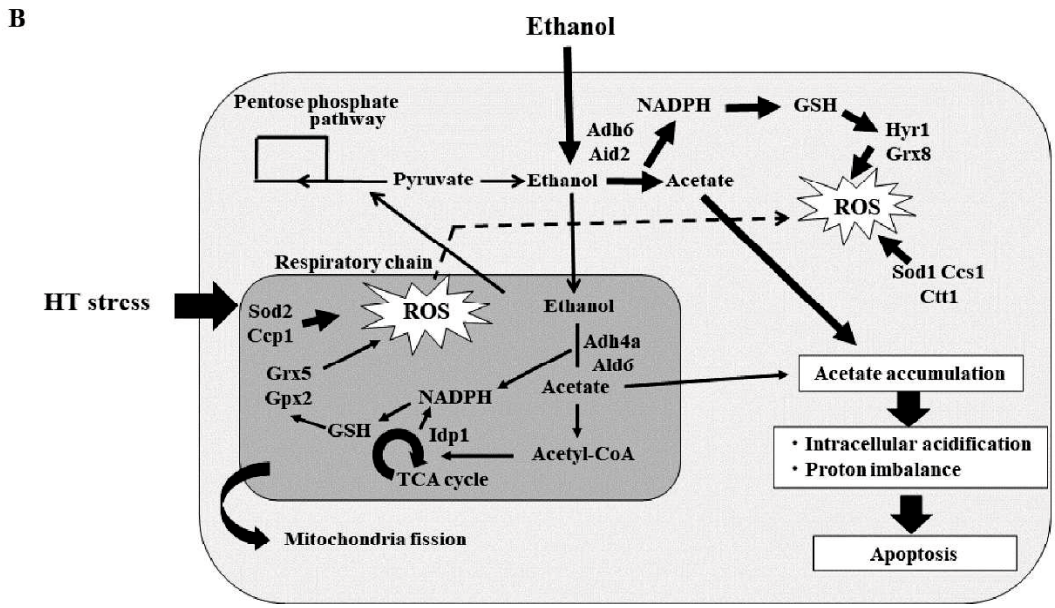


**Fig. 2.9** Models of metabolic flow at a high temperature (HT) in *K. marxianus.* **(**A) Log phase, in which glucose is present in the culture. (B) Acetate-accumulation phase, in which there is no glucose in the culture.

In *S. cerevisiae*, intracellular formation of ROS increases when the temperature rises to 42º (Zhang *et al*. 2015) and GSH decreases with exposure to $H_2O_2$ (Manfredini *et al*. 2004). Similarly, in *K. marxianus*, cellular and mitochondrial levels of ROS in the log phase at 45ºC were higher than those at 30ºC (Fig. 2.3A and B), and GSH concentrations in both the log and acetate accumulation phases were lower at 45ºC than at 30ºC, and the difference between GSH concentrations at 45ºC and 30ºC in the acetate accumulation phase was much larger than that in the log phase (Fig. 2.3C). The low level of GSH at 45ºC appeared to be related to the increase in ROS because GSH is required for the repair of oxidative damage. These results suggest that the high temperature is responsible for the increase in the cellular and mitochondrial levels of ROS and the decrease in GSH in *K. marxianus*. Probably to compensate for the decrease in GSH, NADPH levels in both the log and acetate accumulation phases at 45ºC were higher than those at 30ºC (Fig. 2.3G).

In the temperature upshift experiments, a delay in oxygen consumption similar to that under the 45ºC constant conditions was observed immediately after the upshift, but the patterns of cell proliferation, glucose consumption, and ethanol production were hardly changed from those under the 30ºC constant conditions (Fig. 2.5B and C). The temperature transition resulted in a change of mitochondrial morphology with an increase in the fission form ratio and in an elevation of the level of ROS to a level about 11-fold higher than that under the 30ºC constant conditions (Fig. 2.6). Given the results of studies showing that mitochondria tend to change their morphology with several stresses (Youle and van der Bliek 2012) and ROS induce mitochondrial fission (Wai and Langer 2016), it is assumed that the accumulation of ROS is the cause of mitochondrial morphological change in *K. marxianus*. Moreover, the fission form ratio was close to that under the 45°C constant conditions, athough the levels of ROS were very different (Fig. 2.6A and B). Another candidate for triggering the mitochondrial morphological change is acetic acid, but for about 4 h after the temperature upshift, there was almost no difference in the acetate concentration in the culture medium from that under the 30°C constant condition (Fig. 2.5D). Therefore, these findings imply that the mitochondrial morphological change is caused not by acetate accumulation but by exposure to ROS. Notably, given that respiratory-active fusion mitochondria may generate more ROS than fission mitochondria (Youle and van der Bliek 2012), fission mitochondria could be a beneficial form for the yeast at high temperatures in terms of keeping ROS levels low.

*K. marxianus* was able to ferment with glucose at 45°C to an extent close to that at 30ºC despite a high level of ROS and the mitochondrial morphological change. These facts led us to conduct transcriptome analysis with samples obtained under temperature upshift conditions to further understand the mechanism of survival at high temperatures and the differences between low- and high-temperature metabolisms. The highly significant response to the temperature upshift appeared to be a general heat shock, that is, the upregulation of genes for heat shock proteins and chaperones and the downregulation of genes for ribosomal proteins and rRNA processing-related metabolism (Tables S1, S4, S7, S10). Such downregulation of genes for ribosomal proteins has been reported for *Escherichia coli* at a critical high temperature (Murata

*et al*. 2011), which may be for saving energy. As a significant response, genes for the pathways of GSH biosynthesis and lipid metabolism were upregulated, and genes for the pathways of amino acid synthesis, glycolysis, the TCA cycle, oxidative phosphorylation, and the PPP were downregulated (Tables S3, S6, S9, S12). Considering the fact that the cells are able to grow and survive at 45ºC after inoculation of cells precultured at 30ºC and the fact that the tendency for the upregulation and downregulation of genes for the central metabolic pathway is in close agreement with that of a 6-h culture at 45ºC (Lertwattanasakul *et al*. 2015), such an alteration in transcription in response to a temperature upshift may reflect metabolic changes that are presumably required for the growth and survival of *K. marxianus* at 45ºC.

In mitochondrial metabolism, *ADH4a*, *ALD4,* and *ACS1* for catalysis between ethanol and acetyl-CoA and *CIT3* and *IDP1* for the TCA cycle, some of which encode enzymes to generate NADPH, were upregulated at the temperature upshift (Fig. 2.7B) or under a 6-h 45ºC constant condition (Lertwattanasakul *et al*. 2015). In the cytosol, downregulation of *RAG2*, *PFK1,* and *PFK2* and upregulation of *GLK1*, *FBP1,* and *SOL1*, most of which were significantly changed 2 h after the temperature upshift, were found (Fig. 2.7A). Especially, the strong negative and positive regulations of *RAG2* for glucose-6-phosphate isomerase and *FBP1* for fructose-1,6-diphosphatase, respectively, might have an impact on metabolic flow, nearly equivalent to that of a *RAG2* (*PGI1*)-disrupted mutant (Zhang *et al*. 2020), and lead to a reduction in the flow of glycolysis and, consequently, an increase in the flow of the PPP despite the moderately decreased expression of many genes for PPP under the temperature upshift condition. These expression changes of genes for glycolysis, the PPP, and gluconeogenesis roughly agreed with the activity changes of the corresponding enzymes tested in these pathways. In particular, the activity of fructose-1,6-diphosphatase in gluconeogenesis was increased, the activity of glucose-6-phosphate dehydrogenase in the PPP was maintained, and the activity of glyceraldehyde-3-phosphate dehydrogenase was reduced, suggesting enhanced metabolic flow to the PPP and a pentose phosphate cycle consisting of the PPP and a reverse reaction in glycolysis from glyceraldehyde-3-phosphate to glucose-6-phosphate. The switch of metabolic flow allows cells to produce NADPH as a reducing power for the removal

of ROS. On the other hand, *ALD4* in mitochondria, but not *ALD* in the cytosol, was upregulated in the temperature upshift experiments, while *ALD2* and *ALD6* in the cytosol, but not *ALD* in mitochondria, were upregulated under the 5°C constant condition, implying that mitochondrial Ald(s) and cytosolic Ald(s) are involved in the production of NADPH immediately after and shortly after a temperature rise, respectively.

*K. marxianus*, which is a Crabtree-negative species, produces a low level of ethanol in the presence of sufficient glucose under aerobic conditions in contrast to *S. cerevisiae*, which is a Crabtree-positive species (Fonseca *et al*. 2008). However, at 45°C, glucose consumption and ethanol accumulation started with a relatively high DOC, and the ethanol level became nearly equivalent to that at 30°C (Fig. 2.5). Such a Crabtree-positive-like fermentation at 45°C, at least at the beginning of fermentation (Later, DOC became very low.), may be due to the regulation of the expression of specific genes. *S. cerevisiae* produces a high level of ethanol even under aerobic conditions via the reduction of the acetyl-CoA synthetic pathway and the inhibition of pyruvate dehydrogenase (Sakihama *et al*. 2019). Similarly, *ADH2* and *ALD2* for the acetyl-CoA synthetic pathway and *PDA1* and *PDB1* for pyruvate dehydrogenase were downregulated at 45°C (Fig. 2.7A and B). This downregulation and the reduced expression of *FUM1*, *MDH1,* and *CIT2* for the TCA cycle contribute to the accumulation of pyruvate, thereby increasing ethanol production at a high temperature.

## 2.6 Conclusions

This study was conducted to understand the mechanism of thermotolerance that is distinct from that at a low temperature in *K. marxianus.* The yeast was exposed to relatively high levels of ROS at a high temperature but maintained levels of CFU for about 36 h. The accumulation of ROS up to a level that threatens cell survival may be prevented by the ROS-scavenging pathway with NADPH, which is generated mainly by the PPP in the presence of glucose and subsidiarily by the catalytic reactions of Adhs-Alds. Relatively high NADH oxidase activity and an increase in the fission form of mitochondria, which may allow dispersal inside cells, might reduce the intracellular oxygen concentration to suppress the generation of ROS. On the other

hand, maintenance of the DOC at the lowest level was observed after about 9 h at 45ºC. When glucose is consumed and the production of NADPH by the PPP ceases, catalytic reactions of Adhs-Alds may become the main NADPH supplier because of the presence of a sufficient amount of ethanol. However, insufficient oxygen and downregulation of vital genes for the TCA cycle may reduce the oxidation of acetic acid, so that acetic acid accumulation to more than a critical level. At 45°C, ethanol consumption started when glucose was almost consumed, and concomitantly, acetate accumulation was promoted (Fig. 2.1), suggesting that glucose is a crucial factor for avoiding acetic acid accumulation and CFU reduction in addition to ethanol consumption. Therefore, ethanol production by HTF for industrial applications may require maintaining at least low levels of glucose (sugar) in the medium.

# CHAPTER 3

# Evolutionary adaptation by repetitive long-term cultivation with gradual increase in temperature for acquiring multi-stress tolerance and high ethanol productivity in *Kluyveromyces marxianus* DMKU 3-1042

## 3.1 Abstract

During ethanol fermentation, yeast cells are exposed to various stresses that have negative effects on cell growth, cell survival, and fermentation ability. This study, therefore, aimed to develop *Kluyveromyces marxianus*-adapted strains that are multi-stress tolerant and to increase ethanol production at high temperatures through a novel evolutionary adaptation procedure. *K. marxianus* DMKU 3-1042 was subjected to repetitive long-term cultivation with gradual increases of temperature (RLCGT), which exposed cells to various stresses, including high temperatures. In each cultivation step, 1% of the previous culture was inoculated into a medium containing 1% yeast extract, 2% peptone, and 2% glucose, and cultivation was performed under a shaking condition. Four adapted strains showed increased tolerance to ethanol, furfural, hydroxymethylfurfural, and vanillin, and they also showed higher production of ethanol in a medium containing 16% glucose at high temperatures. One showed stronger ethanol tolerance. Others had similar phenotypes, including acetic acid tolerance, though genome analysis revealed that they had different mutations. Based on genome and transcriptome analyses, we discuss possible mechanisms of stress tolerance in adapted strains. All adapted strains gained a useful capacity for ethanol fermentation at high temperatures and improved tolerance to multi-stress. This suggests that RLCGT is a simple and efficient procedure for the development of robust strains.

## 3.2 Introduction

*Kluyveromyces marxianus* is a thermotolerant yeast that has beneficial properties for industrial ethanol fermentation, including efficient production of ethanol at high temperatures, high growth rate, short doubling times, weak glucose repression,

and the ability to assimilate various sugars, such as glucose, xylose, and sucrose, that are present in various raw materials (Limtong *et al*. 2007; Goshima *et al*. 2013; Kosaka *et al.* 2018; Nitiyon *et al.* 2016; Saini *et al.* 2017; Kosaka *et al.* 2018). Studies on *K. marxianus* have been increasing rapidly, and the high potential of *K. marxianus* for industrial applications has been reviewed (Lertwattanasakul *et al.* 2015; Nachaiwieng *et al.* 2015; Nurcholis *et al.* 2019; Kılmanoğlu *et al*. 2021; Tinôco *et al.* 2021). Among the *K. marxianus* strains studied, DMKU 3-1042, one of the most thermotolerant strains that was isolated in Thailand, has been extensively analyzed (Limtong *et al*. 2007; Rodrussamee *et al.* 2011; Nurcholis *et al.* 2019), and its complete genome sequence has been determined by transcriptomic analysis under four different growth conditions (Lertwattanasakul *et al.* 2015).

Attention has been given to bioethanol worldwide as an alternative to fossil fuels, as it is one of the cleanest and most renewable energy sources (Auesukaree 2017; Zhang *et al.* 2019). In the ethanol industry, the temperature inside fermenters rises during the fermentation process, and the increase in temperature suppresses cell growth, cell viability and ethanol production, thus increasing production costs (Auesukaree 2017; Taweecheep *et al.* 2019). Accordingly, fermenting microbes that can withstand high temperatures, such as *K. marxianus*, are beneficial and also allow high-temperature fermentation (HTF). HTF has several advantages, including reduced cooling costs, reduced risk of contamination, and reduced amounts of hydrolysis enzymes for simultaneous saccharification and fermentation (Abdel-Banat *et al.* 2010; Murata *et al.* 2015; Nuanpeng *et al.* 2016; Kosaka *et al.* 2018). It is also beneficial for fermentation in tropical countries and under global warming conditions. In addition to temperature tolerance, fermenting microbes are required to be resistant to various stressors present during fermentation, such as ethanol, acetic acid, osmotic stress, and oxidative stress (Gibson *et al*. 2007; Auesukaree 2017; Zhang *et al*. 2015). Therefore, HTF that uses stress-tolerant microbes can reduce the total cost of ethanol production, bring cheaper ethanol compared to commercial materials, and provide benefits for industrial application (Lertwattanasakul *et al.* 2015, Nurcholis *et al.* 2020).

Various strategies such as adaptation, mutagenesis, sexual breeding, and genetic engineering have been reported for the amelioration of yeast properties such as enhanced stress tolerance and ethanol production (Bro *et al*. 2006; Watanabe *et al*.

2011; Chen and Xu 2014; Pattanakittivorakul *et al*. 2019). Of these, the use of various stress adaptation techniques has resulted in improvement of the properties of several yeast strains (Nigam 2001; Cakar *et al*. 2012; Chen and Xu 2014; Zhang *et al*. 2014; Gurdo *et al.* 2017; Saini *et al.* 2017; Zhang *et al*. 2019). For example, Saini *et al*. (2017) adapted a *K. marxianus* strain to a whey permeate medium containing a high concentration of lactose for 65 days and acquired one adapted strain with an ethanol yield of 17.5%. Zhang *et al*. (2014) obtained an *S. cerevisiae* strain via a 266 nm laser radiation treatment followed by repeated cultures in the presence of ethanol, and the strain produced a larger amount of ethanol than that produced by the parental strain. In most cases, yeast cells were repeatedly subjected to short-term cultures at fixed temperatures under certain stress conditions; therefore, most adapted strains acquired predominantly a single enhanced property (see Table S15). However, since cells are exposed to various types of stress during fermentation, improvements of multiple properties are desired. Repetitive long-term cultivation with gradual increases in temperature (RLCGT) was performed by repeatedly cultivating yeast at a low temperature and then by transferring it to a higher temperature and cultivating repeatedly in the same temperature. Yeast cells can adapt to high temperatures during exposure with stepwise increased temperatures.

In this study, in order to develop a simple and effective adaptation procedure for cells to be exposed to various stressors, we examined RLCGT close to the critical high temperature for growth, which is expected to provide various stresses such as those from metabolites including ethanol or organic acids, by-products formed by chemical reactions, nutrient starvation, high temperatures, and oxidative stress in addition to large changes in substrate sugar concentration. Therefore, each cultivation step may optimize resistance to not only temperature but also to other various stresses. The adapted *K. marxianus* strains obtained by RLCGT exhibited increased tolerance to several stresses and enhanced ethanol production compared to the parental strain. Genomic and transcriptomic analyses of the strains were performed.

## 3.3 Materials and Methods

### 3.3.1 Yeast strains

*K. marxianus* DMKU 3-1042, which is a thermotolerant ethanol-fermenting yeast that was isolated in Thailand (Limtong *et al*. 2007), and its derivatives were used in this study. The yeast strains were preserved in YPD medium (10 g $L^{-1}$ yeast extract, 20 g $L^{-1}$ peptone and 20 g $L^{-1}$ glucose) supplemented with 100 g $L^{-1}$ glycerol at −80ºC.

### 3.3.2 Determination of cell growth and viability

The pre-culture was prepared by transferring a single colony of 18 h culture on a YPD agar plate into 30 mL of YPD medium in a 100 mL Erlenmeyer flask, followed by incubation in a rotary shaker at 160 rpm for 18 h at 30ºC. The pre-culture was inoculated into YPD medium or YP medium containing 160 g $L^{-1}$ glucose at the initial optical density at 660 nm ($OD_{660}$) of 0.1, and the culture was carried out at 30-47ºC under a shaking condition at 100 or 160 rpm. Cell growth was determined by measuring the $OD_{660}$ on a UV-VIS spectrophotometer (Shimadzu, Japan). Cell viability was determined as colony-forming units (CFU) by counting the number of colonies on YPD agar plates. Samples were diluted with sterile distilled water and were spread on plates, and colonies were counted after 48-h of incubation at 30ºC. Experiments were performed in triplicate.

### 3.3.3 Determination of fermentation parameters

During cultivation, samples were taken and subjected to an analysis of fermenta-tion parameters. Glucose, acetate, and ethanol were analyzed by using a high-performance liquid chromatography (HPLC) system (Hitachi, Japan) consisting of a Hitachi Model D-2000 Elite HPLC system Manager, column oven L-2130, pump L-2130, auto-sampler L-2200, and RI detector L-2490, equipped with a GL-C610H-S gel pack column at 60ºC with 0.5 mL $min^{-1}$ eluent of 0.1% phosphoric acid. pH was measured by using a twin pH meter (Horiba, Japan).

### 3.3.4 Evolutionary adaptation by RLCGT

For improvement of the stress tolerance of *K. marxianus* DMKU 3-1042, RLCGT was carried out. The pre-culture was inoculated into ten test tubes including

3 mL of YPD medium and was incubated at 40ºC and 160 rpm for 7 days. The adaption started at 40ºC because *K. marxianus* DMKU 3-1042 was found to be unable to survive under long-term cultivation at 41ºC. After that, 1% of the culture was transferred into a fresh medium (other inoculation sizes were not tested), and cultivation was repeated under the same conditions. After two cultivations at 40ºC, 1% of the culture at the second time was transferred into a fresh medium and cultivated at 41ºC and 160 rpm for 7 days. Cultivation was repeated with a gradual increase in temperature from 40ºC to 45ºC (Fig. S7). Cultivation was performed twice at each temperature. Finally, the RLCGT cultures that survived at 45ºC were streaked on YPD plates, and a single colony from each tube was isolated as an adapted strain. This method introduces random mutations and cannot reproduce the same characteristics as the improved strains.

### 3.3.5 Characterization of adapted strains

The tolerance of the adapted strains to various stresses found during the fermentation process was investigated. To prepare an inoculum, cells were grown in YPD medium at 30ºC for 18 h and recovered by low-speed centrifugation. The cells were suspended with sterile distilled water, adjusted to $OD_{660}$ of 1.0, and ten-fold sequentially diluted. Five microliters of cell suspension was spotted onto the surface of YPD agar plates supplemented with various stress materials; the agar plates were adjusted to pH 3 or supplemented with 0.3% (v/v) (52.45 mM) acetic acid, 0.1% (v/v) (26.50 mM) formic acid, 8% (1.37 M) (v/v) ethanol, 15 mM furfural, 15 mM hydroxymethylfurfural (HMF), 0.1% (w/v) (0., 70 mM) vanillin, multiple inhibitors (0.3% (v/v) acetic acid, 15 mM furfural and 0.15% (w/v) (1.05 mM) vanillin or 0.15% (v/v) (26.23 mM) acetic acid, 7.5 mM furfural and 0.075% (w/v) (0.52 mM) vanillin), 35% (w/v) (0.30 M) glucose, or 5 mM hydrogen peroxide ($H_2O_2$). YP agar plates supplemented with 10% (w/v) (0.10 M) xylose were also used. The plates after spotting were incubated at 30ºC, 37ºC, 40ºC, and 45ºC for 48 h. Moreover, growth and fermentation ability of the adapted strains were examined in YPD medium supplemented with 0.2% or 0.3% acetic acid, 10 mM or 15 mM furfural, or multiple inhibitors (0.15% acetic acid, 7.5 mM furfural and 0.075% vanillin) and/or a high

concentration of glucose (8% (0.07 M), 12% (0.10 M) or 16% (0.14 M)) at high temperatures for 6 h to 48 h. All experiments were performed in triplicate.

### 3.3.6 Preparation of genomic DNA, genomic sequencing, and genome mapping analysis

The genomic DNA of adapted strains was extracted as described previously (Sambrook and Russell 2001) from cells grown in YPD medium for 18 h under a shaking condition at 30ºC and was further purified using a Genomic-tip 20 kit (Qiagen, Hilden, Germany) according to the manufacturer's instructions. Genome sequencing was carried out by a massively parallel sequencer (MiSeq; Illumina KK, Tokyo, Japan) as reported previously (Akuzawa *et al*. 2016). The sequenced reads were screened by a quality score higher than the Phred score of 30 and were trimmed 12 bases from the 5' end and 20 bases from the 3'end. Truncated reads less than 150 bases or with mbiguous nucleotides were excluded from further analysis. Accession numbers of all sequence data are DRR305124-DRR305128.

For genome mapping analysis, the reference genome sequence of *K. marxianus* DMKU 3-1042 (GenBank acc. No: AP012213-AP012221) was downloaded from NCBI ftp site, https://ftp.ncbi.nlm.nih.gov/ (accessed on 5 March 2022). Mutation sites were searched for by read mapping using CLC Genomics Workbench version 7.5 (Qiagen, Venlo, Netherland) with the following parameters: match score: 1, mismatch cost: 2, insertion/deletion cost: 3, length fraction: 0.7, and similarity fraction: 0.9. The filter settings for SNP and Indel calling were the same as those use in a previous study (Hirokawa *et al*. 2018). All mutations in coding and non-coding regions in all adapted mutants were confirmed by the Sanger method (Sanger *et al*. 1997) after amplification of individual regions by PCR using primers listed in Table S15. Physiological functions of mutated genes were analyzed by a BLAST search at NCBI (https://www.ncbi.nlm.nih.gov (accessed on 5 March 2022)) or with the STRING database (https://string-db.org (accessed on 5 March 2022)).

### 3.3.7 RNA-Seq analysis

RNA for RNA-Seq analysis was prepared as described previously (Nurcholis *et al.* 2019). The parental and ACT001 strains were inoculated into YPD medium, and

pre-culture was carried out with a rotary shaker at 30ºC and 160 rpm for 18 h. The pre-culture was inoculated into 30 mL of YPD medium in a 100 mL Erlenmeyer flask at $OD_{660}$ of 0.1, and culture was carried out at 45ºC for 8 h under a shaking condition at 160 rpm. The cells were harvested by centrifugation at 5000 rpm for 5 min at 4ºC and subjected to an RNA preparation process. RNA was prepared by a modified procedure on the basis of the procedure reported previously (Lertwattanasakul *et al.* 2015). The RNA samples then were subjected to RNase-free DNase treatment. All RNA samples were purified by using an RNeasy plus mini kit (Qiagen, Hilden, Germany) according to the protocol provided by supplier.

The purified RNA samples were analyzed on an Illumina MiniSeq at the Research Center of Yamaguchi University. The detailed procedure for RNA-Seq has been described previously (Kim *et al*. 2013). All of the data were deposited under accession numbers DRR305122 and DRR305124. The sequencing results were analyzed using CLC genomic workbench version 10.1.1. All mapped reads at exons were counted, and the numbers were converted to unique exon reads. The unique exon reads from two biological replicates of ACT001 were compared to those of the parental strain.

Gene expression profiles of ACT001 and the parental strain were compared to find differentially expressed genes (DEGs) based on unique exon read values from CLC genomic workbench outputs using DESeq2 R package (Ander and Huber 2010). The resulting *p* values were adjusted using Benjamin–Hochberg's method for controlling the false discovery rate. Genes with adjusted *p* values less than 0.05 and $\log_2$ fold change values greater than 1 or lower than −1 were assigned as significant DEG**s.**

### 3.4 Results

#### 3.4.1 Effects of long-term cultivation on *K. marxianus* DMKU 3-1042

In general, adaptive laboratory evolution depends on selection pressure for accumulating adapted strains in the designed cultivation. In this study, as selection pressure, we used long-term cultivation at high temperatures, which provides various stressors that prevent cell growth or cause cell damage, such as organic acids excreted into the culture medium, limitation of nutrients, and high temperatures. Before the

adaptation experiments, several parameters of *K. marxianus* DMKU 3-1042 during long-term cultivation in YPD medium including 2% glucose were compared between two different temperatures for 1 week (Fig. 3.1). The results showed that cell growth and cell viability at 45°C were lower than those at 30°C. Glucose was almost completely utilized within 12 h at both temperatures (Fig. 3.1d). The maximum ethanol concentrations were 7.53 g $L^{-1}$ and 6.46 g $L^{-1}$ at 30°C and 45°C, respectively (Fig. 3.1e). During fermentation, ethanol was converted to acetic acid, and its accumulation was significantly high at 45ºC compared to that at 30ºC (Fig. 3.1f). The concentration of acetate continued to rise, reaching 5.44 g $L^{-1}$ at 168 h, consistently lowering the pH of the medium (Fig. 3.1c). The viability at 45°C approached zero at 120 h, whereas that at 30°C was maintained, though the level decreased after 120 h (Fig. 3.1b). The decline in viability at 45°C began when the pH fell below the pKa of acetic acid, a condition under which acetic acid enters cells in a non-dissociated form by facilitated diffusion, causing cytotoxicity. The production of acetic acid that causes low pH may be a major cause of reduced viability, but other factors such as high temperature, limitation of nutrients, and/or other by-product accumulation could be directly or indirectly associated with the earlier decline in cell viability at 45°C. These findings suggest that various stressors that cause a decline in viability by long-term cultivation at high temperatures are useful selection pressures for this yeast.

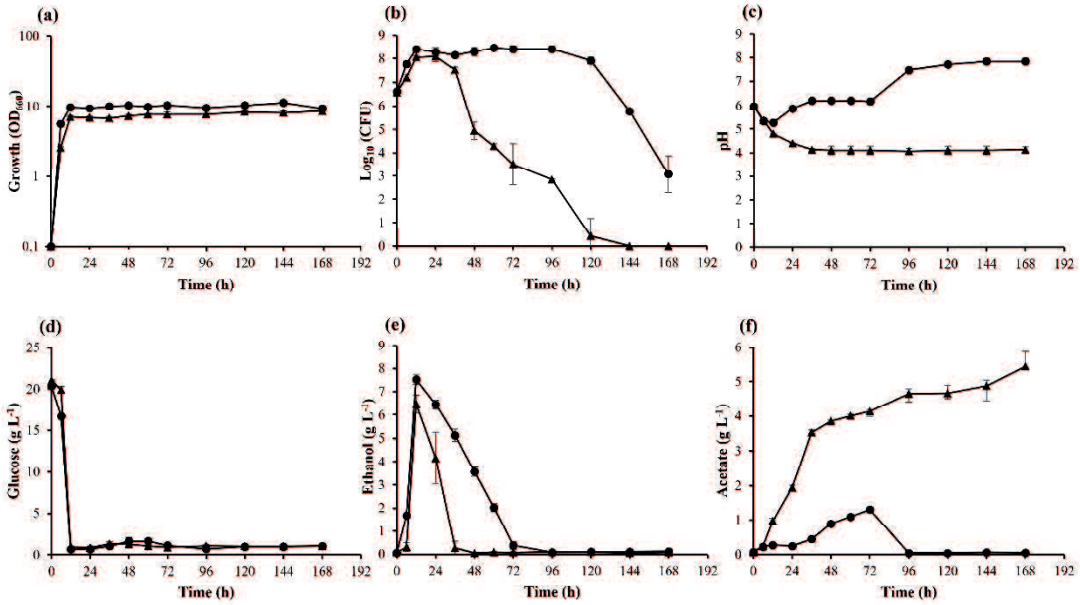


**Fig. 3.1** Growth, CFU, and fermentation parameters of *K. marxianus* DMKU 3-1042 in YPD medium at 30ºC and 45ºC. Cells were cultivated in YPD medium at 30ºC (●) and 45°C (▲) under a shaking condition at 160 rpm for 7 days. Growth (a) was determined by measuring $OD_{660}$. CFUs (b) were determined by counting colonies on YPD plates incubated at 30 °C. pH (c) was measured by using a twin pH meter. Glucose (d), ethanol (e), and acetate (f) were determined by HPLC. Error bars represent SD for triplicate experiments.

### 3.4.2 Adaptive laboratory evolution of *K. marxianus* DMKU 3-1042 by RLCGT

In order to obtain strains with multi-stress tolerance, *K. marxianus* DMKU 3-1042 was subjected to RLCGT while gradually increasing the temperature from 40°C to 45°C. Cells were inoculated into 10 tubes containing 3 mL YPD and cultivated at 40°C for 7 days, and a portion of the culture in each tube was inoculated into a tube containing fresh YPD medium, cultivated at 40ºC for 7 days, and so on (Fig. S7). For 7 days, cells were exposed to several stresses such as ethanol, acetate, other by-products, and nutrient starvation in addition to high temperature. These combinations may significantly reduce survival. The temperature was increased by 1°C every 2 weeks. No growth was observed in 6 tubes at 44°C, and no growth was observed in the remaining 4 tubes above 45ºC. After repetitive cultivation for 12 weeks, a portion of each culture in the remaining 4 tubes was spread on YPD agar plates to obtain

ACT001, ACT002, ACT003, and TML001, which were used in the following experiments.

### 3.4.3 Fermentation ability of adapted strains at high temperatures

In industrial ethanol production, heat generated by fermentation is one of the most serious problems for achieving stable and efficient fermentation. The effects of temperature on growth and fermentation parameters of the four adapted strains were thus examined in YP medium containing 160 g $L^{-1}$ glucose at 40ºC, 42ºC, 45ºC, and 47ºC (Fig. 3.2). At 40ºC and 42ºC, three adapted strains, ACT001, ACT002, and ACT003, utilized glucose almost completely within 24 h, whereas glucose remained in the culture of TML001 and the parental strain. Maximal ethanol concentrations of ACT001, ACT002, and ACT003 at 40ºC were 69.7 g $L^{-1}$, 68.5 g $L^{-1}$, and 70.3 g $L^{-1}$, respectively, whereas maximal ethanol concentrations of TML001 and the parental strain were 46.9 g $L^{-1}$ and 49.6 g $L^{-1}$, respectively. As a result of the evaporation of ethanol increasing with increasing temperature (Abdel-Banat *et al.* 2010), the amount of ethanol produced at high temperatures may be underestimated. At higher temperatures of 45ºC, and 47ºC, glucose in the medium remained even in ACT strains after 48 h of fermentation, and the four adapted strains produced higher ethanol concentrations than that produced by the parental strain. Maximal ethanol concentrations produced by these strains were in the range of 41.5–56.2 g $L^{-1}$ (Table 3.1). At 42ºC, and 45ºC, higher ethanol concentrations and lower acetate accumulation were achieved by the four adapted strains in comparison to the parental strain. The ethanol productivities and ethanol yields of ACT001, ACT002, and ACT003 were almost the same at each temperature and were higher than or equal to those of TML001 (Table 3.1).

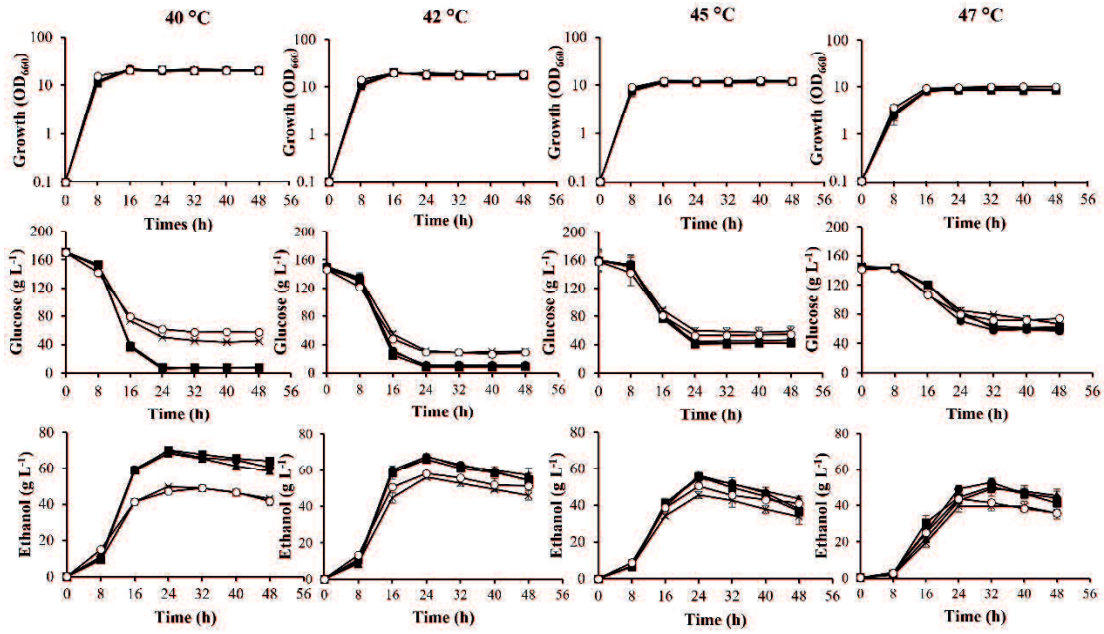


**Fig. 3.2** Fermentation of adapted strains in YP medium containing 16% glucose at high temperatures. Wild-type (×), ACT001 (●), ACT002 (▲), ACT003 (■), and TML001 (○) strains were cultivated in YP medium containing 16% glucose at 40-47 ºC under a shaking condition at 100 rpm, and samples were taken every 8 h until 48 h. Growth was determined by measuring $OD_{660}$. Glucose, ethanol, and acetate were determined by HPLC. Error bars represent SD for triplicate experiments.

**Table 3.1** Comparison of growth and fermentation parameters among various adapted strains and previously reported strains

| Strains | Temp. (°C) | Medium | Cultivation Time (h) | Growth ($OD_{660}$) | Remaining Sugar (g $L^{-1}$) | Acetic Acid Accumulation (g $L^{-1}$) | Ethanol Production (g $L^{-1}$) | Increased Ethanol (%) | Ethanol Productivity (g $L^{-1}$ $h^{-1}$) | Ethanol Yield (g $g^{-1}$) | Ref |
|---|---|---|---|---|---|---|---|---|---|---|---|
| *K. marxianus* DMKU 3-1042 | | | | | | | | | | | |
| Wild-type | 40 | YP + 160 g $L^{-1}$ glucose | 24 | 19.0 ± 0.8 | 50.1 ± 1.2 | 1.7 ± 0.1 | 49.6 ± 0.7 | - | 2.1 ± 0.0 | 0.3 ± 0.0 | This study |
| ACT001 | 40 | YP + 160 g $L^{-1}$ glucose | 24 | 19.4 ± 0.7 | 7.3 ± 2.4 | 1.5 ± 0.1 | 69.7 ± 0.7 | 40 | 2.9 ± 0.0 | 0.4 ± 0.0 | This study |
| ACT002 | 40 | YP + 160 g $L^{-1}$ glucose | 24 | 20.3 ± 1.2 | 5.8 ± 2.0 | 1.5 ± 0.0 | 68.5 ± 0.7 | 38 | 2.9 ± 0.0 | 0.4 ± 0.0 | This study |
| ACT003 | 40 | YP + 160 g $L^{-1}$ glucose | 24 | 20.7 ± 1.0 | 8.1 ± 0.4 | 1.5 ± 0.0 | 70.3 ± 0.7 | 42 | 2.9 ± 0.0 | 0.4 ± 0.0 | This study |
| TML001 | 40 | YP + 160 g $L^{-1}$ glucose | 24 | 20.7 ± 0.9 | 61.5 ± 0.4 | 1.3 ± 0.1 | 46.9 ± 0.7 | 0 | 2.0 ± 0.1 | 0.3 ± 0.0 | This study |
| Wild-type | 42 | YP + 160 g $L^{-1}$ glucose | 24 | 19.6 ± 1.1 | 31.2 ± 2.2 | 1.7 ± 0.1 | 56.1 ± 1.1 | - | 2.3 ± 0.1 | 0.4 ± 0.0 | This study |
| ACT001 | 42 | YP + 160 g $L^{-1}$ glucose | 24 | 17.5 ± 1.3 | 11.3 ± 1.1 | 1.4 ± 0.0 | 67.6 ± 0.3 | 20 | 2.8 ± 0.0 | 0.4 ± 0.0 | This study |
| ACT002 | 42 | YP + 160 g $L^{-1}$ glucose | 24 | 17.5 ± 0.9 | 8.7 ± 1.4 | 1.5 ± 0.0 | 67.9 ± 1.2 | 21 | 2.8 ± 0.0 | 0.4 ± 0.0 | This study |
| ACT003 | 42 | YP + 160 g $L^{-1}$ glucose | 24 | 17.0 ± 0.8 | 8.8 ± 1.4 | 1.5 ± 0.0 | 66.2 ± 1.0 | 18 | 2.8 ± 0.0 | 0.4 ± 0.0 | This study |
| TML001 | 42 | YP + 160 g $L^{-1}$ glucose | 24 | 17.9 ± 1.2 | 29.0 ± 0.8 | 1.3 ± 0.0 | 58.1 ± 0.4 | 3 | 2.4 ± 0.0 | 0.4 ± 0.0 | This study |
| Wild-type | 45 | YP + 160 g $L^{-1}$ glucose | 24 | 12.1 ± 0.6 | 59.5 ± 4.0 | 1.6 ± 0.0 | 45.5 ± 1.8 | - | 1.9 ± 0.1 | 0.3 ± 0.0 | This study |
| ACT001 | 45 | YP + 160 g $L^{-1}$ glucose | 24 | 11.3 ± 0.5 | 44.5 ± 2.0 | 1.4 ± 0.0 | 54.5 ± 3.0 | 20 | 2.3 ± 0.1 | 0.3 ± 0.0 | This study |
| ACT002 | 45 | YP + 160 g $L^{-1}$ glucose | 24 | 11.9 ± 1.0 | 42.8 ± 1.6 | 1.4 ± 0.0 | 56.2 ± 1.8 | 23 | 2.3 ± 0.1 | 0.4 ± 0.0 | This study |
| ACT003 | 45 | YP + 160 g $L^{-1}$ glucose | 24 | 11.6 ± 0.6 | 41.4 ± 1.6 | 1.4 ± 0.1 | 55.4 ± 2.0 | 22 | 2.3 ± 0.1 | 0.4 ± 0.0 | This study |
| TML001 | 45 | YP + 160 g $L^{-1}$ glucose | 24 | 12.2 ± 0.7 | 52.9 ± 2.3 | 1.4 ± 0.0 | 50.3 ± 1.7 | 11 | 2.1 ± 0.1 | 0.3 ± 0.0 | This study |
| Wild-type | 47 | YP + 160 g $L^{-1}$ glucose | 32 | 9.3 ± 1.1 | 78.9 ± 1.6 | 1.9 ± 0.1 | 39.5 ± 2.8 | - | 1.2 ± 0.1 | 0.3 ± 0.0 | This study |
| ACT001 | 47 | YP + 160 g $L^{-1}$ glucose | 32 | 8.9 ± 0.9 | 57.8 ± 1.4 | 1.8 ± 0.2 | 52.6 ± 2.5 | 33 | 1.7 ± 0.1 | 0.3 ± 0.0 | This study |
| ACT002 | 47 | YP + 160 g $L^{-1}$ glucose | 32 | 9.0 ± 0.7 | 60.2 ± 3.2 | 1.8 ± 0.1 | 49.0 ± 3.8 | 24 | 1.5 ± 0.1 | 0.3 ± 0.0 | This study |
| ACT003 | 47 | YP + 160 g $L^{-1}$ glucose | 32 | 8.5 ± 0.5 | 63.5 ± 1.3 | 1.7 ± 0.1 | 50.2 ± 1.8 | 27 | 1.6 ± 0.1 | 0.3 ± 0.0 | This study |
| TML001 | 47 | YP + 160 g $L^{-1}$ glucose | 32 | 10.0 ± 0.8 | 71.4 ± 2.0 | 1.8 ± 0.1 | 41.5 ± 1.7 | 5 | 1.3 ± 0.1 | 0.3 ± 0.0 | This study |
| *S. cerevisiae* G85 | 28 | Sugar juice (207.25 g $L^{-1}$ sugar) | 480 | NR | 10.4 ± 0.8 | NR | 126.6 ± 5.6 | - | 0.3 | 0.6 | Chen and Xu 2014 |
| *S. cerevisiae* G85X-8 | 28 | Sugar juice (207.25 g $L^{-1}$ sugar) | 480 | NR | 7.0 ± 1.0 | NR | 130.0 ± 4.5 | 3 | 0.3 | 0.6 | Chen and Xu 2014 |
| *S. cerevisiae* YE0 | 34 | YP + 300 g $L^{-1}$ glucose + 50 g $L^{-1}$ ethanol | 72 | NR | 31.5 | NR | 106.8 | - | 1.5 | 0.4 | Zhang *et al*. 2014 |
| *S. cerevisiae* SM4 | 34 | YP + 300 g $L^{-1}$ glucose + 50 g $L^{-1}$ ethanol | 72 | NR | 2.1 | NR | 138.1 | 29 | 1.9 | 0.5 | Zhang *et al*. 2014 |
| *K. marxianus* MTCC1389 (Wild-type) | 37 | Whey permeate (200 g $L^{-1}$ lactose) | 50 | NR | 0.7 ± 0.0 | NR | 66.8 ± 0.9 | - | 1.3 ± 0.0 | 0.3 ± 0.0 | Saini *et al*. 2017 |
| *K. marxianus* MTCC1389 (Adapted strain) | 37 | Whey permeate (200 g $L^{-1}$ lactose) | 42 | NR | 0.8 ± 0.0 | NR | 79.3 ± 0.8 | 19 | 1.7 ± 0.1 | 0.4 ± 0.1 | Saini *et al*. 2017 |
| *S. cerevisiae* Y-1 | 30 | Fermentation medium (350 g $L^{-1}$ glucose) | 60 | NR | 75.7 | NR | 125.0 | - | 2.1 ± 0.0 | 0.3 | Zhang *et al*. 2019 |
| *S. cerevisiae* YF10-5 | 30 | Fermentation medium (350 g $L^{-1}$ glucose) | 60 | NR | 5.5 | NR | 145.8 | 16.6 | 2.43 ± 0.1 | 0.4 | Zhang *et al*. 2019 |

### 3.4.4 Characterization of the adapted strains

During the fermentation process, yeast cells are exposed to various stresses that have negative effects on cell viability and ethanol production (Gibson *et al*. 2007; Auesukaree 2017; Pattanakittivorakul *et al*. 2019), and it is desirable that yeast cells are resistant to these stresses. We thus compared the stress tolerance of the four adapted strains that had experienced stressful conditions during the adaptation process with that of the parental strain (Fig. 3.3). Their growth was examined on YPD agar plates supplemented with 0.3% (v/v) acetic acid, 0.1% (v/v) formic acid, or an adjusted pH of 3 at different temperatures up to 45°C. ACT001, ACT002, and ACT003 grew well except for in 0.3% (v/v) acetic acid at 45ºC, but TML001 and the pa-rental strain did not grow (Fig. 3.3a). When examined on YPD agar plates supplemented with 8% (v/v) ethanol, which also inhibits cell growth (Chen and Xu 2014), all of the adapted strains grew better than did the parental strain at 40°C, and TML001 showed much stronger growth (Fig. 3.3b). When examined on YPD agar plates supplemented with 15 mM furfural or 15 mM HMF, which are inhibitors found in lignocellulosic hydrolysate and browning reaction products (Modig *et al*. 2002; Gurdo *et al*. 2018), all of the adapted strains grew better than did the parental strain at 40ºC and 45ºC (Fig. 3.3b). The tolerance to vanillin as a phenolic compound (Hemansi *et al.* 2022) was also examined, showing that all adapted strains were more resistant to 0.1% (w/v) vanillin than the parental strain (Fig. 3.3c).

Further experiments were carried out with a YPD liquid medium supplemented with 0.2% (v/v) and 0.3% (v/v) acetic acid under a shaking condition at 40ºC. In the case of 0.2% (v/v) acetic acid, ACT001, ACT002, and ACT003 showed much better growth than that of TML001 and the parental strain, and they completely utilized glucose and produced the highest concentration of ethanol within 12 h, whereas TML001 and the parental strain completely utilized glucose and produced the highest concentration of ethanol at 48 h. In the case of 0.3% (v/v) acetic acid, only ACT strains grew and utilized glucose and produced ethanol (Fig. 3.4). These results are consistent with the results of the above-described experiments using agar plates, indicating that ACT strains are resistant to acetic acid. Moreover, all adapted strains except ACT002 showed better growth and ethanol production than the parental strain in a YPD medium supplemented with 10 mM furfural at 45 °C (Fig. S8). These results combined with

the results obtained from experiments with formic acid, furfural, and HMF suggest that the adapted strains have acquired abilities to withstand multiple stressors.

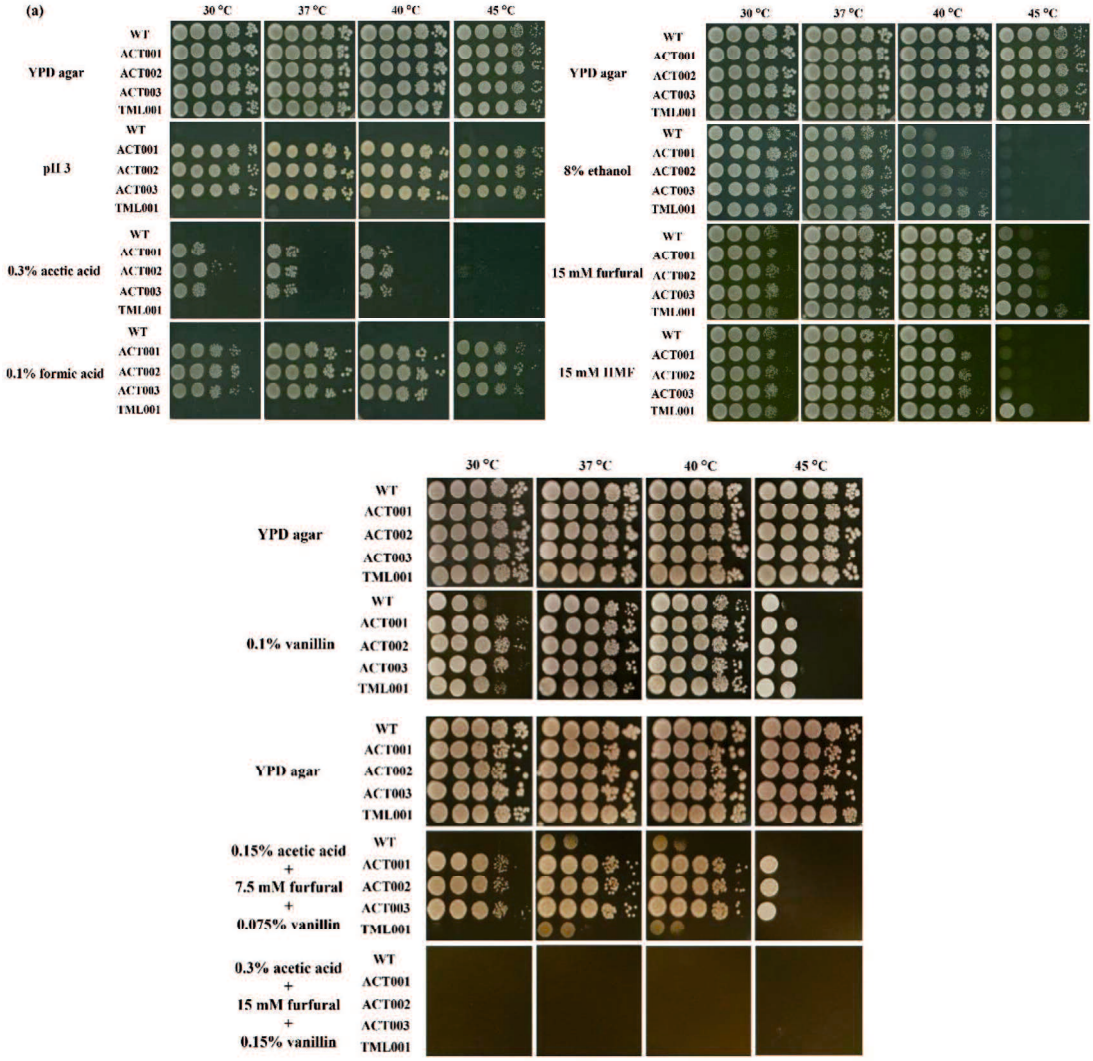


**Fig. 3.3** Characterization of adapted strains. Growth of adapted strains on YPD agar plates with pH adjusted to 3 or supplemented with 0.3% acetic acid, 0.1% formic acid (a), 8% ethanol, 15 mM furfural, 15 mM HMF (b), 0.1% vanillin or multiple inhibitors (0.15% acetate, 7.5 mM furfural and 0.075% vanillin or 0.3% acetate, 15 mM furfural and 0.15% vanillin) (c) were compared. The plates were incubated at 30-45°C for 48 h.

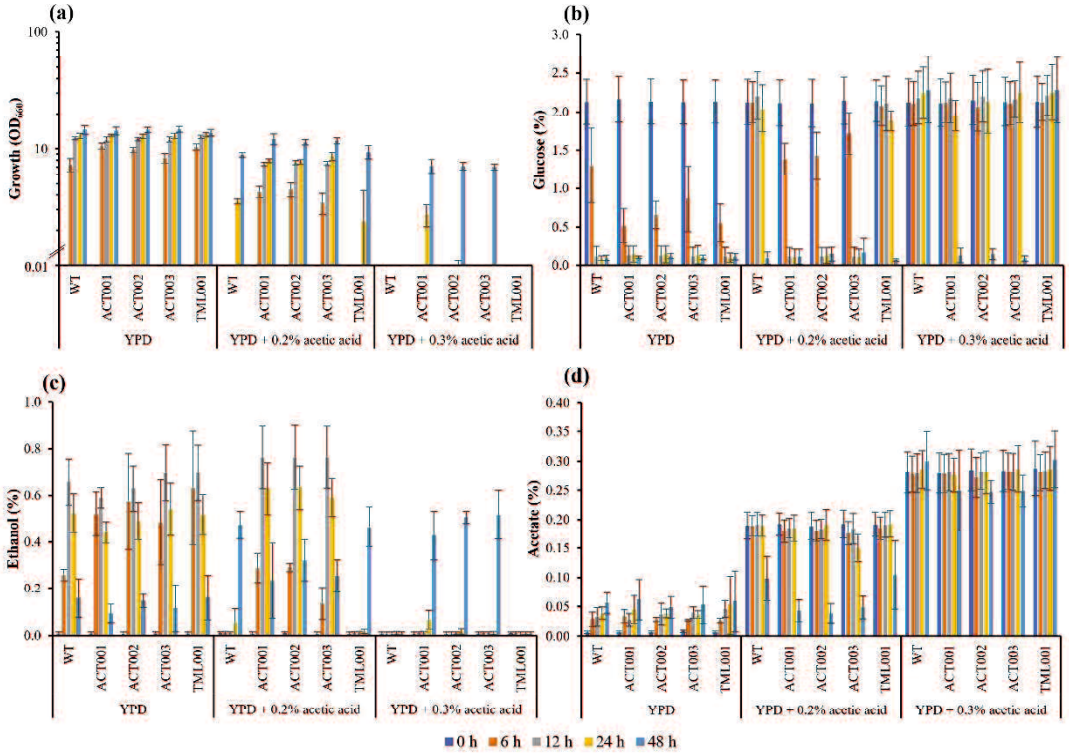


**Fig. 3.4** Effects of acetic acid on growth and fermentation parameters of adapted strains at 40°C. Adapted strains were cultivated in YPD medium supplemented with 0.2% or 0.3% acetic acid at 40°C under a shaking condition at 160 rpm for 48 h. Growth (a) was determined by measuring $OD_{660}$. Glucose (b), ethanol (c), and acetate (d) were determined by HPLC. Error bars represent SD for triplicate experiments.

Considering that the stresses in biofuel production from lignocellulosic biomass are synergistic, the effects of multiple inhibitors including acetate, furfural, and vanillin were examined (Fig. 3.3c). The synergistic effects of inhibitors were seen when each inhibitor in the experiments with multiple inhibitors was added at the same concentration as used in the experiments with a single inhibitor (Fig. 3.3a and b). Under these conditions, all the adapted strains did not grow. However, when the concentrations of inhibitors were reduced, all adapted strains except for TML001 grew, but the parental strain did not grow at 30°C and 45°C. These findings suggest that ACTs have acquired resistance to multiple stresses. Furthermore, ACT003, which was most tolerant to acetic acid (Fig. 3.4) and furfural (Fig. S8), was subjected to

fermentation experiments in a YPD medium containing 0.15% acetate, 7.5 mM furfural, and 0.075% vanillin in the presence of 8-16% glucose at 40°C (Fig. S9). ACT003 showed much better growth and ethanol production than the parental strain.

To examine the effects of osmotic stress and oxidative stress, which are known to accumulate in cells at high temperatures (Zhang *et al*. 2015), growth experiments were carried out on YP agar plates supplemented with 10% (w/v) xylose or 35% (w/v) glucose and supplemented with 5 mM $H_2O_2$. In the former experiments, the growth of all the adapted strains was almost the same as that of the parental strain, except that the growth of TML001 was weaker in the presence of 35% glucose at 45ºC (Fig. S10). Additionally, in the latter experiments, ACT strains exhibited a level of growth similar to that of the parental strain, but the growth of TML001 was slightly weaker at 45°C (Fig. S10).

### 3.4.5 Mutation points of adapted strains

Next-generation sequencing was performed to find mutations in the four adapted strains, and candidate mutations were further confirmed by direct sequencing. The results showed that ACT001, ACT002, ACT003, and TML001 strains have two, four, one, and seven mutation points, respectively (Table 3.2). There were no shared mutations in ACT strains, though they exhibited a similar tolerance phenotype against several stresses tested. The two mutations in ACT001 are the following: the insertion of one nucleotide in the coding region of *KLMA_10738* for a PH domain-containing protein as an orthologue of YHR131C in *S. cerevisiae*, causing a frame shift mutation, and the deletion of one nucleotide in the non-coding region. All mutations in ACT002 and ACT003 are single nucleotide polymorphisms (SNPs) either in the coding or non-coding regions, causing one missense and two synonymous mutations in the case of ACT002. The missense mutation occurs in *GAL1* for galactokinase, and the synonymous mutations occur in *ALY2* for UPF0675 protein as an orthologue of YJL084C in *S. cerevisiae* and in *KLMA_40563* for ATP-dependent protease La. YHR131C contains a PH domain that occurs in a wide range of proteins involved in

intracellular signaling or as constituents of the cytoskeleton (Ingley and Hemmings 1994; Saraste *et al*. 1995; Breslow *et al*. 2008; Ren *et al*. 2016). There are six SNPs and one triple-nucleotide insertion in TML001. Of these, four are missense or nonsense mutations in coding regions, and one causes a single amino acid insertion. The missense mutations occur in *FSH3* for the family of serine hydrolase 3 and in *TNA1* for a high-affinity nicotinic acid transporter; the nonsense mutations occur in *KLMA_40326* for an orthologue of YPL014W in *S. cerevisiae* and in *SVL3* for styryl dye vacuolar localization protein 3; and the amino acid insertion mutation occurs in *PMA1* for plasma membrane ATPase. YPL014W (Cip1) is a novel negative regulator of cyclin-dependent kinase (Ren *et al*. 2016).

### 3.4.6 Transcriptome analysis

The three strains ACT001, ACT002, and ACT003 had similar phenotypes of multi-stress tolerance and higher ethanol production but had obtained distinct mutations, indicating that it is difficult to understand the mechanism of expression of similar phenotypes only by genome mutation analysis. We thus carried out transcriptome analysis of ACT001 as a representative strain and of the parental strain as a control by RNA-Seq using total RNAs prepared from cells grown in a YPD medium at 45ºC for 8 h. Reads per kilobase of exon per million (RPKM) of each gene were estimated as a transcript abundance. The difference of each gene in ACT001 strain from that in the parental strain was reflected as the ratio of the RPKM value in ACT001 strain to that in the parental strain. To further explore the transcriptional changes, analysis of differentially expressed genes (DEGs) based on the RNA-Seq data was conducted. DEGs showed significant changes at the transcription level with $\log_2$ fold change > 1 and $\log_2$ fold change < −1. A total of 7 genes were significantly up-regulated in ACT001 strain (Table 3.3), and 10 genes were significantly down-regulated (Table 3.3).

**Table 3.2** Summary of mutations of adapted strains

| Adapted Strain | Gene/Locus_Tag | Product | Region | Ref | Allele | Type | Amino Acid Change |
|---|---|---|---|---|---|---|---|
| ACT001 | KLMA_10738 | PH domain-containing protein Orthologue of YHR131C | 1552906^1552907 | - | G | Insertion | Lle812fs |
| | | | 47658 | T | - | Deletion | Non-coding region |
| ACT002 | | | 1161817 | G | A | SNP | Non-coding region |
| | GAL1 | Galactokinase | 712698 | G | T | SNP | Lue391Phe |
| | ALY2 | UPF0675 protein Orthologue of YJL084C | 385614 | G | A | SNP | synonymous |
| | KLMA_40563 | ATP-dependent protease La | 1269738 | T | C | SNP | synonymous |
| ACT003 | | | 1107715 | T | C | SNP | Non-coding region |
| TML001 | FSH3 | Family of serine hydrolase 3 | 613476 | C | G | SNP | Lle253Met |
| | PMA1 | Plasma membrane ATPase | 968552^968553 | - | GCT | Insertion | Ala255_Leu256insAla |
| | TNA1 | High-affinity nicotinic acid transporter | 1010140 | C | G | SNP | Phe467Leu |
| | | | 1714543 | G | A | SNP | Non-coding region |
| | KLMA_40326 | Hypothetical protein Orthologue of YPL014W | 767036 | G | T | SNP | Glu106 * |
| | | | 724738 | T | G | SNP | Non-coding region |
| | SVL3 | Styryl dye vacuolar localization protein 3 | 815396 | C | A | SNP | Ser629 * |

SNPs: Single nucleotide polymorphisms; fs: frame-shift mutation; * stop codon.

**Table 3.3** Up-regulated ($log_2 > 1$) and down-regulated ($log_2 < -1$) genes in ACT001 strain

| Locus_Tag | Gene | $Log_2$ Fold Change | Product |
|---|---|---|---|
| **Up-regulated** | | | |
| KLMA_70179 | *ICL1* | 1.90 | Isocitrate lyase |
| KLMA_70444 | *CIT3* | 1.43 | Citrate synthase 3 |
| KLMA_30101 | *SPG4* | 1.24 | stationary phase protein 4 |
| KLMA_20819 | *KLMA_20819* | 1.20 | hypothetical protein |
| KLMA_60471 | *RRT12* | 1.12 | putative subtilase-type proteinase YCR045C |
| KLMA_60452 | *FBP1* | 1.08 | fructose-1,6-bisphosphatase |
| KLMA_20009 | *ADY2_1* | 1.04 | acetate transporter |
| **Down-regulated** | | | |
| KLMA_50379 | *HAK1* | −1.99 | high-affinity potassium transporter |
| KLMA_50489 | *ZRT2* | −1.39 | zinc-regulated transporter 2 |
| KLMA_10655 | *CDR4* | −1.37 | ATPase-coupled transporter |
| KLMA_50332 | *SEO1* | −1.33 | probable transporter SEO1 |
| KLMA_10677 | *MET17* | −1.18 | protein MET17 |
| KLMA_30339 | *KLMA_30339* | −1.17 | ATP synthase subunit b |
| KLMA_30724 | *SNZ3* | −1.17 | pyridoxal-5′-phosphate synthase |
| KLMA_30338 | *KLMA_30338* | −1.08 | protein ICY2 |
| KLMA_60029 | *ACAD11* | −1.01 | acyl-CoA dehydrogenase family member 11 |
| KLMA_30726 | *SNO3* | −1.00 | probable pyridoxal-5′-phosphate synthase subunit |

Each strain was performed in duplicate.

Of the significantly up-regulated genes (Table 3.3), *ICL1*, *CIT3*, and *ADY2* may be related to acetic acid tolerance by maintaining a low level of intracellular acetate. The former two genes enhance the TCA cycle or glyoxylate cycle to assimilate acetic acid, and the latter exports acetate. Consistent with the assimilation enhancement, the acetate accumulation level in ACT001 was lower than that in the parental strain at high temperatures (Fig. 3.2). *ICL1* encodes isocitrate lyase, which catalyzes the cleavage of isocitrate to succinate and glyoxylate and which is a key enzyme for the glyoxylate cycle to utilize two carbon compounds, such as acetate (Paik *et al*. 2019). *CIT3* encodes the dual specificity mitochondrial citrate and methylcitrate synthase, which catalyzes the condensation of acetyl-CoA and oxaloacetate to form citrate, and which catalyzes that of propionyl-CoA and oxaloacetate to form 2-methylcitrate, respectively, in *S. cerevisiae* (Graybill *et al*. 2007). *ADY2* is an acetate transporter that has a key role in acetic acid sensitivity, and disruption of *ADY2* abolishes the active transport of acetate in *S. cerevisiae* (Paiva *et al*. 2004). The up-

regulation of *ADY2* may reduce the intracellular acetate level. Therefore, it is possible that the enhanced expression of these three genes is responsible for acid tolerance in ACT001. Given that three ACT mutants exhibited similar levels of acetic acid tolerance and similar glucose utilization patterns at high temperatures, ACT002 and ACT003 can enhance the TCA cycle or glyoxylate cycle as well as export the activity of acetate.

Four genes, *HAK1*, *ZRT2*, *CDR4*, and, for transporters including a high-affinity potassium transporter, a low-affinity zinc transporter, an ATPase-coupled transporter, and a putative allantoate transporter were down-regulated. Two genes, *SNZ3* and *SNO3*, for probable pyridoxal 5′-phosphatae biosynthesis were also down-regulated. The relationship between these negative regulations and stress resistance is not clear.

### 3.5 Discussion

There are many reports showing improvement of yeasts via evolutionary adaptation (Nigam 2001; Chen and Xu 2014; Zhang *et al*. 2014; Gurdo *et al*. 2017; Saini *et al*. 2017; Sharma *et al*. 2017; Kim *et al*. 2019; Zhang *et al*. 2019). In most of them, cells were exposed to a single stress, for example, a high concentration of ethanol, by repetitive cultivation in a short cycle, such as 1 to 2 days at a fixed temperature (Table S16). The procedure applied in this study is relatively simple and not laborious because of the transfer to a fresh medium once a week, which gives a chance to enrich multi-stress-resistant mutants and to obtain characteristically different mutants if cultivated in multiple test tubes. We successfully acquired 4 different mutants from cultivation with 10 test tubes in this study.

Long-term cultivation causes nutrient starvation and toxic compounds to accumulate in the medium. *K. marxianus* DMKU 3-1042 was found to accumulate acetate at high temperatures (Fig. 3.1), which may be responsible for a marked decrease in cell viability after 36 h. It suggests that this yeast tends to convert ethanol to acetic acid and/or has a weak metabolism with acetic acid at high temperatures. High temperatures may be not a primary factor affecting cell viability because it can

grow even at 48°C (Abdel-Banat *et al*. 2010), but high temperatures may lead to the accumulation of acetate. On the other hand, the accumulation of acetic acid is relatively low at low temperatures, and the decline of cell viability after 120 h could be due to limitation of nutrients. Therefore, the acquisition of acetic acid resistant mutants of ACTs at high temperatures is reasonable. Notably, the accumulation levels of acetate were lower than that of the parental strain in the medium containing 160 g $L^{-1}$ of glucose at 40°C to 45°C. Given the high ethanol production in ACT mutants, their ethanol-to-acetic acid conversion activity may be relatively low, or acetic acid metabolic activity may be high as expected from the results of the transcriptome analysis. TML001, which is sensitive to acetic acid like the parental strain, may have a distinct strategy for survival in the presence of acetic acid. The mutant somehow kept a lower level of acetate compared to the other adapted mutants as seen in the medium containing 160 g $L^{-1}$ of glucose at 40°C to 45°C. Notably, *K. marxianus* DMKU 3-1042 as well as adapted strains exhibited a stronger resistance to high temperatures (up to 48°C) on agar plates (Abdel-Banat *et al*. 2010). It is assumed that only the surface cells of colonies on agar plates are exposed to oxidative stress, which increases with rising temperature (Cuny *et al*. 2007), and individual cells in liquid media are directly exposed to the stress. The thermal stability of *K. marxianus* DMKU 3-1042 is one of the most important application criteria for different applications, and this property is crucial for the preparation strategy of the strain or its stabilization. The stability of *K. marxianus* DMKU 3-1042 is beneficial for a wide range of applications in synthesis processes, which currently are in great demand from the industrial point of view (Lertwattanasakul *et al*. 2022; Nurcholis *et al*. 2020).

By RLCGT, adapted mutants were acquired at a relatively high frequency (4 mutants/10 tubes). One of the reasons may be a significant reduction in viability at each 7-day cultivation step. Gradual rising temperatures may reduce survival because, in addition to temperature stress, higher temperatures tend to accumulate more reactive oxygen species (ROS) that damage cells (Kosaka *et al*. 2018; Nurcholis *et al*. 2020). The combinations of various stresses including acetic acid, high temperatures, ROS, ethanol, and other by-products are thought to influence viability, resulting in enrichment of adapted mutants. The other may be due to the gradual accumulation of

ethanol, acetic acid, and other by-products at each long-term cultivation step. The high acquisition frequency of adapted mutants and their enhanced capacity of ethanol fermentation at high temperatures demonstrate the usefulness of RLCGT for evolutionary adaptation. This procedure can be applied to improve other microbes once the initial temperature for RLCGT is properly determined. Recently, *Candida tropicalis* X-17 was subjected to RLCGT in the presence of a high concentration of glucose, and the resultant adapted strain increased ethanol production and improved multi-stress tolerance (Phommachan *et al.* 2022).

Spontaneous mutations occur during cultivation, and some of the mutations contribute to adaptation to environmental conditions. Such adaptations are also accompanied by phenotypic alterations (Saini *et al.* 2017; Pereira *et al*. 2018). In this study, all of the adapted strains exhibited phenotypes of resistance to furfural, HMF, and vanillin in addition to ethanol or acetic acid. The phenotypes were stable rather than transient, which may be conferred by underlying mutations, unlike an adaptive response and tolerance to stress encountered during ethanol fermentation (Kim *et al*. 2013; Auesukaree 2017). ACT strains were clearly tolerant to acetic acid, formic acid, and low pH compared to TML001 and the parental strain (Fig. 3.3). Acetic acid resistance may have promoted glucose assimilation and ethanol production more than the parental strain (Fig. 3.2). One to seven mutations in coding or non-coding regions were found in the adapted strains, some of which may be responsible for altered phenotypes. Unfortunately, the mutations in the adapted strains were different, and mutations responsible for the common phenotypes were therefore not identified. Mutations causing drastic alterations in protein structure could be related to adaptations under stress conditions, including the frame-shift mutation of *KLMA_10738* in ACT001 and the nonsense mutations of *KLMA_40326* and *SVL3* in TML001. Null mutants of their orthologue genes, *YHR131C*, *YPL014W*, and *SVL3*, in *S. cerevisiae* exhibited an increase in competitive fitness in minimum medium (Breslow *et al*. 2018), and a resistance to oxidative stress (Helsen *et al*. 2020), respectively. Therefore, it is assumed that the accumulation of some mutations except for ACT003, not only in coding regions but also non-coding regions, is responsible for

a phenotype such as acetic acid resistance. In the future, it is necessary to confirm stress tolerance by constructing individual mutations in the wild-type background.

Nonetheless, transcriptome analysis suggests possible mechanisms of acetic acid tolerance in ACT001 as mentioned above, though the relationship between its genomic mutations and acetic acid tolerance is unclear. Like these adapted strains, adapted strains with multi-stress tolerance were previously isolated in *S. cerevisiae* (Chen and Xu 2014; Zhang *et al*. 2019). The mechanism of multi-stress tolerance may be complicated, given previous evidence which suggests that many genes are involved in certain stress resistances (Dhar *et al*. 2011), that genes required for specific stress tolerance contribute to other stress resistances (Berry *et al.* 2011), and that the integration of selected genes can improve tolerance to multiple inhibitors in lignocellulose fermentations (Brandt *et al.* 2021).

No direct association between up-regulation of those three genes and mutations in ACT001 can be found in the literature or databases. ACT001 was suggested to have two mutations: a frame-shift mutation in KLMA_10738 for the Pleckstrin homology (PH) domain-containing protein and an SNP in the non-coding region (Table 3.2). PH domains are small protein modules known for their ability to bind to phosphoinositides, and they are involved in intracellular signaling or in being constituents of the cytoskeleton (Ingley and Hemmings 1994; Saraste and Hyvönen 1995; Yu *et al*. 2004; Breslow *et al*. 2008). The STRING database indicates that *YHR131C* in *S. cerevisiae*, which is the orthologue of *KIMA_10738* in *K. marxianus*, interacts with 10 proteins, including a putative transcription factor required for growth of superficial pseudohyphae. Therefore, it is speculated that the defective mutation of *KLMA_10738* is directly or indirectly related to stress resistance and/or the up-regulation of *ICL1*, *CIT3*, and *ADY2* in ACT001. Further works are needed in the future, including the disruption of *KLMA_10738* and its effects on the expression of these genes, and including the overexpression of these genes and their effects on acetic acid and other stress tolerances.

The four mutants obtained in this study produced higher ethanol concentration than the parental strain in a YP medium containing 160 g $L^{-1}$ at high temperatures

under a shaking condition, which provided oxygen and avoided aggregations of cells. Ethanol concentrations in ACT mutants increased by about 20-40% of that of the parental strain (Table 3.1). The increment was consistent with greater consumption of glucose compared to that of the parental strain. The ratios of increase in ethanol production are higher than or equivalent to those of adapted mutants in several reports. The ratios of increase in ethanol concentration in *S. cerevisiae* SM4 adapted in a YP medium containing 300 g $L^{-1}$ glucose and 50 g $L^{-1}$ ethanol at 34°C, an adapted strain from *K. marxianus* MTCC1389 in whey permeate containing 200 g $L^{-1}$ lactose at 37°C, and *S. cerevisiae* YF10-5 adapted in a fermentation medium containing 350 g $L^{-1}$ glucose at 30°C, were in the range of 16.6% to 29.3% (Zhang *et al*. 2014; Saini *et al*. 2017; Zhang *et al*. 2019) Therefore, the adaptation procedure used in this study may allow efficient improvement of ethanol productivity at high temperatures.

## 3.6 Conclusions

This study showed that (1) RLCGT is an effective evolutionary adaptation procedure and provided evidence that (2) adapted strains have the ability to achieve high ethanol concentrations at high temperatures and are (3) capable of tolerating multiple stresses, especially ACT strains, which are strongly resistant to acetic acid and formic acid. These beneficial properties are useful for industrial ethanol fermentation using lignocellulosic biomass as a substrate.

## REFERENCES


Abbott DA, Zelle RM, Pronk JT, van Maris AJ. 2009. Metabolic engineering of *Saccharomyces cerevisiae* for production of carboxylic acids: current status and challenges. FEMS Yeast Res. 9:1123-1136. https://doi.org/10.1111/j.1567-1364.2009.00537.x.

Abdel-Banat BA, Hoshida H, Ano A, Nongklang S, Akada R. 2010. High-temperature fermentation: how can processes for ethanol production at high temperatures become superior to traditional process using mesophilic yeast?. Appl. Microbiol. Biotechnol. 85:861-867. https://doi.org/10.1007/s00253-009-2248-5.

Akuzawa S, Nagaoka J, Kanekatsu M, Kanesaki Y, Suzuki T. 2016. Draft genome sequence of *Oceanobacillus picturae* Heshi-B3, isolated from fermented rice bran in a traditional Japanese seafood dish. Genome Announc. 4:e01621-15. https://doi.org/10.1128/genomeA.01621-15.

Amelunxen RE, Carr DO. 1975. Glyceraldehyde-3-phosphate dehydrogenase from rabbit muscle. Meth. Enzymol. 41:264-267. https://doi.org/10.1016/s0076-6879(75)41060-6.

Anders S, Huber W. 2010. Differential expression analysis for sequence count data. Genome Biol. 11:R106. https://doi.org/10.1186/gb-2010-11-10-r106.

Auesukaree C. 2017. Molecular mechanisms of the yeast adaptive response and tolerance to stresses encountered during ethanol fermentation. J. Biosci. Bioeng. 124:133-142. https://doi.org/10.1016/j.jbiosc.2017.03.009.

Axe DD, Bailey JE. 1995. Transport of lactate and acetate through the energized cytoplasmic membrane of *Escherichia coli*. Biotechnol. Bioeng. 47:8-19. https://doi.org/10.1002/bit.260470103.

Banat IM, Nigam P, Singh D, Marchantand R, McHale AP. 1998. Ethanol production at elevated temperatures and alcohol concentrations, I. Yeasts in

general. World J. Microbiol. Biotechnol. 14:809-821. https://doi.org/10.1023/A:1008802704374.

Berry DB, Guan Q, Hose J, Haroon S, Gebbia M, Heisler LE, Nislow C, Giaever G, Gasch AP. 2011. Multiple means to the same end: the genetic basis of acquired stress resistance in yeast. PLoS Genet. 7:e1002353. https://doi.org/10.1371/journal.pgen.1002353.

Brandt BA, García-Aparicio MD, Görgens JF, Zyl WHV. 2021. Rational engineering of *Saccharomyces cerevisiae* towards improved tolerance to multiple inhibitors in lignocellulose fermentations. Biotechnol. Biofuels. 14:173. https://doi.org/10.1186/s13068-021-02021-w.

Breslow D, Cameron D, Collins S, Schuldiner M, Stewart-Ornstein J, Newman H, Madhani H, Krogan N, Weiss-man JA. 2008. A comprehensive strategy enabling high-resolution functional analysis of the yeast genome. Nat. Methods. 5:711-718. https://doi.org/10.1038/nmeth.1234.

Bro C, Regenberg B, Forster J, Nielsen J. 2006. In silico aided metabolic engineering of *Saccharomyces cerevisiae* for improved bioethanol production. Metab. Eng. 8:102-111. https://doi.org/10.1016/j.ymben.2005.09.007.

Çakar ZP, Turanlı-Yıldız B, Alkım C, Yılmaz Ü. 2012. Evolutionary engineering of *Saccharomyces cerevisiae* for improved industrially important properties. FEMS Yeast Res. 12:171-182. https://doi.org/10.1111/j.1567-1364.2011.00775.x.

Chen S, Xu Y. 2014. Adaptive evolution of *Saccharomyces cerevisiae* with enhanced ethanol tolerance for Chinese rice wine fermentation. Biotechnol. Appl. Biochem. 173:1940-1954. https://doi.org/10.1007/s12010-014-0978-z.

Cunha JT, Romaní A, Costa CE, Sá-correia I, Domingues L. 2019. Molecular and physiological basis of *Saccharomyces cerevisiae* tolerance to adverse lignocellulose-based process conditions. Appl. Microbiol. Biotechnol. 103:159-175. https://doi.org/10.1007/s00253-018-9478-3.

Cuny C, Lesbats M, Dukan S. 2007. Induction of a global stress response during the first step of *Escherichia coli* plate growth. Appl. Environ. Microbiol. 73:885-999. https://doi.org/10.1128/AEM.01874-06.

Davidson JF, Whyte B, Bissinger PH, Schiestl RH. 1996. Oxidative stress is involved in heat-induced cell death in *Saccharomyces cerevisiae*. Proc. Natl. Acad. Sci. U.S.A. 93:5116-5121. https://doi.org/10.1073/pnas.93.10.5116.

Delorme-Axford E, Klionsky DJ. 2018. Transcriptional and post-transcriptional regulation of autophagy in the yeast *Saccharomyces cerevisiae.* J. Biol. Chem. 293:5396-5403. https://doi.org/10.1074/jbc.R117.804641.

Dhar R, Sägesser R, Weikert C, Yuan J, Wagner A. 2011. Adaptation of *Saccharomyces cerevisiae* to saline stress through laboratory evolution. J. Evol. Biol. 24:1135-1153. https://doi.org/10.1111/j.1420-9101.2011.02249.x.

Dinh TN, Nagahisa K, Hirasawa T, Furusawa C, Shimizu H. 2008. Adaptation of *Saccharomyces cerevisiae* cells to high ethanol concentration and changes in fatty acid composition of membrane and cell size. PLoS One. 3:e2623. https://doi.org/10.1371/journal.pone.0002623.

Dulley JR, Grieve PA. 1975. A simple technique for eliminating interference by detergents in the Lowry method of protein determination. Anal. Biochem. 64:136-141. https://doi.org/10.1016/0003-2697(75)90415-7.

Fonseca GG, Heinzle E, Wittmann C, Gombert AK. 2008. The yeast *Kluyveromyces marxianus* and its biotechnological potential. Appl. Microbiol. Biotechnol. 79:339-354. https://doi.org/10.1007/s00253-008-1458-6.

Frank M, Duvezin-Caubet S, Koob S, Occhipinti A, Jagasia R, Petcherski A, Ruonala MO, Priault M, Salin B, Reichert AS. 2012. Mitophagy is triggered by mild oxidative stress in a mitochondrial fission dependent manner. Biochim Biophys Acta. 1823:2297-2310. https://doi.org/10.1016/j.bbamcr.2012.08.007.

Gajendra KA, Singh V, Mandal P, Singh P, Golla U, Baranwal S, Chauhan S, Tomar RS. 2014. Ebselen induces reactive oxygen species (ROS)-mediated

cytotoxicity in *Saccharomyces cerevisiae* with inhibition of glutamate dehydrogenase being a target. FEBS Open Bio. 4:77-89. https://doi.org/10.1016.j.fob.2014.01.002.

Gibson BR, Lawrence SJ, Leclaire JP, Powell CD, Smart KA. 2007. Yeast responses to stresses associated with industrial brewery handling. FEMS Microbiol. Rev. 31:535-569. https://doi.org/10.1111/j.1574-6976.2007.00076.x.

Goshima T, Tsuji M, Inoue H, Yano S, Hoshino T, Matsushika A. 2013. Bioethanol production from lignocellulosic biomass by a novel *Kluyveromyces marxianus* strain. Biosci. Biotechnol. Biochem. 77:1505-1510. https://doi.org/10.1271/bbb.130173.

Graybill ER, Rouhier MF, Kirby CE, Hawes JW. 2007. Functional comparison of citrate synthase isoforms from *S. cerevisiae*. Arch. Biochem. Biophys. 465:26-37. https://doi.org/10.1016/j.abb.2007.04.039.

Guaragnella N, Passarella S, Marra E, Giannattasio S. 2010. Knock-out of metacaspase and/or cytochrome *c* results in the activation of a ROS-independent acetic acid-induced programmed cell death pathway in yeast. FEBS Lett. 584:3655-3660. https://doi.org/10.1016/j.febslet.2010.07.044.

Gurdo N, Novelli Poisson GF, Juárez ÁB, Rios de Molina MC, Galvagno MA. 2018. Improved robustness of an ethanologenic yeast strain through adaptive evolution in acetic acid is associated with its enzymatic antioxidant ability. J. Appl. Microbiol. 125:766-776. https://doi.org/10.1111/jam.13917.

Helsen J, Voordeckers K, Vanderwaeren L, Santermans T, Tsontaki M, Verstrepen, KJ, Jelier R. 2020. Gene loss predictably drives evolutionary adaptation. Mol. Biol. Evol. 37:2989-3002. https://doi.org/10.1093/molbev/msaa172.

Hemansi, Himanshu, Patel AK, Saini JK, Singhania RR. 2021. Development of multiple inhibitor tolerant yeast via adaptive laboratory evolution for sustainable bioethanol production. Bioresour. Technol. 344:126247. https://doi.org/10.1016/j.biortech.2021.126247.

Hirokawa Y, Kanesaki Y, Arai S, Saruta F, Hayashihara K, Murakami A, Shimizu K, Honda H, Yoshikawa H, Hanai T. 2018. Mutations responsible for alcohol tolerance in the mutant of *Synechococcus elongatus* PCC 7942 (SY1043) obtained by single-cell screening system. J. Biosci. Bioeng. 125:572-577. https://doi.org/10.1016/j.jbiosc.2017.11.012.

Hughes DB, Tuoroszen NJ, Moye CJ. 1984. The effect of temperature on the kinetics of ethanol production by a thermotolerant strain *Kluyveromyces marxianus*. Biotechnol. Lett. 6:1-6. https://doi.org/10.1128/AEM.01854-08.

Ibraheem O, Ndimba BK. 2013. Molecular adaptation mechanisms employed by ethanologenic bacteria in response to lignocellulose-derived inhibitory compounds. Int. J. Biol. Sci. 9:598-612. https://doi.org/10.7150/ijbs.6091.

Ingley E, Hemmings BA. 1994. Pleckstrin homology (PH) domains in signal transduction. J. Cell. Biochem. 56:436-443. https://doi.org/10.1002/jcb.240560403.

Itsumi M, Inoue S, Elia AJ, Murakami K, Sasaki M, Lind EF, Brenner D, Harris IS, Chio II, Afzal S, Cairns RA, Cescon DW, Elford AR, Ye J, Lang PA, Li WY, Wakeham A, Duncan GS, Haight J, You-Ten A, Snow B, Yamamoto K, Ohashi PS, Mak TW. 2015. Idh1 protects murine hepatocytes from endotoxin induced oxidative stress by regulating the intracellular $NADP^+$/NADPH ratio. Cell Death Differ. 22:1837-1845. https://doi.org/10.1038/cdd.2015.38.

Jönsson LJ, Martín C. 2016. Pretreatment of lignocellulose: Formation of inhibitory by-products and strategies for minimizing their effects. Bioresour. Technol. 199:103-112. https://doi.org/10.1016/j.biortech.2015.10.009.

Kanki T, Furukawa K, Yamashita S. 2015. Mitophagy in yeast: Molecular mechanisms and physiological role. Biochim Biophys Acta. 1853:2756-2765. https://doi.org/10.1016/j.bbamcr.2015.01.005.

Kılmanoğlu H, Hoşoğlu Mİ, Güneşer O, Yüceer YK. 2020. Optimization of pretreatment and enzymatic hydrolysis conditions of tomato pomace for production of alcohols and esters by *Kluyveromyces marxianus*. LWT. 138:110728. https://doi.org/10.1016/j.lwt.2020.110728.

Kim IS, Kim YS, Kim H, Jin I, Yoon HS. 2013. *Saccharomyces cerevisiae* KNU5377 stress response during high-temperature ethanol fermentation. Mol. Cells. 35:210-218. https://doi.org/10.1007/s10059-013-2258-0.

Kim SB, Kwon DH, Park JB, Ha SJ. 2019. Alleviation of catabolite repression in *Kluyveromyces marxianus*: the thermotolerant SBK1 mutant simultaneously coferments glucose and xylose. Biotechnol. Biofuels. 12:90. https://doi.org/10.1186/s13068-019-1431-x.

Kosaka T, Lertwattanasakul N, Rodrussamee N, Nurcholis M, Dung NTP, Keo-Oudone C, Murata M, Götz P, Theodoropoulos C, Suprayogi, Maligan JM, Limtong S, Yamada M. 2018. Potential of thermotolerant ethanologenic yeasts isolated from ASEAN countries and their application in high-temperature fermentation. In *Fuel Ethanol Production from Sugarcane*. IntechOpen: London. UK. pp. 121-154.

Kotiadis VN, Duchen MR, Osellame LD. 2014. Mitochondrial quality control and communications with the nucleus are important in maintaining function and cell death. Biochim Biophs Acta. 1840:1254-1265. https://doi.org/10.1016/j.bbagen.2013.10.041.

Kruger NJ, von Schaewen A. 2003. The oxidative pentose phosphate pathway: structure and organization. Curr. Opin. Plant. Biol. 6:236-246. https://doi.org/10.1016/S1369-5266(03)00039-6.

Kuby SA, Noltmann EA. 1966. Glucose 6-phosphate dehydrogenase (crystalline) from brewers' yeast. Meth. Enzymol. 9:116-125. https://doi.org/10.1016/0076-6879(66)09029-3.

Kumari R, Pramanik K. 2012. Improvement of multiple stress tolerance in yeast strain by sequential mutagenesis for enhanced bioethanol production. J. Biosci. Bioeng. 114: 622-629. https://doi.org/10.1016/j.jbiosc.2012.07.007.

Lau MW, Gunawan C, Balan V, Dale BE. 2010. Comparing the fermentation performance of *Escherichia coli* KO11, *Saccharomyces cerevisiae* 424A(LNH-ST) *and Zymomonas mobilis* AX101 for cellulosic ethanol

production. Biotechnol. Biofuels. 3:11. https://doi.org/10.1186/1754-6834-3-11.

Lertwattanasakul N, Shigemoto E, Rodrussamee N, Limtong S, Thanonkeo P, Yamada M. 2009. The crucial role of alcohol dehydrogenase Adh3 *in Kluyveromyces marxianus* mitochondrial metabolism. Biosci. Biotechnol. Biochem. 73:2720-2726. https://doi.org/10.1271/bbb.90609.

Lertwattanasakul N, Rodrussamee N, Suprayogi, Limtong S, Thanonkeo P, Kosaka T, Yamada M. 2011. Utilization capability of sucrose, raffinose and inulin and its less-sensitiveness to glucose repression in thermotolerant yeast *Kluyveromyces marxianus* DMKU 3-1042. AMB Express. 1:20. https://doi.org/10.1186/2191-0855-1-20.

Lertwattanasakul N, Kosaka T, Hosoyama A, Suzuki Y, Rodrussamee N, Matsutani M, Murata M, Fujimoto N, Suprayogi, Tsuchikane K, Limtong S, Fujita N, Yamada M. 2015. Genetic basis of the highly efficient yeast *Kluyveromyces marxianus*: complete genome sequence and transcriptome analyses. Biotechnol. Biofuels. 8:47. https://doi.org/10.1186/s13068-015-0227-x.

Lertwattanasakul N, Nurcholis M, Rodrussamee N, Kosaka T, Murata M, Yamada M. 2022. *Kluyveromyces marxianus* as a platform in synthetic biology for the production of useful materials. In Synthetic Biology of Yeasts. Darvishi Harzevili F. Ed. Springer International Publishing. Cham. Switzerland. pp. 293–335.

Limtong S, Sringiew C, Yongmanitchai W. 2007. Production of fuel ethanol at high temperature from sugar cane juice by a newly isolated *Kluyveromyces marxianus.* Bioresour. Technol. 98:3367-3374. https://doi.org/10.1016/j.biortech.2006.10.044.

López-Mirabal HR, Winther JR. 2008. Redox characteristics of the eukaryotic cytosol. Biochem Biophys Acta. 1783:629-640. https://doi.org/10.1016/j.bbamcr.2007.10.013.

Ludovico P, Sousa MJ, Silva MT, Leão CL, Côrte-Real M. 2001. *Saccharomyces cerevisiae* commits to a programmed cell death process in response to acetic acid. Microbiology. 147:2409-2415. https://doi.org/10.1099/00221287-147-9-2409.

Ludovico P, Rodrigues F, Almeida A, Silva MT, Barrientos A, Côrte-Real M. 2002. Cytochrome c release and mitochondria involvement in programmed cell death induced by acetic acid in *Saccharomyces cerevisiae.* Mol. Biol. Cell. 13:2598-2606. https://doi.org/10.1091/mbc.e01-12-0161.

Madeo F, Fröhlich E, Ligr M, Grey M, Sigrist SJ, Wolf DH, Fröhlich KU. 1999. Oxygen stress: a regulator of apoptosis in yeast. J. Cell Biol 145:757–767. https://doi.org/10.1083/jcb.145.4.757.

Manfredini V, Roehrs R, Peralba MC, Henriques JA, Saffi J, Ramos AL, Benfato MS. 2004. Glutathione peroxidase induction protects *Saccharomyces cerevisiae sod1D sod2D* double mutants against oxidative damage. Braz. J. Med. Biol. Res. 37:159-165. https://doi.org/10.1590/S0100-879X2004000200001.

Mobini-Dehkordi M, Nahvi I, Zarkesh-Esfahani H, Ghaedi K, Tavassoli M, Akada R. 2008. Isolation of a novel mutant strain of *Saccharomyces cerevisiae* by an ethyl methane sulfonate-induced mutagenesis approach as a high producer of bioethanol. J. Biosci. Bioeng. 105:403-408. https://doi.org/10.1263/jbb.105.403.

Modig T, Lidén G, Taherzadeh MJ. 2002. Inhibition effects of furfural and alcohol dehydrogenase, aldehyde dehydrogenase and pyruvate dehydrogenase. Biochem. J. 363: 769-776. https://doi.org/10.1042/bj3630769.

Murata M, Fujimoto H, Nishimura K, Charoensuk K, Nagamitsu H, Raina S, Kosaka T, Oshima T, Ogasawara N, Yamada M. 2011. Molecular strategy for survival at a critical high temperature in *Eschierichia coli.* PLoS ONE. 6:e20063. https://doi.org/10.1371/journal.pone.0020063.

Murata M, Nitiyon S, Lertwattanasakul N, Sootsuwan K, Kosaka T, Thanonkeo P, Limtomg S, Yamada M. 2015. High-temperature fermentation technology for low-cost bioethanol. J Jpn Inst Energy. 94:1154-1162. https://doi.org/10.3775/jie.94.1154.

Nachaiwieng W, Lumyong S, Yoshioka K, Watanabe T, Khanongnuch C. 2015. Bioethanol production from rice husk under elevated temperature simultaneous saccharification and fermentation using *Kluyveromyces marxianus* CK8. Biocatal. Agric. Biotechnol. 4:543-549. https://doi.org/10.1016/j.bcab.2015.10.003.

Nasuno R, Aitoku M, Manago Y, Nishimura A, Sasano Y, Takagi H. 2014. Nitric oxide-mediated antioxidative mechanism in yeast through the activation of the transcription factor Mac1. PLoS One. 9:e113788. https://doi.org/10.1371/journal.pone.0113788.

Natarajan K, Meyer MR, Jackson BM, Slade D, Roberts C, Hinnebusch AG, Marton MJ. 2001. Transcriptional profiling shows that Gcn4p is a master regulator of gene expression during amino acid starvation in yeast. Mol. Cell. Biol. 21:4347-4368. https://doi.org/10.1128/MCB.21.13.4347-4368.2001.

Nigam JN. 2001. Development of xylose-fermenting yeast *Pichia stipites* for ethanol zproduction through adaptation on hardwood hemicellulose acid prehydrolysate. J. Appl. Microbiol. 90:208-215. https://doi.org/10.1046/j.1365-2672.2001.01234.x.

Nitiyon S, Keo-Oudone C, Murata M, Lertwattanasakul N, Limtong S, Kosaka T, Yamada M. 2016. Efficient conversion of xylose to ethanol by stress-tolerant *Kluyveromyces marxianus* BUNL-21. Springerplus. 5:185. https://doi.org/10.1186/s40064-016-1881-6.

Noltmann EA. 1966. Phosphoglucose isomerase. Meth. Enzymol. 9:557-565.

Nuanpeng S, Thanonkeo S, Yamada M, Thanonkeo P. 2016. Ethanol production from sweet sorghum juice at high temperatures using a newly isolated

thermotolerant yeast *Saccharomyces cerevisiae* DBKKU Y-53. Energies. 9:253. https://doi.org/10.3390/en9040253

Nurcholis M, Murata M, Limtong S, Kosaka T, Yamada M. 2019. *MIG1* as a positive regulator for the histidine biosynthesis pathway and as a global regulator in thermotolerant yeast *Kluyveromyces marxianus*. Sci. Rep. 9:9926. https://doi.org/10.1038/s41598-019-46411-5.

Nurcholis M, Nitiyon S, Suprayogi, Rodrussamee N, Lertwattanasakul N, Limtong S, Kosaka T, Yamada M. 2019. Functional analysis of Mig1 and Rag5 as expressional regulators in thermotolerant yeast *Kluyveromyces marxianus*. Appl. Microbiol. Biotechnol. 103:395-410. https://doi.org/10.1007/s00253-018-9462-y.

Nurcholis M, Lertwattanasakul N, Rodrussamee N, Kosaka T, Murata M, Yamada M. 2020. Integration of comprehensive data and biotechnological tools for industrial applications of *Kluyveromyces marxianus*. Appl. Microbiol. Biotechnol. 104:475-488. https://doi.org/10.1007/s00253-019-10224-3.

Paik SM, Kim J, Jin E, Jeon NL. 2019. Overproduction of recombinant *E. coli* malate synthase enhances *Chlamydomonas reinhardtii* biomass by upregulating heterotrophic metabolism. Bioresour. Technol. 272:594-598. https://doi.org/10.1016/j.biortech.2018.10.029.

Paiva S, Devaux F, Barbosa S, Jacq C, Casal M. 2004. Ady2p is essential for the acetate permease activity in the yeast *Saccharomyces cerevisiae.* Yeast. 21:201-210. https://doi.org/10.1002/yea.1056.

Palikaras K, Tavernarakis N. 2014. Mitochondrial homeostasis: The interplay between mitophagy and mitochondrial biogenesis. Exp. Gerontol. 56:182-188. https://doi.org/10.1016/j.exger.2014.01.021.

Pan Y. 2011. Mitochondria, reactive oxygen species, and chronological aging: A message from yeast. Exp. Gerontol. 46:847-852. https://doi.org/10.1016/j.exger.2011.08.007.

Pattanakittivorakul S, Lertwattanasakul N, Yamada M, Limtong, S. 2019. Selection of thermotolerant *Saccharomyces cerevisiae* for high temperature ethanol production from molasses and increasing ethanol production by strain improvement. Antonie van Leeuwenhoek. 112:975-990. https://doi.org/10.1007/s10482-019-01230-6.

Pereira T, Vilaprinyo E, Belli G, Sorribas A, Alte G, Pereira T, Vilaprinyo E, Belli G, Herrero E, Salvado B, Sorribas A. 2018. Quantitative operating principles of yeast metabolism during adaptation to heat stress. Cell Rep. 22:2421-2430. https://doi.org/10.1016/j.celrep.2018.02.020.

Pérez-Gallardo RV, Briones LS, Díaz-Pérez AL, Gutiérrez S, Rodríguez-Zavala JS, Campos-García J. 2013. Reactive oxygen species production induced by ethanol in *Saccharomyces cerevisiae* increases because of a dysfunctional mitochondrial iron-sulfur cluster assembly system. FEMS Yeast Res. 13:804-819. https://doi.org/10.1111/1567-1364.12090.

Petitjean M, Teste MA, Léger-Silvestre I, François JM, Parrou JL. 2017. RETRACTED: A new function for the yeast trehalose-6P synthase (Tps1) protein, as key pro-survival factor during growth, chronological ageing, and apoptotic stress. Mech. Ageing Dev. 161:234-246. https://doi.org/10.1016/j.mad.2016.07.01.

Phommachan K, Keo-oudone C, Nurcholis M, Vongvilaisak N, Chanhming M, Savanhnaly V, Bounphanmy S, Matsutani M, Kosaka T, Limtong S, Yamada M. 2022. Adaptive laboratory evolution for multistress tolerance, including fermentability at high glucose concentrations in thermotolerant *Candida tropicalis*. Energies. 15:561. https://doi.org/10.3390/en15020561.

Ren P, Malik A, Zeng F. 2016. Identification of YPL014W (Cip1) as a novel negative regulator of cyclin-dependent kinase in *Saccharomyces cerevisiae*. Genes Cells. 21:543–552. https://doi.org/10.1111/gtc.12361.

Rodrussamee N, Lertwattanasakul N, Hirata K, Suprayogi, Limtong S, Kosaka T, Yamada M. 2011. Growth and ethanol fermentation ability on hexose and

pentose sugars and glucose effect under various conditions in thermotolerant yeast *Kluyveromyces marxianus*. Appl. Microbiol. Biotechnol. 90:1573-1586. https://doi.org/10.1007/s00253-011-3218-2.

Rosen OM. 1975. Purification of fructose-1,6-diphosphatase from *Polysphondylium palidum*. Meth. Enzymol. 42:360-363. https://doi.org/10.1016/0076-6879(75)42141-3.

Rozakis S, Haque MI, Natsis A, Borzecka-Walker M, Mizak K. 2013. Cost-effectiveness of bioethanol policies to reduce carbon dioxide emissions in Greece. Int J Life Cycle Assess. 18:306-318. https://doi.org/10.1007/s11367-012-0471-2.

Russell JB. 1991. Resistance of *Streptococcus bovis* to acetic acid at low pH: relationship between intracellular pH and anion accumulation. Appl. Environ. Microbiol. 57:255-259. https://doi.org/10.1128/AEM.57.1.255-259.1991.

Saini P, Beniwal A, Kokkiligadda A, Vij S. 2017. Evolutionary adaptation of *Kluyveromyces marxianus* strain for efficient conversion of whey lactose to bioethanol. Process Biochem. 62:69-79. https://doi.org/10.1016/j.procbio.2017.07.013

Sakihama Y, Hidese R, Hasunuma T, Kondo A. 2019. Increased flux in acetyl-CoA synthetic pathway and TCA cycle of *Kluyveromyces marxianus* under respiratory conditions. Sci. Rep. 9:5319. https://doi.org/10.1038/s41598-019-41863-1.

Sambrook J, Russell DW. 2001. Molecular cloning a laboratory manual, Third edition. Volume 3. Cold Spring Harbor Laboratory Press, New York.

Sanger F, Nicklen S, Coulson AR. 1997. DNA sequencing with chain-terminating inhibitors. Proc. Natl. Acad. Sci. USA. 74:5463-5467. https://doi.org/10.1073/pnas.74.12.5463.

Saraste M, Hyvönen M. 1995. Pleckstrin homology domains: A fact file. Curr. Opin. Struct. Biol. 5:403-408. https://doi.org/10.1016/0959-440x(95)80104-9.

Satomura A, Katsuyama Y, Miura N, Kuroda K, Tomio A, Bamba T, Fukusaki E, Ueda M. 2013. Acquisition of thermotolerant yeast *Saccharomyces cerevisiae* by breeding via stepwise adaptation. Biotechnol. Prog. 29:1116-1123. https://doi.org/10.1002/btpr.1754.

Scherz-Shouval R, Elazar Z. 2007. ROS, mitochondria and the regulation of autophagy. Trends Cell Biol. 17:422-427. https://doi.org/10.1016/j.tcb.2007.07.009.

Scott WA, Abramsky T. 1975. 6-Phosphogluconate dehydrogenase from *Neurospora crassa*. Meth. Enzymol. 41:227-231. https://doi.org/10.1016/s0076-6879(75)41052-7.

Sharma NK, Behera S, Arora R, Kumar S. 2017. Evolutionary adaptation of *Kluyveromyces marxianus* NIRE-K3 for enhanced xylose utilization. Front. Energy Res. 5. https://doi.org/10.3389/fenrg.2017.00032.

Shaw JM, Nunnari J. 2002. Mitochondrial dynamics and division in budding yeast. Trends Cell Biol. 12:178-184. https://doi.org/10.1016/s0962-8924(01)02246-2.

Singer MA, Lindquist S. 1998. Thermotolerance in *Saccharomyces cerevisiae*: the Yin and Yang of trehalose. Trends Biotechnol. 16:460-468. https://doi.org/10.1016/S0167-7799(98)01251-7.

Sootsuwan K, Lertwattanasakul N, Thanonkeo P, Matsushita K, Yamada M. 2008. Analysis of the respiratory chain in ethanologenic *Zymomonas mobilis* with a cyanide-resistant bd-type ubiquinol oxidase as the only terminal oxidase and its possible physiological roles. J. Mol. Microbiol. Biotechnol. 14:163-175. https://doi.org/10.1159/000112598.

Sun Y, Cheng Z. 2002. Hydrolysis of lignocellulosic materials for ethanol production: A review. Bioresour. Technol. 83:1-11. https://doi.org/10.1016/S0960-8524(01)00212-7.

Tarrío N, García-Leiro A, Cerdán ME, González-Siso MI. 2008. The role of glutathione reductase in the interplay between oxidative stress response and

turnover of cytosolic NADPH in *Kluyveromyces lactic.* FEMS Yeast Res. 8:597-606. https://doi.org/10.1111/j.1567-1364.2008.00366.x.

Taweecheep P, Naloka K, Matsutani M, Yakushi T, Matsushita K, Theeragool G. 2019. In vitro thermal and ethanol adaptations to improve vinegar fermentation at high temperature of *Komagataeibacter oboediens* MSKU 3. Biotechnol. Appl. Biochem. 189:144-159. https://doi.org/10.1007/s12010-019-03003-3.

Techaparin A, Thanonkeo P, Klanrit P. 2017. High-temperature ethanol production using thermotolerant yeast newly isolated from Greater Mekong Subregion. Braz. J. Microbiol. 48:461-475. https://doi.org/10.1016/j.bjm.2017.01.006.

Tinôco D, Genier HLA, da Silveira WB. 2021. Technology valuation of cellulosic ethanol production by *Kluyveromyces marxianus* CCT 7735 from sweet sorghum bagasse at elevated temperatures. Renew. Energy. 173:188-196. https://doi.org/10.1016/j.renene.2021.03.132.

Thevelein JM. 1984. Regulation of trehalose mobilization in fungi. Microbio. Rev. 48:42-59. https://doi.org/10.1128/mr.48.1.42-59.1984.

Yu JW, Mendrola JM, Audhya A, Singh S, Keleti D, DeWald DB, Murray D, Emr SD. Lemmon MA. 2004. Genome-wide analysis of membrane targeting by *S. cerevisiae* pleckstrin homology domains. Mol. Cell. 13:677-688. https://doi.org/10.1016/S1097-2765(04)00083-8.

Youle RJ, van der Bliek AM. 2012. Mitochondrial fission, fusion, and stress. Science. 337:1062-1065. https://doi.org/10.1126/science.1219855.

Wai T, Langer T. 2016. Mitochondrial dynamics and metabolic regulation. Trends Endocrinol. Metab. 27:105-117. https://doi.org/10.1016/j.tem.2015.12.001.

Watanabe T, Watanabe I, Yamamoto M, Ando A, Nakamura T. 2011. A UV-induced mutant of *Pichia stipitis* with increased ethanol production from xylose and selection of a spontaneous mutant with increased ethanol tolerance. Bioresour. Technol. 102:1844-1848. https://doi.org/10.1016/j.biortech.2010.09.087.

Woo JM, Yang KM, Kim SU, Blank LM, Park JB. 2014. High temperature stimulates acetic acid accumulation and enhances the growth inhibition and ethanol production by *Saccharomyces cerevisiae* under fermenting conditions. Appl. Microbiol. Biotechnol. 98:6085-6094. https://doi.org/10.1007/s00253-014-5691-x.

Xia W, Wang Z, Wang Q, Han J, Zhao C, Hong Y, Zeng L, Tang L, Ying W. 2009. Roles of $NAD^+$/NADH and $NADP^+$/NADPH in cell death. Curr. Pharm. Des. 15:12-19. https://doi.org/10.2174/138161209787185832.

Zhang J, ten Pierick A, van Rossum HM, Seifar RM, Ras C, Daran JM, Heijnen JJ, Wahl SA. 2015. Determination of the cytosolic NADPH/NADP ratio in *Saccharomyces cerevisiae* using shikimate dehydrogenase as sensor reaction. Sci. Rep. 5:12846. https://doi.org/10.1038/srep12846.

Zhang M, Zhu R, Zhang M, Wang S. 2014. Creation of an ethanol-tolerant *Saccharomyces cerevisiae* strain by 266 nm laser radiation and repetitive cultivation. J. Biosci. Bioeng. 118:508-513. https://doi.org/10.1016/j.jbiosc.2014.04.016.

Zhang M, Shi J, Jiang L. 2015. Modulation of mitochondrial membrane integrity and ROS formation by high temperature in *Saccharomyces cerevisiae.* Electron. J. Biotechnol. 18:202-209. https://doi.org/10.1016/j.ejbt.2015.03.008.

Zhang Q, Lin YL, Fang Y, Zhao H. 2019. Adaptive evolution and selection of stress resistant *Saccharomyces cerevisiae* for very high-gravity bioethanol fermentation. Electron. J. Biotechnol. 41:88-94. https://doi.org/10.1016/j.ejbt.2019.06.003.

Zhang B, Ren L, Zeng S, Zhang S, Xu D, Zeng X, Li F. 2020. Functional analysis of *PGI1* and *ZWF1* in thermotolerant yeast *Kluyveromyces marxianus*. Appl. Microbiol. Biotechnol. https://doi.org/10.1007/s00253-020-10808-4.

## ACKNOWLEDGEMENTS

I would like to express my deepest gratitude to my supervisors, Prof. Dr. Mamoru Yamada and Assoc. Prof. Dr. Tomoyuki Kosaka, for excellent guidance, attentive supervision and encouragement throughout this research. Besides, they also provide good opportunities and good suggestions, which are benefit to my future career.

Beside my supervisors, I would like to thank Prof. Dr. Kazunobu Matsushita, Prof. Dr. Toshiharu Yakushi, and Assistant Prof. Dr. Naoya Kataoka for their helpful and valuable advice.

I am particularly grateful to Dr. Masayuki Murata, Dr. Noppon Lertwattanasakul, Dr. Mochamad Nurcholis, Sakuda Anggarini, Koudkeo Phommachan, all members of Josei laboratory and International students who study in Yamaguchi University for their value comments, discussion, suggestions and friendship during my study.

I am thankful to the Japanese Government through Monbukagakusho (MEXT) Scholarship for financial support during my study and Department of Biological Chemistry, Yamaguchi University for providing laboratory facilities.

Finally, I greatly appreciate and grateful to my parents, my family and my friends for their understanding, encouragement and powerful support during my study.



Sornsiri Pattanakittivorakul

PhD Student of Graduate School of

Science and Technology for Innovation

Yamaguchi University

## LIST OF PUBLICATION

1. **Distinct metabolic flow in response to temperature in thermotolerant *Kluyveromyces marxianus***

   Tomoyuki Kosaka, Tatsuya Tsuzuno, Seiki Nishida, Sornsiri Pattanakittivorakul, Masayuki Murata, Isamu Miyakawa, Noppon Lertwattanasakul, Savitree Limtong, Mamoru Yamada

   Applied and Environmental Microbiology, 2022, 88:e02006-21, DOI: https://doi.org/10.1128/aem.02006-21

2. **Evolutionary adaptation by repetitive long-term cultivation with gradual increase in temperature for acquiring multi-stress tolerance and high ethanol productivity in *Kluyveromyces marxianus* DMKU 3-1042**

   Sornsiri Pattanakittivorakul, Tatsuya Tsuzuno, Tomoyuki Kosaka, Masayuki Murata, Yu Kanesaki, Hirofumi Yoshikawa, Savitree Limtong and Mamoru Yamada

   Microorganisms, 10:798, DOI: https://doi.org/10.3390/microorganisms10040798

# APPENDIX

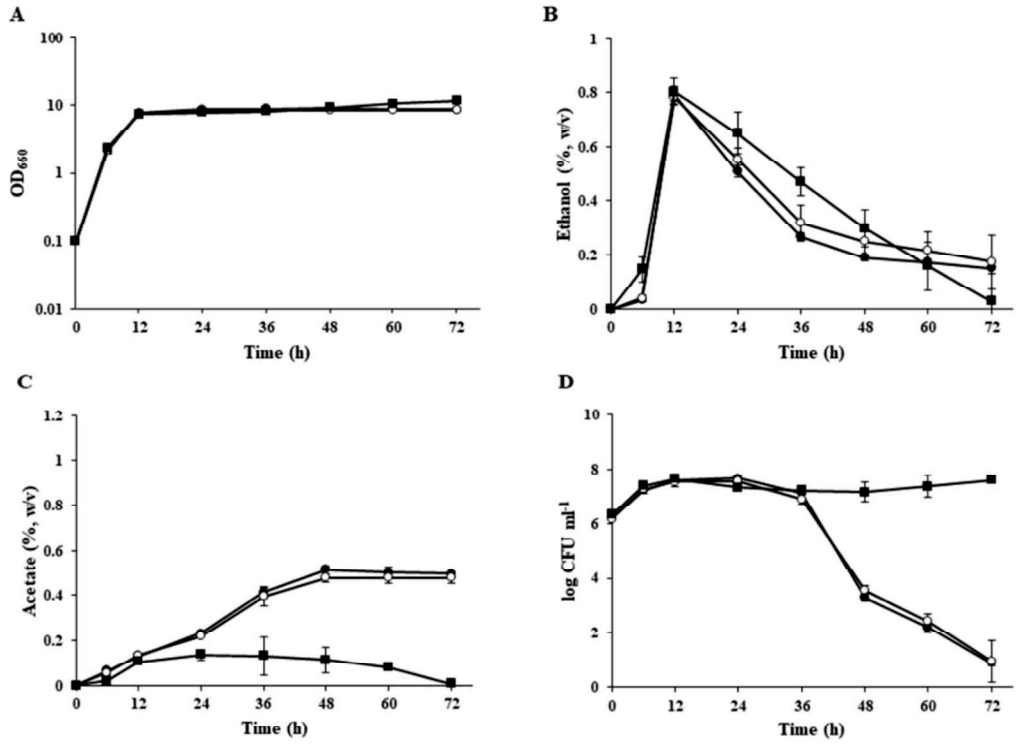


**Fig. S1** Effects of exogenous GSH on ethanol consumption, acetate accumulation and cell viability of *K. marxianus* at 45ºC. Cells were cultivated in 2% YPD medium containing 1 mM (open circles) or 4 mM (close squares) GSH or not containing GSH (close circles) at 45ºC under shaking conditions at 160 rpm. The cell density (A), concentrations of ethanol (B) and acetate (C), and CFU (D) were determined as described in the legend of Fig. 2.1. Error bars represent standard deviations (SD) for triplicate experiments.

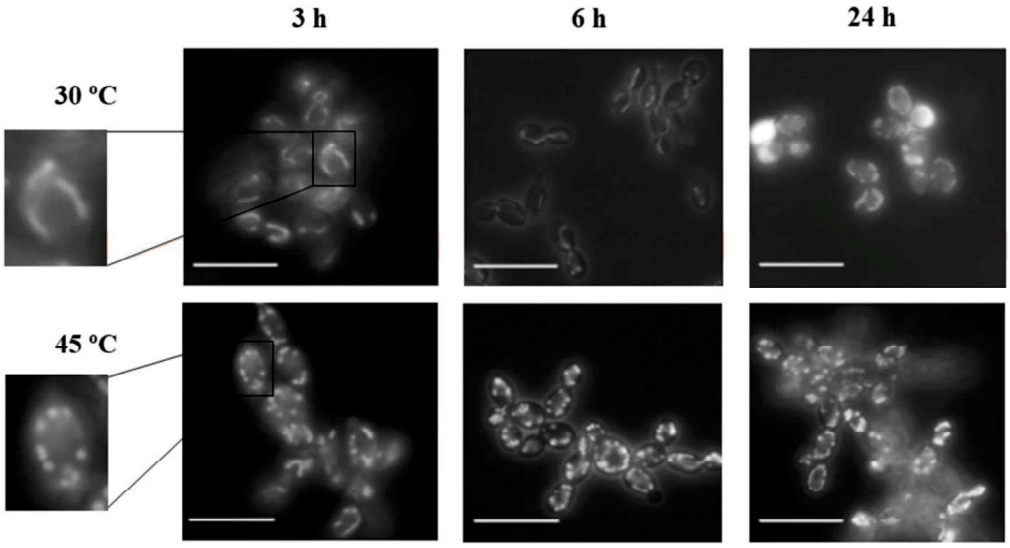


**Fig. S2** Mitochondrial morphology of *K. marxianus* at 30ºC and 45ºC. Cells were cultivated in 2% YPD medium at 30ºC and 45ºC under shaking conditions. Mitochondrial morphology was observed with samples taken at 3 h, 6 h, and 24 h.

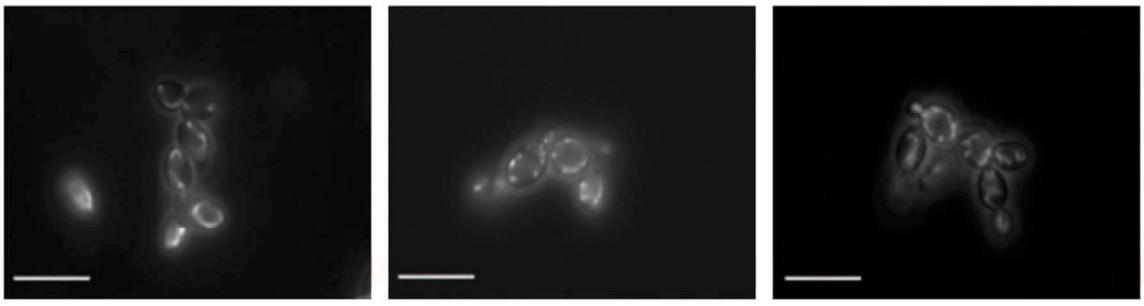


**Fig. S3** Effects of temperature upshift on mitochondrial morphology. Cells were cultivated in 2 % YPD medium at 30ºC, 45ºC or 30ºC to 45ºC under a shaking condition. The temperature upshift was performed as described in the legend of Fig. 2.5. Photos of mitochondrial morphology were taken 3 h (30-45ºC, 3 h) after the temperature upshift or 7 h under the condition of continuous cultivation at 30ºC or 45ºC.

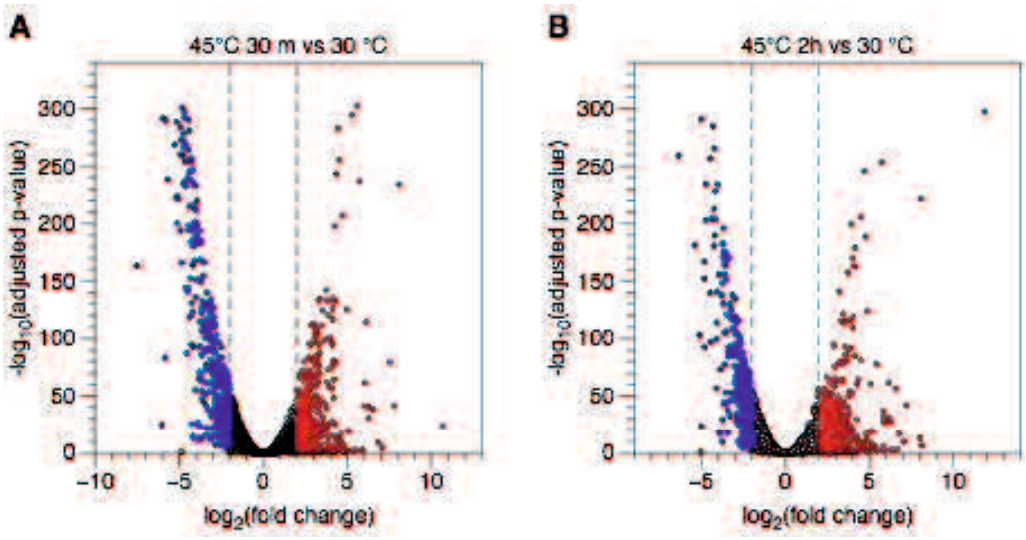


**Fig. S4** Volcano plots of differentially expressed genes (DEGs) for 45ºC for 30 min (4H30-30M45) (A) and 45ºC for 2 h (4H30-2H45) (B) vs 30ºC (6H30). Genes with adjusted *P* values less than 0.01 and $\log_2$ fold change values greater than 1 and less than -1, respectively, were assigned as differential expression. Red symbols, significantly upregulated genes; blue symbols. significantly downregulated genes.

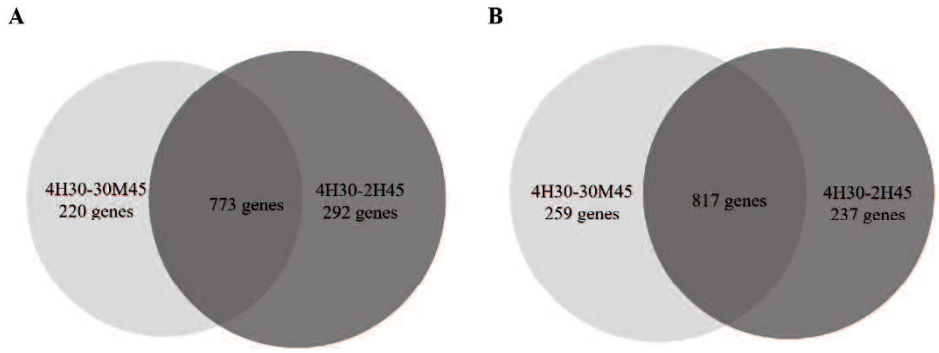


**Fig. S5** The number of shared and non-shared genes between 4H30-30M45 and 4H30-2H45 conditions in downregulated (A) and upregulated (B) DEGs.

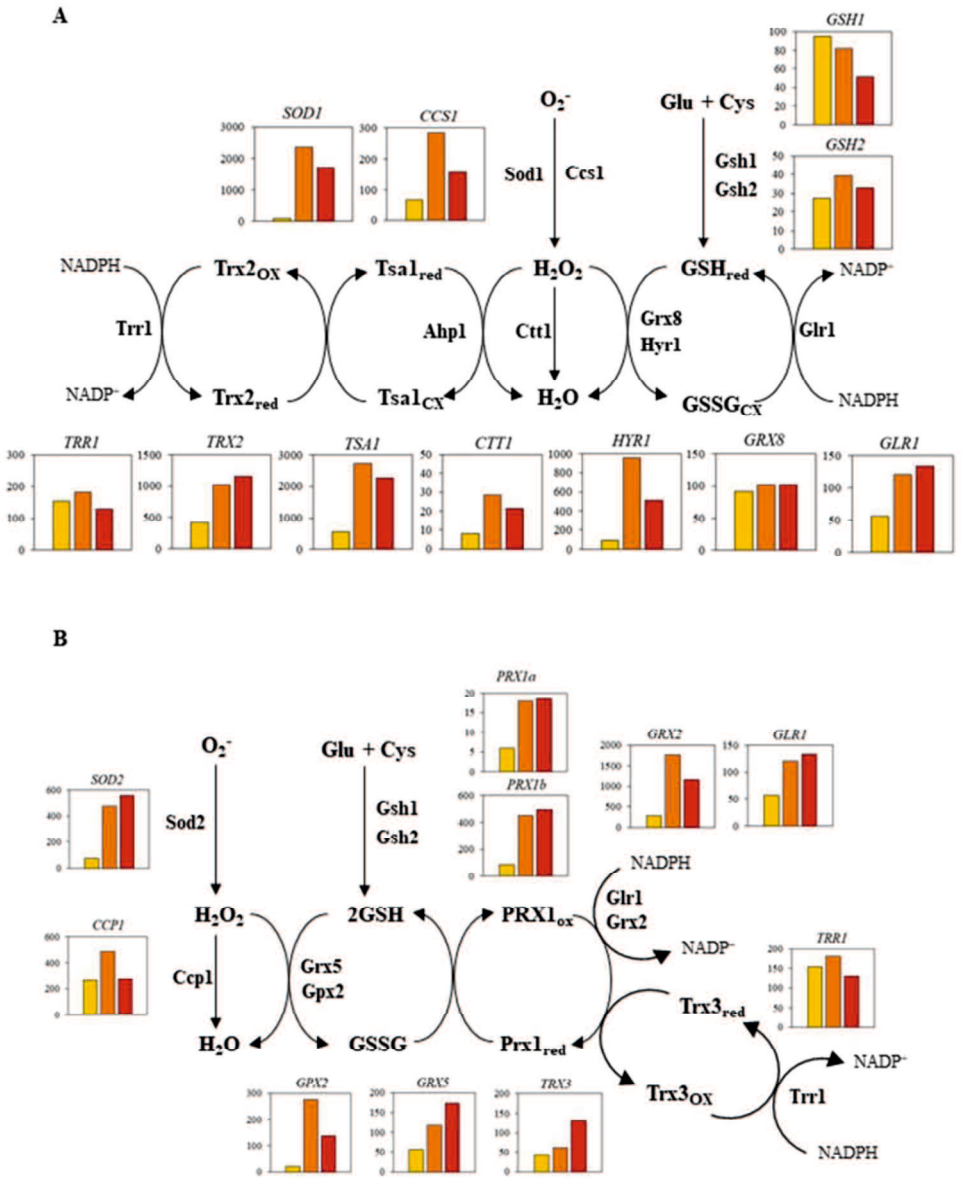


**Fig. S6** Transcriptome analysis of the effect of temperature upshift in *K. marxianus*. Cells were cultivated in YPD medium at 30ºC for 4 h under shaking conditions and flasks were transferred from a 30ºC incubator to a 45ºC incubator for further culture for 30 min (4H30-30M45, orange) or for 2 h (4H30-2H45, red). The control was the culture at 30ºC for 6 h under a shaking condition (6H30, yellow). Total RNA was then isolated, purified, and subjected to RNA-Seq analysis. The Y axis of each graph represents the reads per kilobase of exon per million (RPKM) of each gene under the conditions. Data for cytosolic (A) and mitochondrial (B) oxidative stress responses are shown. The RPKM value of each gene represents the average value of two independent experiments.

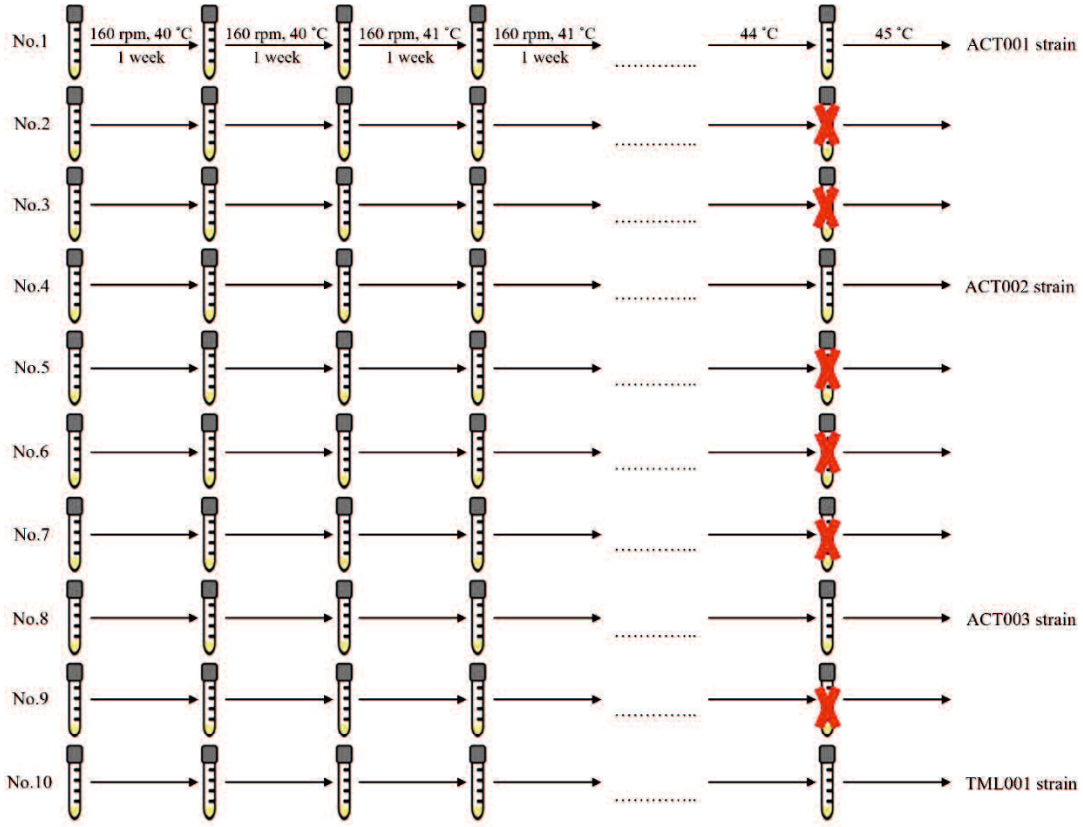


**Fig. S7** Schematic diagram of RLCGT for *K. marxianus* DMKU 3-1042. *K. marxianus* DMKU 3-1042 was subjected to RLCGT in YPD medium at temperatures from 40ºC to 45ºC, and finally 4 adapted strains were obtained. Cultivation for 7 days at each temperature was performed twice. Details are given in Materials and Methods.

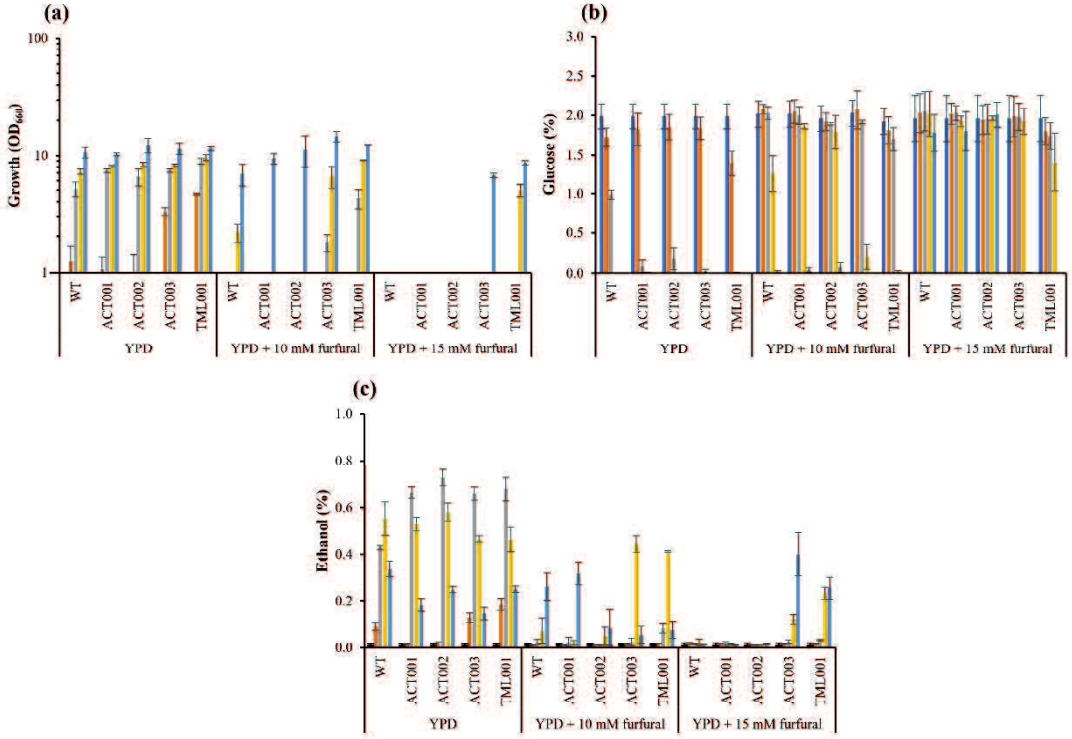


**Fig. S8** Effects of furfural on growth and fermentation parameters of adapted strains at 45ºC. Adapted strains were cultivated in YPD medium supplemented with 10 mM or 15 mM furfural at 45ºC under a shaking condition at 160 rpm for 48 h. Growth (a) was determined by measuring $OD_{660}$. Glucose (b) and ethanol (c) were determined by HPLC. Error bars represent SD for triplicate experiments.

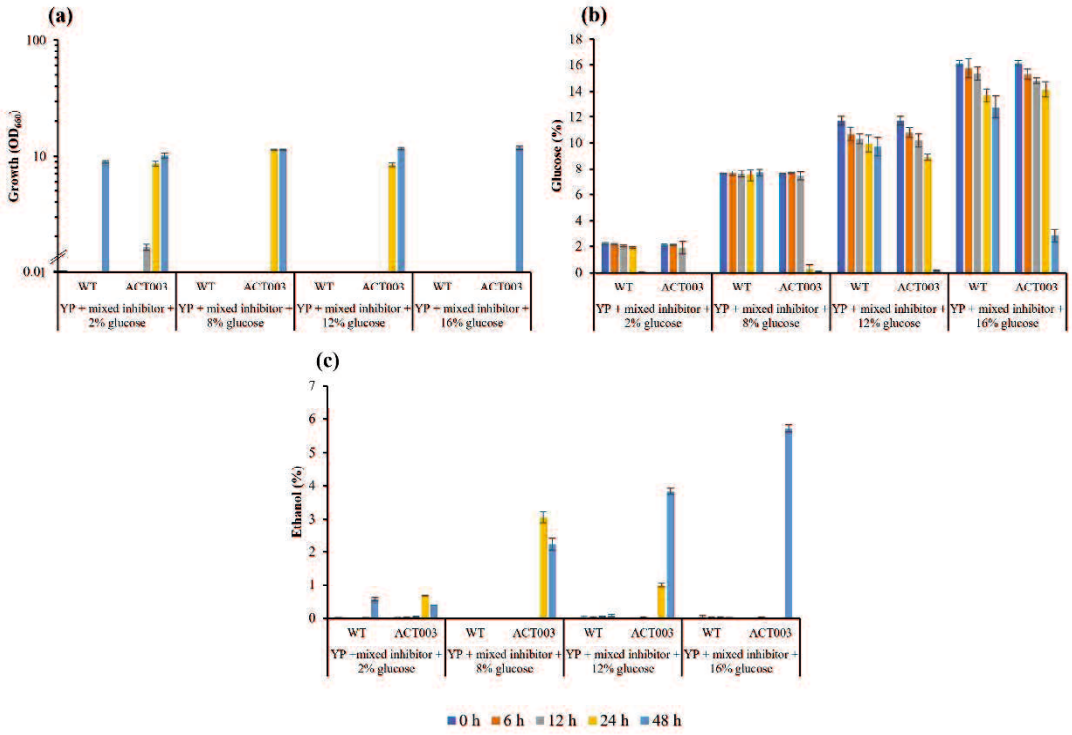


**Fig. S9** Effects of multiple inhibitors on growth and fermentation parameters of adapted strains at 45ºC. Adapted strains were cultivated in YPD medium supplemented with three inhibitors of 0.15% acetate, 7.5 mM furfural and 0.075% vanillin and with 8%, 12% or 16% glucose at 40ºC under a shaking condition at 160 rpm for 48 h. Growth (a) was determined by measuring $OD_{660}$. Glucose (b) and ethanol (c) were determined by HPLC. Error bars represent SD for triplicate experiments.

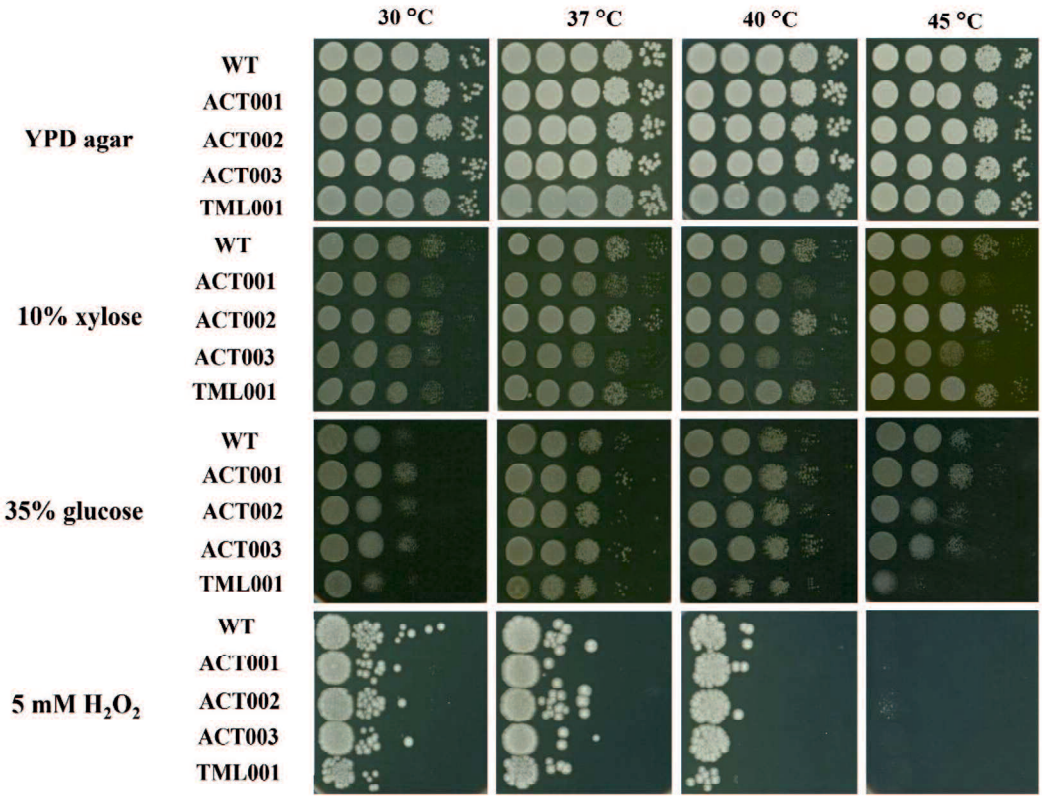


**Figure S10.** Characterization of adapted strains. Growth of adapted strains on YP agar plates supplemented with 10% xylose and YPD agar plates supplemented with 35% glucose or 5 mM $H_2O_2$ were compared. The plates were incubated at 30ºC-45 ºC for 48 h.

**Table S1** Upregulated genes (> 4 $log_2$) at 30 min after temperature upshift

| Locus_tag | $Log_2$ Fold Change | Product |
|---|---|---|
| KLMA_40128 | 12.5 | heat shock protein 26 |
| KLMA_60124 | 10.7 | RCR super family protein |
| KLMA_20427 | 8.4 | hypothetical protein |
| KLMA_20547 | 8.1 | protein BTN2 |
| KLMA_80019 | 7.8 | probable chaperone protein HSP31 |
| KLMA_30555 | 7.5 | conserved hypothetical transmembrane protein |
| KLMA_60356 | 7.1 | mating factor alpha-1 |
| KLMA_50268 | 6.8 | hypothetical protein |
| KLMA_80226 | 6.5 | mitochondrial carnitine carrier |
| KLMA_10830 | 6.4 | ribosyldihydronicotinamide dehydrogenase [quinone] |
| KLMA_60268 | 6.4 | uncharacterized protein YNL134C |
| KLMA_40532 | 6.4 | cell membrane protein YLR414C |
| KLMA_10782 | 6.3 | alkaline ceramidase YDC1 |
| KLMA_40247 | 6.3 | SDO1-like protein YHR087W |
| KLMA_80004 | 6.1 | putative uncharacterized oxidoreductase YGL039W |
| KLMA_70103 | 6.1 | protein yippee-like MOH1 |
| KLMA_20612 | 6.0 | sporulation-specific chitinase 2 |
| KLMA_80307 | 5.9 | hypothetical protein |
| KLMA_80367 | 5.8 | heat shock protein SSA3 |
| KLMA_70458 | 5.7 | uncharacterized protein ywnB |
| KLMA_50124 | 5.6 | hsp90 co-chaperone AHA1 |
| KLMA_40564 | 5.5 | hypothetical protein |
| KLMA_50589 | 5.5 | probable diacylglycerol pyrophosphate phosphatase 1 |
| KLMA_30561 | 5.3 | co-chaperone protein SBA1 |
| KLMA_70425 | 5.3 | uncharacterized protein MBB1 |
| KLMA_60409 | 5.0 | protein ZIP2 |
| KLMA_30331 | 5.0 | hypothetical protein |
| KLMA_40062 | 4.8 | meiotic recombination protein |
| KLMA_20771 | 4.8 | 12 kDa heat shock protein |
| KLMA_60511 | 4.7 | peptidyl-prolyl cis-trans isomerase D |
| KLMA_40061 | 4.7 | cell wall protein YLR040C |
| KLMA_80339 | 4.7 | NADP-dependent alcohol dehydrogenase 6 |
| KLMA_40250 | 4.6 | hypothetical protein |
| KLMA_10637 | 4.6 | hypothetical protein |
| KLMA_70050 | 4.6 | probable metabolite transport protein YFL040W |
| KLMA_60101 | 4.5 | heat shock protein 78 |
| KLMA_50236 | 4.5 | factor-induced gene 1 protein |
| KLMA_20442 | 4.4 | Ubiquitin |
| KLMA_20819 | 4.4 | hypothetical protein |
| KLMA_10806 | 4.4 | hypothetical protein |
| KLMA_40099 | 4.4 | heat shock protein 104 |
| KLMA_10754 | 4.3 | uncharacterized protein YPL071C |
| KLMA_30729 | 4.3 | putative uncharacterized oxidoreductase YGL039W |
| KLMA_70087 | 4.3 | superoxide dismutase [Cu-Zn] |
| KLMA_40102 | 4.2 | alcohol dehydrogenase 1 |
| KLMA_80094 | 4.2 | uncharacterized oxidoreductase SSP0419 |
| KLMA_30672 | 4.2 | probable metabolite transport protein C1271.09 |

| | | |
|---|---|---|
| KLMA_40420 | 4.2 | conserved hypothetical protein |
| KLMA_10044 | 4.2 | cell wall mannoprotein PST1 |
| KLMA_60369 | 4.2 | ribosome assembly 1 protein |
| KLMA_60029 | 4.2 | acyl-CoA dehydrogenase family member 11 |
| KLMA_80192 | 4.2 | conserved hypothetical membrane protien |
| KLMA_10814 | 4.1 | oxidored-like super family |
| KLMA_30691 | 4.1 | conserved hypothetical protein |
| KLMA_50024 | 4.1 | Arginase |
| KLMA_20807 | 4.1 | protein TBF1 |
| KLMA_20010 | 4.1 | protein crtK |
| KLMA_10012 | 4.1 | uncharacterized protein C11D3.14c |
| KLMA_70074 | 4.0 | DNA repair protein RAD59 |
| KLMA_40308 | 4.0 | hypothetical protein |
| KLMA_20352 | 4.0 | protein OPI10 |
| KLMA_10783 | 4.0 | sorbose reductase SOU1 |

**Table S2** GO enrichment analysis in biological process for upregulated genes (> 2 $\log_2$) at 30 min after temperature up-shift

| GO.ID | Term | classic |
|---|---|---|
| GO:0022613 | ribonucleoprotein complex biogenesis | 4.3E-08 |
| GO:0042254 | ribosome biogenesis | 9.1E-08 |
| GO:0006364 | rRNA processing | 1.5E-07 |
| GO:0016072 | rRNA metabolic process | 2E-07 |
| GO:0000462 | maturation of SSU-rRNA from tricistronic... | 2.2E-07 |
| GO:0034470 | ncRNA processing | 2.4E-07 |
| GO:0000460 | maturation of 5.8S rRNA | 2.8E-07 |
| GO:0000466 | maturation of 5.8S rRNA from tricistroni... | 2.8E-07 |
| GO:0006396 | RNA processing | 3E-07 |
| GO:0042274 | ribosomal small subunit biogenesis | 5.8E-07 |
| GO:0030490 | maturation of SSU-rRNA | 1.1E-06 |
| GO:0000447 | endonucleolytic cleavage in ITS1 to sepa... | 1.6E-06 |
| GO:0034660 | ncRNA metabolic process | 2E-06 |
| GO:0000478 | endonucleolytic cleavage involved in rRN... | 1.2E-05 |
| GO:0000479 | endonucleolytic cleavage of tricistronic... | 1.2E-05 |
| GO:0090502 | RNA phosphodiester bond hydrolysis, endo... | 1.2E-05 |
| GO:0044085 | cellular component biogenesis | 2E-05 |
| GO:0000469 | cleavage involved in rRNA processing | 0.0001 |
| GO:0000472 | endonucleolytic cleavage to generate mat... | 0.00013 |
| GO:0000480 | endonucleolytic cleavage in 5'-ETS of tr... | 0.00017 |
| GO:0072353 | cellular age-dependent response to react... | 0.00017 |
| GO:0006457 | protein folding | 0.00018 |
| GO:0000967 | rRNA 5'-end processing | 0.00021 |
| GO:0090304 | nucleic acid metabolic process | 0.00034 |
| GO:0000966 | RNA 5'-end processing | 0.00043 |
| GO:0034471 | ncRNA 5'-end processing | 0.00043 |
| GO:0034605 | cellular response to heat | 0.00065 |
| GO:0001315 | age-dependent response to reactive oxyge... | 0.00066 |
| GO:0042273 | ribosomal large subunit biogenesis | 0.00087 |
| GO:0071840 | cellular component organization or bioge... | 0.00109 |
| GO:0090501 | RNA phosphodiester bond hydrolysis | 0.00123 |
| GO:0006077 | (1->6)-beta-D-glucan metabolic process | 0.00159 |
| GO:0006078 | (1->6)-beta-D-glucan biosynthetic proces... | 0.00159 |
| GO:0042026 | protein refolding | 0.0023 |
| GO:0000463 | maturation of LSU-rRNA from tricistronic... | 0.00271 |
| GO:0001306 | age-dependent response to oxidative stre... | 0.00304 |
| GO:0007571 | age-dependent general metabolic decline | 0.00304 |
| GO:0001320 | age-dependent response to reactive oxyge... | 0.00312 |
| GO:0032220 | plasma membrane fusion involved in cytog... | 0.00312 |
| GO:0045026 | plasma membrane fusion | 0.00312 |
| GO:0051274 | beta-glucan biosynthetic process | 0.0033 |
| GO:0009408 | response to heat | 0.00344 |
| GO:0000470 | maturation of LSU-rRNA | 0.00377 |
| GO:0009266 | response to temperature stimulus | 0.00395 |
| GO:0033692 | cellular polysaccharide biosynthetic pro... | 0.00507 |
| GO:0070590 | spore wall biogenesis | 0.00507 |

| | | |
|---|---|---|
| GO:0070591 | ascospore wall biogenesis | 0.00507 |
| GO:0016925 | protein sumoylation | 0.00511 |
| GO:0048869 | cellular developmental process | 0.00529 |
| GO:0044264 | cellular polysaccharide metabolic proces... | 0.00544 |
| GO:0034614 | cellular response to reactive oxygen spe... | 0.0061 |
| GO:0051273 | beta-glucan metabolic process | 0.0061 |
| GO:0000271 | polysaccharide biosynthetic process | 0.00627 |
| GO:0016070 | RNA metabolic process | 0.00742 |
| GO:0016559 | peroxisome fission | 0.00783 |
| GO:0032502 | developmental process | 0.00803 |
| GO:0071852 | fungal-type cell wall organization or bi... | 0.00812 |
| GO:0000715 | nucleotide-excision repair, DNA damage r... | 0.009 |
| GO:0090305 | nucleic acid phosphodiester bond hydroly... | 0.00902 |

**Table S3** KEGG pathway analysis for upregulated genes (> 2 $\log_2$) at 30 min after temperature upshift

| | |
|---|---|
| kmx04141 | Protein processing in endoplasmic reticulum (8) |
| kmx03040 | Spliceosome (8) |
| kmx01110 | Biosynthesis of secondary metabolites (8) |
| kmx01130 | Biosynthesis of antibiotics (6) |
| kmx04113 | Meiosis - yeast (6) |
| kmx04011 | MAPK signaling pathway - yeast (6) |
| kmx04146 | Peroxisome (6) |
| kmx00240 | Pyrimidine metabolism (5) |
| kmx04213 | Longevity regulating pathway - multiple species (5) |
| kmx00561 | Glycerolipid metabolism (4) |
| kmx03008 | Ribosome biogenesis in eukaryotes (4) |
| kmx00071 | Fatty acid degradation (4) |
| kmx00230 | Purine metabolism (4) |
| kmx03440 | Homologous recombination (3) |
| kmx00480 | Glutathione metabolism (3) |
| kmx01212 | Fatty acid metabolism (3) |
| kmx04144 | Endocytosis (3) |
| kmx00010 | Glycolysis / Gluconeogenesis (3) |
| kmx00600 | Sphingolipid metabolism (3) |
| kmx04139 | Mitophagy - yeast (2) |
| kmx04111 | Cell cycle - yeast (2) |
| kmx01200 | Carbon metabolism (2) |
| kmx03030 | DNA replication (2) |
| kmx00051 | Fructose and mannose metabolism (2) |
| kmx00620 | Pyruvate metabolism (2) |
| kmx00564 | Glycerophospholipid metabolism (2) |
| kmx03013 | RNA transport (2) |
| kmx00500 | Starch and sucrose metabolism (2) |
| kmx03020 | RNA polymerase (2) |
| kmx02010 | ABC transporters (2) |
| kmx03410 | Base excision repair (2) |
| kmx00590 | Arachidonic acid metabolism (2) |
| kmx00520 | Amino sugar and nucleotide sugar metabolism (2) |
| kmx03018 | RNA degradation (2) |

**Table S4** Downregulated genes (< -4 $log_2$) at 30 min after temperature upshift

| Locus_tag | $Log_2$ Fold Change | Product |
|---|---|---|
| KLMA_20184 | -7.52 | endo-1,3-beta-glucanase |
| KLMA_10079 | -6.19 | S-adenosylmethionine synthetase 2 |
| KLMA_10829 | -6.03 | hypothetical protein |
| KLMA_50200 | -6.00 | 60S acidic ribosomal protein P0 |
| KLMA_20355 | -5.98 | 60S acidic ribosomal protein P2-alpha |
| KLMA_60222 | -5.85 | uncharacterized aminotransferase C660.12c |
| KLMA_20495 | -5.84 | 60S ribosomal protein L22-A |
| KLMA_60069 | -5.71 | 40S ribosomal protein S0 |
| KLMA_20625 | -5.69 | hypothetical protein |
| KLMA_50473 | -5.62 | 60S ribosomal protein L2 |
| KLMA_30115 | -5.61 | guanine nucleotide-binding protein subunit beta-like |
| KLMA_20054 | -5.47 | 60S ribosomal protein L24 |
| KLMA_60438 | -5.39 | 40S ribosomal protein S5 |
| KLMA_30664 | -5.35 | 60S ribosomal protein L12 |
| KLMA_50363 | -5.28 | low-affinity glucose transporter |
| KLMA_50529 | -5.28 | HYALURONIC ACID-BINDING PROTEIN 4 |
| KLMA_20403 | -5.16 | ribosomal_L18e super family |
| KLMA_80348 | -5.13 | 5-methyltetrahydropteroyltriglutamate homocysteine methyltransferase |
| KLMA_10826 | -5.13 | hypothetical protein |
| KLMA_70068 | -5.13 | 40S ribosomal protein S29 |
| KLMA_20742 | -5.12 | 40S ribosomal protein S3 |
| KLMA_10180 | -5.11 | argininosuccinate synthase |
| KLMA_80096 | -5.10 | 60S ribosomal protein L9-B |
| KLMA_80222 | -5.06 | 40S ribosomal protein S7-A |
| KLMA_50194 | -5.06 | 60S ribosomal protein L26-B |
| KLMA_10652 | -4.94 | hypothetical protein |
| KLMA_50474 | -4.92 | 60S ribosomal protein L29 |
| KLMA_10700 | -4.92 | 40S ribosomal protein S16 |
| KLMA_60491 | -4.87 | 60S acidic ribosomal protein P1-beta |
| KLMA_20268 | -4.87 | 40S ribosomal protein S2 |
| KLMA_20762 | -4.84 | conserved hypothetical protein |
| KLMA_40482 | -4.83 | 40S ribosomal protein S4 |
| KLMA_80413 | -4.79 | 60S ribosomal protein L8-B |
| KLMA_40436 | -4.77 | delta(24(24(1)))-sterol reductase |
| KLMA_20492 | -4.76 | 40S ribosomal protein S26-A |
| KLMA_20356 | -4.75 | 40S ribosomal protein S15 |
| KLMA_60532 | -4.70 | 60S ribosomal protein L16-A |
| KLMA_20318 | -4.69 | 60S ribosomal protein L20 |
| KLMA_40405 | -4.69 | 40S ribosomal protein S24 |
| KLMA_70190 | -4.66 | 60S ribosomal protein L34-B |
| KLMA_60313 | -4.63 | 40S ribosomal protein S20 |
| KLMA_20053 | -4.62 | 60S ribosomal protein L30 |
| KLMA_50361 | -4.60 | hexose transporter 2 |
| KLMA_10347 | -4.57 | GT8_Glycogenin |
| KLMA_40443 | -4.56 | 60S ribosomal protein L6-B |
| KLMA_10518 | -4.53 | inulinase |

| | | |
|---|---|---|
| KLMA_10786 | -4.48 | 40S ribosomal protein S5 |
| KLMA_50264 | -4.48 | 40S ribosomal protein S14 |
| KLMA_50288 | -4.45 | 40S ribosomal protein S10-A |
| KLMA_10701 | -4.45 | ribosomal_L13e super family |
| KLMA_80198 | -4.44 | probable family 17 glucosidase SCW4 |
| KLMA_30066 | -4.43 | 60S ribosomal protein L14-B |
| KLMA_80365 | -4.41 | 40S ribosomal protein S8 |
| KLMA_40393 | -4.41 | ribosomal protein L23 |
| KLMA_20105 | -4.39 | citrate synthase |
| KLMA_10560 | -4.38 | glutathione transferase 3 |
| KLMA_10376 | -4.36 | ribosomal_L22 |
| KLMA_40558 | -4.34 | 60S ribosomal protein L10a |
| KLMA_60504 | -4.34 | 60S ribosomal protein L35 |
| KLMA_50402 | -4.32 | 2-isopropylmalate synthase |
| KLMA_10702 | -4.32 | 60S acidic ribosomal protein P1-alpha |
| KLMA_30148 | -4.31 | acetolactate synthase small subunit |
| KLMA_70398 | -4.30 | PHO85 cyclin-1 |
| KLMA_50170 | -4.28 | 40S ribosomal protein S1 |
| KLMA_80064 | -4.28 | alpha-1,3-mannosyltransferase |
| KLMA_50223 | -4.28 | peroxisomal ATPase PEX1 |
| KLMA_50210 | -4.26 | 40S ribosomal protein S25 |
| KLMA_40419 | -4.24 | probable mitochondrial transport protein FSF1 |
| KLMA_80119 | -4.23 | histone H3 |
| KLMA_80177 | -4.22 | succinate/fumarate mitochondrial transporter |
| KLMA_70383 | -4.22 | peptide transporter PTR2 |
| KLMA_80163 | -4.21 | mitochondrial outer membrane protein porin 1 |
| KLMA_10828 | -4.20 | hypothetical protein |
| KLMA_10769 | -4.20 | 60S ribosomal protein L21-A |
| KLMA_50453 | -4.18 | 3-oxoacyl-(acyl-carrier-protein) reductase |
| KLMA_70155 | -4.17 | 60S ribosomal protein L23 |
| KLMA_30035 | -4.14 | methylene-fatty-acyl-phospholipid synthase |
| KLMA_10621 | -4.12 | cytochrome b2 |
| KLMA_60118 | -4.11 | histone H2B.2 |
| KLMA_70358 | -4.11 | 60S ribosomal protein L19 |
| KLMA_20590 | -4.08 | 60S acidic ribosomal protein P2-B |
| KLMA_10770 | -4.07 | hypothetical protein |
| KLMA_30712 | -4.07 | ubiquitin-60S ribosomal protein L40 |
| KLMA_50008 | -4.06 | 40S ribosomal protein S12 |
| KLMA_20800 | -4.05 | 60S ribosomal protein L5 |
| KLMA_70178 | -4.04 | uncharacterized protein YIL057C |
| KLMA_20339 | -4.03 | 60S ribosomal protein L11 |
| KLMA_30671 | -4.02 | sterol 24-C-methyltransferase |

**Table S5** GO enrichment analysis in biological process for downregulated genes (< -2 $log_2$) at 30 min after temperature upshift

| GO.ID | Term | classic |
|---|---|---|
| GO:1901566 | organonitrogen compound biosynthetic pro... | < 1e-30 |
| GO:0006412 | translation | 6.8E-27 |
| GO:0043043 | peptide biosynthetic process | 2.7E-26 |
| GO:0043604 | amide biosynthetic process | 4E-25 |
| GO:0006518 | peptide metabolic process | 8.3E-25 |
| GO:0043603 | cellular amide metabolic process | 6.2E-23 |
| GO:1901576 | organic substance biosynthetic process | 1.2E-18 |
| GO:0009058 | biosynthetic process | 3.8E-18 |
| GO:0044283 | small molecule biosynthetic process | 3.2E-17 |
| GO:0044249 | cellular biosynthetic process | 1.2E-16 |
| GO:0019752 | carboxylic acid metabolic process | 1E-15 |
| GO:0043436 | oxoacid metabolic process | 1.3E-15 |
| GO:0006082 | organic acid metabolic process | 1.9E-15 |
| GO:0044281 | small molecule metabolic process | 4E-15 |
| GO:1901564 | organonitrogen compound metabolic proces... | 1.2E-14 |
| GO:0016053 | organic acid biosynthetic process | 3.9E-13 |
| GO:0046394 | carboxylic acid biosynthetic process | 3.9E-13 |
| GO:0008652 | cellular amino acid biosynthetic process | 1.5E-11 |
| GO:1901607 | alpha-amino acid biosynthetic process | 2E-10 |
| GO:1902652 | secondary alcohol metabolic process | 6.4E-10 |
| GO:1902653 | secondary alcohol biosynthetic process | 6.4E-10 |
| GO:0006520 | cellular amino acid metabolic process | 7.7E-10 |
| GO:0006696 | ergosterol biosynthetic process | 4.7E-09 |
| GO:0008204 | ergosterol metabolic process | 4.7E-09 |
| GO:0016128 | phytosteroid metabolic process | 4.7E-09 |
| GO:0016129 | phytosteroid biosynthetic process | 4.7E-09 |
| GO:0044108 | cellular alcohol biosynthetic process | 4.7E-09 |
| GO:0097384 | cellular lipid biosynthetic process | 4.7E-09 |
| GO:1901605 | alpha-amino acid metabolic process | 6.2E-09 |
| GO:0046165 | alcohol biosynthetic process | 1.3E-08 |
| GO:0044107 | cellular alcohol metabolic process | 1.7E-08 |
| GO:0006694 | steroid biosynthetic process | 8.9E-08 |
| GO:0016126 | sterol biosynthetic process | 8.9E-08 |
| GO:0016125 | sterol metabolic process | 2.3E-07 |
| GO:0044267 | cellular protein metabolic process | 2.6E-07 |
| GO:0008202 | steroid metabolic process | 3.6E-07 |
| GO:1901617 | organic hydroxy compound biosynthetic pr... | 7.5E-07 |
| GO:0006066 | alcohol metabolic process | 1.4E-06 |
| GO:0019538 | protein metabolic process | 1.4E-06 |
| GO:0044271 | cellular nitrogen compound biosynthetic ... | 3.8E-06 |
| GO:0008610 | lipid biosynthetic process | 7.5E-06 |
| GO:0009082 | branched-chain amino acid biosynthetic p... | 1.1E-05 |
| GO:1901615 | organic hydroxy compound metabolic proce... | 2.2E-05 |
| GO:0017144 | drug metabolic process | 2.4E-05 |
| GO:0016999 | antibiotic metabolic process | 4E-05 |
| GO:0009097 | isoleucine biosynthetic process | 4E-05 |
| GO:0006407 | rRNA export from nucleus | 5.8E-05 |
| GO:0051029 | rRNA transport | 5.8E-05 |
| GO:0006637 | acyl-CoA metabolic process | 0.00012 |

| | | |
|---|---|---|
| GO:0035383 | thioester metabolic process | 0.00012 |
| GO:0009059 | macromolecule biosynthetic process | 0.00015 |
| GO:0009066 | aspartate family amino acid metabolic pr... | 0.00016 |
| GO:0032787 | monocarboxylic acid metabolic process | 0.00018 |
| GO:0006099 | tricarboxylic acid cycle | 0.00018 |
| GO:0006101 | citrate metabolic process | 0.00018 |
| GO:0072350 | tricarboxylic acid metabolic process | 0.00018 |
| GO:0006549 | isoleucine metabolic process | 0.00019 |
| GO:0009081 | branched-chain amino acid metabolic proc... | 0.00019 |
| GO:0034645 | cellular macromolecule biosynthetic proc... | 0.00021 |
| GO:0071704 | organic substance metabolic process | 0.00022 |
| GO:0009084 | glutamine family amino acid biosynthetic... | 0.00029 |
| GO:0006526 | arginine biosynthetic process | 0.00031 |
| GO:0008152 | metabolic process | 0.00046 |
| GO:0006732 | coenzyme metabolic process | 0.00056 |
| GO:0072330 | monocarboxylic acid biosynthetic process | 0.00059 |
| GO:0044255 | cellular lipid metabolic process | 0.00067 |
| GO:0044238 | primary metabolic process | 0.00079 |
| GO:0009067 | aspartate family amino acid biosynthetic... | 0.00088 |
| GO:0006629 | lipid metabolic process | 0.00105 |
| GO:0009185 | ribonucleoside diphosphate metabolic pro... | 0.00157 |
| GO:0046500 | S-adenosylmethionine metabolic process | 0.00191 |
| GO:0009064 | glutamine family amino acid metabolic pr... | 0.00199 |
| GO:0000105 | histidine biosynthetic process | 0.00218 |
| GO:0006547 | histidine metabolic process | 0.00218 |
| GO:0052803 | imidazole-containing compound metabolic ... | 0.00218 |
| GO:0006084 | acetyl-CoA metabolic process | 0.00239 |
| GO:0006525 | arginine metabolic process | 0.00239 |
| GO:0006090 | pyruvate metabolic process | 0.00267 |
| GO:0009132 | nucleoside diphosphate metabolic process | 0.00267 |
| GO:0044237 | cellular metabolic process | 0.00285 |
| GO:0015850 | organic hydroxy compound transport | 0.00367 |
| GO:0046031 | ADP metabolic process | 0.0037 |
| GO:2000601 | positive regulation of Arp2/3 complex-me... | 0.0045 |
| GO:0009135 | purine nucleoside diphosphate metabolic ... | 0.00484 |
| GO:0009179 | purine ribonucleoside diphosphate metabo... | 0.00484 |
| GO:0006104 | succinyl-CoA metabolic process | 0.0064 |
| GO:0009099 | valine biosynthetic process | 0.0064 |
| GO:0019284 | L-methionine salvage from S-adenosylmeth... | 0.0064 |
| GO:0033212 | iron assimilation | 0.0064 |
| GO:0033215 | iron assimilation by reduction and trans... | 0.0064 |
| GO:0033353 | S-adenosylmethionine cycle | 0.0064 |
| GO:0046439 | L-cysteine metabolic process | 0.0064 |
| GO:1901684 | arsenate ion transmembrane transport | 0.0064 |
| GO:0006555 | methionine metabolic process | 0.00665 |
| GO:0097064 | ncRNA export from nucleus | 0.00665 |
| GO:0006091 | generation of precursor metabolites and ... | 0.00697 |
| GO:0051186 | cofactor metabolic process | 0.00727 |
| GO:0061013 | regulation of mRNA catabolic process | 0.00846 |
| GO:0006568 | tryptophan metabolic process | 0.00848 |
| GO:0006586 | indolalkylamine metabolic process | 0.00848 |
| GO:0042430 | indole-containing compound metabolic pro... | 0.00848 |
| GO:0051127 | positive regulation of actin nucleation | 0.00848 |

| | | |
|---|---|---|
| GO:0006096 | glycolytic process | 0.00881 |
| GO:0006757 | ATP generation from ADP | 0.00881 |
| GO:0042866 | pyruvate biosynthetic process | 0.00881 |
| GO:1903311 | regulation of mRNA metabolic process | 0.00881 |
| GO:0006414 | translational elongation | 0.00979 |

**Table S6** KEGG pathway analysis for down-regulated genes (< -2 $\log_2$) at 30 min after temperature up-shift

| | |
|---|---|
| kmx03010 | Ribosome (71) |
| kmx01110 | Biosynthesis of secondary metabolites (67) |
| kmx01130 | Biosynthesis of antibiotics (58) |
| kmx01230 | Biosynthesis of amino acids (38) |
| kmx01200 | Carbon metabolism (20) |
| kmx00620 | Pyruvate metabolism (12) |
| kmx00010 | Glycolysis / Gluconeogenesis (12) |
| kmx01210 | 2-Oxocarboxylic acid metabolism (11) |
| kmx00100 | Steroid biosynthesis (10) |
| kmx00270 | Cysteine and methionine metabolism (10) |
| kmx04111 | Cell cycle - yeast (9) |
| kmx00630 | Glyoxylate and dicarboxylate metabolism (9) |
| kmx00020 | Citrate cycle (TCA cycle) (8) |
| kmx00340 | Histidine metabolism (7) |
| kmx00190 | Oxidative phosphorylation (7) |
| kmx00260 | Glycine, serine and threonine metabolism (7) |
| kmx00220 | Arginine biosynthesis (6) |
| kmx01212 | Fatty acid metabolism (6) |
| kmx00970 | Aminoacyl-tRNA biosynthesis (6) |
| kmx00290 | Valine, leucine and isoleucine biosynthesis (6) |
| kmx04011 | MAPK signaling pathway - yeast (6) |
| kmx00400 | Phenylalanine, tyrosine and tryptophan biosynthesis (6) |
| kmx00230 | Purine metabolism (5) |
| kmx04144 | Endocytosis (5) |
| kmx00520 | Amino sugar and nucleotide sugar metabolism (5) |
| kmx00650 | Butanoate metabolism (5) |
| kmx04113 | Meiosis - yeast (5) |
| kmx00250 | Alanine, aspartate and glutamate metabolism (5) |
| kmx00350 | Tyrosine metabolism (5) |
| kmx03013 | RNA transport (5) |
| kmx00330 | Arginine and proline metabolism (4) |
| kmx00770 | Pantothenate and CoA biosynthesis (4) |
| kmx00071 | Fatty acid degradation (4) |
| kmx00900 | Terpenoid backbone biosynthesis (4) |
| kmx00052 | Galactose metabolism (4) |
| kmx00380 | Tryptophan metabolism (4) |
| kmx00500 | Starch and sucrose metabolism (4) |
| kmx00300 | Lysine biosynthesis (4) |
| kmx04145 | Phagosome (4) |
| kmx00561 | Glycerolipid metabolism (4) |
| kmx00640 | Propanoate metabolism (4) |
| kmx00730 | Thiamine metabolism (3) |
| kmx00280 | Valine, leucine and isoleucine degradation (3) |
| kmx01040 | Biosynthesis of unsaturated fatty acids (3) |
| kmx03018 | RNA degradation (3) |
| kmx00310 | Lysine degradation (3) |
| kmx00360 | Phenylalanine metabolism (3) |
| kmx00030 | Pentose phosphate pathway (3) |
| kmx00410 | beta-Alanine metabolism (3) |
| kmx00450 | Selenocompound metabolism (3) |

| | |
|---|---|
| kmx04138 | Autophagy - yeast (3) |
| kmx00680 | Methane metabolism (3) |

**Table S7** Upregulated genes ($log_2 > 4$) at 2 h after temperature upshift

| Locus_tag | $Log_2$ Fold Change | Product |
|---|---|---|
| KLMA_40128 | 11.87 | heat shock protein 26 |
| KLMA_60356 | 8.13 | mating factor alpha-1 |
| KLMA_20547 | 8.06 | protein BTN2 |
| KLMA_60124 | 8.01 | RCR super family protein |
| KLMA_20427 | 7.77 | hypothetical protein |
| KLMA_40247 | 7.20 | SDO1-like protein YHR087W |
| KLMA_50268 | 7.05 | hypothetical protein |
| KLMA_20771 | 6.78 | 12 kDa heat shock protein |
| KLMA_10239 | 6.70 | hypothetical protein |
| KLMA_30555 | 6.56 | conserved hypothetical transmembrane protein |
| KLMA_80374 | 6.51 | conserved hypothetical protein |
| KLMA_80307 | 6.29 | hypothetical protein |
| KLMA_20027 | 6.29 | hypothetical protein |
| KLMA_80019 | 6.24 | probable chaperone protein HSP31 |
| KLMA_80226 | 6.18 | mitochondrial carnitine carrier |
| KLMA_70103 | 6.14 | protein yippee-like MOH1 |
| KLMA_10830 | 6.03 | ribosyldihydronicotinamide dehydrogenase [quinone] |
| KLMA_40564 | 5.84 | hypothetical protein |
| KLMA_60409 | 5.83 | protein ZIP2 |
| KLMA_20612 | 5.83 | sporulation-specific chitinase 2 |
| KLMA_40062 | 5.82 | meiotic recombination protein |
| KLMA_10782 | 5.82 | alkaline ceramidase YDC1 |
| KLMA_70458 | 5.73 | uncharacterized protein ywnB |
| KLMA_60268 | 5.54 | uncharacterized protein YNL134C |
| KLMA_70425 | 5.43 | uncharacterized protein MBB1 |
| KLMA_80004 | 5.42 | putative uncharacterized oxidoreductase YGL039W |
| KLMA_50589 | 5.41 | probable diacylglycerol pyrophosphate phosphatase 1 |
| KLMA_20819 | 5.16 | hypothetical protein |
| KLMA_10806 | 5.13 | hypothetical protein |
| KLMA_40250 | 5.09 | hypothetical protein |
| KLMA_30476 | 5.06 | sporulation-specific protein 22 |
| KLMA_10355 | 4.88 | hypothetical protein |
| KLMA_50335 | 4.84 | transposon Ty1-H Gag-Pol polyprotein |
| KLMA_30729 | 4.83 | putative uncharacterized oxidoreductase YGL039W |
| KLMA_70050 | 4.81 | probable metabolite transport protein YFL040W |
| KLMA_40532 | 4.77 | cell membrane protein YLR414C |
| KLMA_50124 | 4.69 | hsp90 co-chaperone AHA1 |
| KLMA_20203 | 4.65 | sporulation-specific protein 2 |
| KLMA_50236 | 4.62 | factor-induced gene 1 protein |
| KLMA_80192 | 4.62 | conserved hypothetical membrane brotien |
| KLMA_30672 | 4.49 | probable metabolite transport protein C1271.09 |
| KLMA_80367 | 4.49 | heat shock protein SSA3 |
| KLMA_10637 | 4.45 | hypothetical protein |
| KLMA_60029 | 4.40 | acyl-CoA dehydrogenase family member 11 |
| KLMA_40061 | 4.37 | cell wall protein YLR040C |
| KLMA_80191 | 4.34 | meiotically up-regulated gene 70 protein |
| KLMA_40420 | 4.34 | conserved hypothetical protein |

| | | |
|---|---|---|
| KLMA_40621 | 4.30 | hypothetical protein |
| KLMA_20010 | 4.26 | protein crtK |
| KLMA_80275 | 4.25 | non-disjunction protein 1 |
| KLMA_10044 | 4.24 | cell wall mannoprotein PST1 |
| KLMA_10521 | 4.22 | protein FMP23 |
| KLMA_20807 | 4.15 | protein TBF1 |
| KLMA_80339 | 4.14 | NADP-dependent alcohol dehydrogenase 6 |
| KLMA_30561 | 4.13 | co-chaperone protein SBA1 |
| KLMA_10814 | 4.02 | oxidored-like super family |
| KLMA_30013 | 4.01 | cytochrome b2 |
| KLMA_50594 | 4.01 | conserved hypothetical protein |
| KLMA_60101 | 4.00 | heat shock protein 78 |
| KLMA_30691 | 4.00 | conserved hypothetical protein |

**Table S8** GO enrichment analysis in biological process for upregulated genes (> 2 $log_2$) at 2 h after temperature upshift

| GO.ID | Term | classic |
|---|---|---|
| GO:0006364 | rRNA processing | 2.4E-15 |
| GO:0034470 | ncRNA processing | 8.3E-15 |
| GO:0016072 | rRNA metabolic process | 8.4E-15 |
| GO:0042254 | ribosome biogenesis | 1.2E-14 |
| GO:0022613 | ribonucleoprotein complex biogenesis | 2.8E-13 |
| GO:0034660 | ncRNA metabolic process | 9.2E-13 |
| GO:0006396 | RNA processing | 6E-12 |
| GO:0042274 | ribosomal small subunit biogenesis | 9.8E-10 |
| GO:0000462 | maturation of SSU-rRNA from tricistronic... | 1.2E-09 |
| GO:0000460 | maturation of 5.8S rRNA | 1.5E-09 |
| GO:0000466 | maturation of 5.8S rRNA from tricistroni... | 1.5E-09 |
| GO:0030490 | maturation of SSU-rRNA | 8.9E-09 |
| GO:0042273 | ribosomal large subunit biogenesis | 1.3E-07 |
| GO:0000447 | endonucleolytic cleavage in ITS1 to sepa... | 2.3E-07 |
| GO:0000470 | maturation of LSU-rRNA | 4.5E-07 |
| GO:0000463 | maturation of LSU-rRNA from tricistronic... | 2E-06 |
| GO:0000478 | endonucleolytic cleavage involved in rRN... | 2.1E-06 |
| GO:0000479 | endonucleolytic cleavage of tricistronic... | 2.1E-06 |
| GO:0090502 | RNA phosphodiester bond hydrolysis, endo... | 2.1E-06 |
| GO:0044085 | cellular component biogenesis | 2.4E-06 |
| GO:0000469 | cleavage involved in rRNA processing | 5.1E-06 |
| GO:0071840 | cellular component organization or bioge... | 1.7E-05 |
| GO:0090304 | nucleic acid metabolic process | 2.1E-05 |
| GO:0090501 | RNA phosphodiester bond hydrolysis | 2.8E-05 |
| GO:0022414 | reproductive process | 8.8E-05 |
| GO:0051321 | meiotic cell cycle | 8.8E-05 |
| GO:0000472 | endonucleolytic cleavage to generate mat... | 0.00015 |
| GO:0000003 | reproduction | 0.00016 |
| GO:0072353 | cellular age-dependent response to react... | 0.00018 |
| GO:0000480 | endonucleolytic cleavage in 5'-ETS of tr... | 0.00019 |
| GO:0000967 | rRNA 5'-end processing | 0.00025 |
| GO:0000054 | ribosomal subunit export from nucleus | 0.00038 |
| GO:0033750 | ribosome localization | 0.00038 |
| GO:0090305 | nucleic acid phosphodiester bond hydroly... | 0.00044 |
| GO:0000966 | RNA 5'-end processing | 0.00049 |
| GO:0034471 | ncRNA 5'-end processing | 0.00049 |
| GO:0001315 | age-dependent response to reactive oxyge... | 0.00071 |
| GO:0048285 | organelle fission | 0.00078 |
| GO:0071428 | rRNA-containing ribonucleoprotein comple... | 0.00079 |
| GO:1903046 | meiotic cell cycle process | 0.00124 |
| GO:0140013 | meiotic nuclear division | 0.00138 |
| GO:0006725 | cellular aromatic compound metabolic pro... | 0.00158 |
| GO:0006077 | (1->6)-beta-D-glucan metabolic process | 0.00169 |
| GO:0006078 | (1->6)-beta-D-glucan biosynthetic proces... | 0.00169 |
| GO:0006139 | nucleobase-containing compound metabolic... | 0.00173 |
| GO:0007127 | meiosis I | 0.00175 |

| | | |
|---|---|---|
| GO:0000055 | ribosomal large subunit export from nucl... | 0.00183 |
| GO:0007129 | synapsis | 0.00249 |
| GO:0044242 | cellular lipid catabolic process | 0.00284 |
| GO:0016070 | RNA metabolic process | 0.00313 |
| GO:0001306 | age-dependent response to oxidative stre... | 0.00324 |
| GO:0007571 | age-dependent general metabolic decline | 0.00324 |
| GO:0001320 | age-dependent response to reactive oxyge... | 0.00325 |
| GO:0046483 | heterocycle metabolic process | 0.00336 |
| GO:0045132 | meiotic chromosome segregation | 0.00348 |
| GO:0030476 | ascospore wall assembly | 0.00444 |
| GO:0042244 | spore wall assembly | 0.00444 |
| GO:0070590 | spore wall biogenesis | 0.00557 |
| GO:0070591 | ascospore wall biogenesis | 0.00557 |
| GO:0070726 | cell wall assembly | 0.00557 |
| GO:0071940 | fungal-type cell wall assembly | 0.00557 |
| GO:0031505 | fungal-type cell wall organization | 0.00562 |
| GO:0000280 | nuclear division | 0.00626 |
| GO:0045229 | external encapsulating structure organiz... | 0.0063 |
| GO:0071555 | cell wall organization | 0.0063 |
| GO:0034614 | cellular response to reactive oxygen spe... | 0.00659 |
| GO:1901360 | organic cyclic compound metabolic proces... | 0.0068 |
| GO:0016042 | lipid catabolic process | 0.00715 |
| GO:0007130 | synaptonemal complex assembly | 0.00832 |
| GO:0016559 | peroxisome fission | 0.00832 |
| GO:0031167 | rRNA methylation | 0.00832 |
| GO:0033313 | meiotic cell cycle checkpoint | 0.00832 |
| GO:0001510 | RNA methylation | 0.00859 |
| GO:0071852 | fungal-type cell wall organization or bi... | 0.00941 |

**Table S9** KEGG pathway analysis for upregulated genes (> 2 $\log_2$) at 2 h after temperature upshift

| | |
|---|---|
| kmx04146 | Peroxisome (8) |
| kmx04113 | Meiosis - yeast (8) |
| kmx01130 | Biosynthesis of antibiotics (6) |
| kmx03040 | Spliceosome (6) |
| kmx04213 | Longevity regulating pathway - multiple species (5) |
| kmx04141 | Protein processing in endoplasmic reticulum (5) |
| kmx04011 | MAPK signaling pathway - yeast (4) |
| kmx00240 | Pyrimidine metabolism (4) |
| kmx03008 | Ribosome biogenesis in eukaryotes (4) |
| kmx00230 | Purine metabolism (4) |
| kmx03440 | Homologous recombination (3) |
| kmx04144 | Endocytosis (3) |
| kmx00600 | Sphingolipid metabolism (3) |
| kmx01200 | Carbon metabolism (3) |
| kmx01212 | Fatty acid metabolism (3) |
| kmx00561 | Glycerolipid metabolism (3) |
| kmx00071 | Fatty acid degradation (3) |
| kmx04139 | Mitophagy - yeast (2) |
| kmx00670 | One carbon pool by folate (2) |
| kmx00564 | Glycerophospholipid metabolism (2) |
| kmx00010 | Glycolysis / Gluconeogenesis (2) |
| kmx00480 | Glutathione metabolism (2) |
| kmx00051 | Fructose and mannose metabolism (2) |
| kmx03013 | RNA transport (2) |
| kmx03020 | RNA polymerase (2) |
| kmx03410 | Base excision repair (2) |
| kmx00620 | Pyruvate metabolism (2) |

**Table S10** Downregulated genes (< -4 $log_2$) at 2 h after temperature upshift

| Locus_tag | $log_2$FoldChange | Product |
|---|---|---|
| KLMA_40220 | -6.38 | alcohol dehydrogenase 2 |
| KLMA_50360 | -6.35 | hexose transporter 2 |
| KLMA_50363 | -6.23 | low-affinity glucose transporter |
| KLMA_50361 | -5.41 | hexose transporter 2 |
| KLMA_10079 | -5.20 | S-adenosylmethionine synthetase 2 |
| KLMA_20587 | -5.11 | ammonia transport outward protein 3 |
| KLMA_50284 | -5.00 | c-4 methylsterol oxidase |
| KLMA_30263 | -5.00 | uncharacterized protein YKR075C |
| KLMA_60075 | -4.98 | pyruvate decarboxylase |
| KLMA_10518 | -4.83 | inulinase |
| KLMA_60219 | -4.83 | pyruvate kinase |
| KLMA_40115 | -4.82 | coproporphyrinogen-III oxidase |
| KLMA_10347 | -4.82 | GT8_Glycogenin |
| KLMA_20105 | -4.75 | citrate synthase |
| KLMA_70383 | -4.73 | peptide transporter PTR2 |
| KLMA_60412 | -4.47 | hexokinase |
| KLMA_80064 | -4.47 | alpha-1,3-mannosyltransferase |
| KLMA_20829 | -4.46 | repressible acid phosphatase |
| KLMA_30671 | -4.41 | sterol 24-C-methyltransferase |
| KLMA_10540 | -4.32 | phosphoglycerate kinase |
| KLMA_80198 | -4.24 | probable family 17 glucosidase SCW4 |
| KLMA_30204 | -4.23 | squalene monooxygenase |
| KLMA_10462 | -4.22 | enolase |
| KLMA_10832 | -4.20 | dihydroorotate dehydrogenase |
| KLMA_40388 | -4.17 | fructose-bisphosphate aldolase |
| KLMA_10057 | -4.16 | hypothetical protein |
| KLMA_10560 | -4.13 | glutathione transferase 3 |
| KLMA_70178 | -4.10 | uncharacterized protein YIL057C |
| KLMA_20184 | -4.10 | endo-1,3-beta-glucanase |
| KLMA_10180 | -4.06 | argininosuccinate synthase |
| KLMA_50200 | -4.05 | 60S acidic ribosomal protein P0 |

**Table S11** GO enrichment analysis in biological process for downregulated genes (< -2 $\log_2$) at 2 h after temperature upshift

| GO.ID | Term | classic |
|---|---|---|
| GO:0044283 | small molecule biosynthetic process | 3.50E-17 |
| GO:0044281 | small molecule metabolic process | 5.40E-17 |
| GO:0043436 | oxoacid metabolic process | 5.20E-13 |
| GO:0006082 | organic acid metabolic process | 6.90E-13 |
| GO:1902652 | secondary alcohol metabolic process | 1.70E-12 |
| GO:1902653 | secondary alcohol biosynthetic process | 1.70E-12 |
| GO:0019752 | carboxylic acid metabolic process | 2.20E-12 |
| GO:0046165 | alcohol biosynthetic process | 3.70E-12 |
| GO:0006696 | ergosterol biosynthetic process | 1.70E-11 |
| GO:0008204 | ergosterol metabolic process | 1.70E-11 |
| GO:0016128 | phytosteroid metabolic process | 1.70E-11 |
| GO:0016129 | phytosteroid biosynthetic process | 1.70E-11 |
| GO:0044108 | cellular alcohol biosynthetic process | 1.70E-11 |
| GO:0097384 | cellular lipid biosynthetic process | 1.70E-11 |
| GO:0044107 | cellular alcohol metabolic process | 7.40E-11 |
| GO:0016125 | sterol metabolic process | 1.10E-10 |
| GO:0032787 | monocarboxylic acid metabolic process | 1.70E-10 |
| GO:0008202 | steroid metabolic process | 2.00E-10 |
| GO:0006694 | steroid biosynthetic process | 5.00E-10 |
| GO:0016126 | sterol biosynthetic process | 5.00E-10 |
| GO:1901617 | organic hydroxy compound biosynthetic pr... | 5.70E-10 |
| GO:1901615 | organic hydroxy compound metabolic proce... | 9.60E-10 |
| GO:0005975 | carbohydrate metabolic process | 1.10E-09 |
| GO:0006066 | alcohol metabolic process | 1.20E-09 |
| GO:0008610 | lipid biosynthetic process | 5.90E-09 |
| GO:0006090 | pyruvate metabolic process | 1.00E-08 |
| GO:0006096 | glycolytic process | 1.40E-08 |
| GO:0006757 | ATP generation from ADP | 1.40E-08 |
| GO:0042866 | pyruvate biosynthetic process | 1.40E-08 |
| GO:0019362 | pyridine nucleotide metabolic process | 2.80E-08 |
| GO:0046496 | nicotinamide nucleotide metabolic proces... | 2.80E-08 |
| GO:0006165 | nucleoside diphosphate phosphorylation | 3.00E-08 |
| GO:0046939 | nucleotide phosphorylation | 3.00E-08 |
| GO:0016053 | organic acid biosynthetic process | 5.10E-08 |
| GO:0046394 | carboxylic acid biosynthetic process | 5.10E-08 |
| GO:0006091 | generation of precursor metabolites and ... | 7.70E-08 |
| GO:0072330 | monocarboxylic acid biosynthetic process | 8.10E-08 |
| GO:0006629 | lipid metabolic process | 8.40E-08 |
| GO:0046031 | ADP metabolic process | 1.10E-07 |
| GO:0006732 | coenzyme metabolic process | 1.30E-07 |
| GO:0019359 | nicotinamide nucleotide biosynthetic pro... | 1.30E-07 |
| GO:0019363 | pyridine nucleotide biosynthetic process | 1.30E-07 |
| GO:0044255 | cellular lipid metabolic process | 1.50E-07 |
| GO:0034404 | nucleobase-containing small molecule bio... | 1.50E-07 |
| GO:1901566 | organonitrogen compound biosynthetic pro... | 1.50E-07 |
| GO:0009135 | purine nucleoside diphosphate metabolic ... | 2.00E-07 |
| GO:0009166 | nucleotide catabolic process | 2.00E-07 |

| | | |
|---|---|---|
| GO:0009179 | purine ribonucleoside diphosphate metabo... | 2.00E-07 |
| GO:0072524 | pyridine-containing compound metabolic p... | 2.00E-07 |
| GO:0006006 | glucose metabolic process | 2.90E-07 |
| GO:1901292 | nucleoside phosphate catabolic process | 3.50E-07 |
| GO:0009185 | ribonucleoside diphosphate metabolic pro... | 5.80E-07 |
| GO:1901576 | organic substance biosynthetic process | 5.90E-07 |
| GO:0005996 | monosaccharide metabolic process | 7.60E-07 |
| GO:0017144 | drug metabolic process | 7.80E-07 |
| GO:0009058 | biosynthetic process | 1.00E-06 |
| GO:0009132 | nucleoside diphosphate metabolic process | 1.50E-06 |
| GO:0019318 | hexose metabolic process | 1.60E-06 |
| GO:0006733 | oxidoreduction coenzyme metabolic proces... | 1.80E-06 |
| GO:0051186 | cofactor metabolic process | 2.20E-06 |
| GO:0016052 | carbohydrate catabolic process | 2.40E-06 |
| GO:0072525 | pyridine-containing compound biosyntheti... | 2.50E-06 |
| GO:0006754 | ATP biosynthetic process | 5.00E-06 |
| GO:1901135 | carbohydrate derivative metabolic proces... | 5.10E-06 |
| GO:0009145 | purine nucleoside triphosphate biosynthe... | 6.90E-06 |
| GO:0009206 | purine ribonucleoside triphosphate biosy... | 6.90E-06 |
| GO:0046434 | organophosphate catabolic process | 7.20E-06 |
| GO:0009201 | ribonucleoside triphosphate biosynthetic... | 1.30E-05 |
| GO:0044249 | cellular biosynthetic process | 2.00E-05 |
| GO:0006793 | phosphorus metabolic process | 2.60E-05 |
| GO:0009142 | nucleoside triphosphate biosynthetic pro... | 2.90E-05 |
| GO:0006637 | acyl-CoA metabolic process | 3.00E-05 |
| GO:0035383 | thioester metabolic process | 3.00E-05 |
| GO:1901137 | carbohydrate derivative biosynthetic pro... | 3.20E-05 |
| GO:0006094 | gluconeogenesis | 5.70E-05 |
| GO:0019319 | hexose biosynthetic process | 5.70E-05 |
| GO:0046364 | monosaccharide biosynthetic process | 5.70E-05 |
| GO:0051188 | cofactor biosynthetic process | 6.00E-05 |
| GO:0072522 | purine-containing compound biosynthetic ... | 9.60E-05 |
| GO:0016999 | antibiotic metabolic process | 0.00016 |
| GO:0009108 | coenzyme biosynthetic process | 0.00016 |
| GO:0009127 | purine nucleoside monophosphate biosynth... | 0.00026 |
| GO:0009168 | purine ribonucleoside monophosphate bios... | 0.00026 |
| GO:0009156 | ribonucleoside monophosphate biosyntheti... | 0.0003 |
| GO:0006099 | tricarboxylic acid cycle | 0.00032 |
| GO:0006101 | citrate metabolic process | 0.00032 |
| GO:0072350 | tricarboxylic acid metabolic process | 0.00032 |
| GO:0055086 | nucleobase-containing small molecule met... | 0.00036 |
| GO:0009124 | nucleoside monophosphate biosynthetic pr... | 0.00041 |
| GO:0009260 | ribonucleotide biosynthetic process | 0.00065 |
| GO:0009084 | glutamine family amino acid biosynthetic... | 0.00066 |
| GO:0072521 | purine-containing compound metabolic pro... | 0.00088 |
| GO:0006084 | acetyl-CoA metabolic process | 0.00092 |
| GO:0019693 | ribose phosphate metabolic process | 0.00098 |
| GO:0006164 | purine nucleotide biosynthetic process | 0.00099 |
| GO:0009152 | purine ribonucleotide biosynthetic proce... | 0.00099 |
| GO:0046390 | ribose phosphate biosynthetic process | 0.00115 |
| GO:0019637 | organophosphate metabolic process | 0.00119 |

| | | |
|---|---|---|
| GO:0046034 | ATP metabolic process | 0.00133 |
| GO:0006526 | arginine biosynthetic process | 0.00167 |
| GO:0009205 | purine ribonucleoside triphosphate metab... | 0.00176 |
| GO:0009144 | purine nucleoside triphosphate metabolic... | 0.00202 |
| GO:0016310 | phosphorylation | 0.00226 |
| GO:0009199 | ribonucleoside triphosphate metabolic pr... | 0.0023 |
| GO:0006796 | phosphate-containing compound metabolic ... | 0.00237 |
| GO:0055114 | oxidation-reduction process | 0.00299 |
| GO:0009117 | nucleotide metabolic process | 0.00322 |
| GO:0009165 | nucleotide biosynthetic process | 0.00347 |
| GO:0006753 | nucleoside phosphate metabolic process | 0.00349 |
| GO:0016051 | carbohydrate biosynthetic process | 0.00414 |
| GO:0006104 | succinyl-CoA metabolic process | 0.00418 |
| GO:0072364 | regulation of cellular ketone metabolic ... | 0.00418 |
| GO:0009141 | nucleoside triphosphate metabolic proces... | 0.00424 |
| GO:1901293 | nucleoside phosphate biosynthetic proces... | 0.00425 |
| GO:0006081 | cellular aldehyde metabolic process | 0.00466 |
| GO:0043242 | negative regulation of protein complex d... | 0.00562 |
| GO:0006633 | fatty acid biosynthetic process | 0.006 |
| GO:0019439 | aromatic compound catabolic process | 0.00601 |
| GO:0009259 | ribonucleotide metabolic process | 0.00622 |
| GO:0006865 | amino acid transport | 0.00647 |
| GO:0034655 | nucleobase-containing compound catabolic... | 0.00707 |
| GO:0009161 | ribonucleoside monophosphate metabolic p... | 0.00712 |
| GO:0015980 | energy derivation by oxidation of organi... | 0.00712 |
| GO:0044270 | cellular nitrogen compound catabolic pro... | 0.00749 |
| GO:0046700 | heterocycle catabolic process | 0.00749 |
| GO:0006525 | arginine metabolic process | 0.00771 |
| GO:0006098 | pentose-phosphate shunt | 0.00774 |
| GO:0006407 | rRNA export from nucleus | 0.00774 |
| GO:0019682 | glyceraldehyde-3-phosphate metabolic pro... | 0.00774 |
| GO:0051029 | rRNA transport | 0.00774 |
| GO:0051051 | negative regulation of transport | 0.00774 |
| GO:0051156 | glucose 6-phosphate metabolic process | 0.00774 |
| GO:0009150 | purine ribonucleotide metabolic process | 0.00782 |
| GO:0009126 | purine nucleoside monophosphate metaboli... | 0.00807 |
| GO:0009167 | purine ribonucleoside monophosphate meta... | 0.00807 |
| GO:0006163 | purine nucleotide metabolic process | 0.00858 |
| GO:0009123 | nucleoside monophosphate metabolic proce... | 0.00858 |
| GO:1901564 | organonitrogen compound metabolic proces... | 0.00978 |
| GO:0015849 | organic acid transport | 0.00979 |
| GO:0046942 | carboxylic acid transport | 0.00979 |
| GO:1901361 | organic cyclic compound catabolic proces... | 0.0099 |

**Table S12** KEGG pathway analysis for downregulated genes (< -2 log2) at 2 h after temperature upshift

| | |
|---|---|
| kmx00010 | Glycolysis / Gluconeogenesis (18) |
| kmx03010 | Ribosome (13) |
| kmx00620 | Pyruvate metabolism (11) |
| kmx00100 | Steroid biosynthesis (11) |
| kmx00030 | Pentose phosphate pathway (10) |
| kmx00630 | Glyoxylate and dicarboxylate metabolism (8) |
| kmx04011 | MAPK signaling pathway - yeast (8) |
| kmx00520 | Amino sugar and nucleotide sugar metabolism (8) |
| kmx00500 | Starch and sucrose metabolism (7) |
| kmx00020 | Citrate cycle (TCA cycle) (7) |
| kmx00052 | Galactose metabolism (7) |
| kmx00680 | Methane metabolism (6) |
| kmx01210 | 2-Oxocarboxylic acid metabolism (6) |
| kmx00270 | Cysteine and methionine metabolism (6) |
| kmx00190 | Oxidative phosphorylation (6) |
| kmx04113 | Meiosis - yeast (6) |
| kmx04111 | Cell cycle - yeast (5) |
| kmx00051 | Fructose and mannose metabolism (5) |
| kmx00220 | Arginine biosynthesis (5) |
| kmx04144 | Endocytosis (5) |
| kmx03018 | RNA degradation (5) |
| kmx01212 | Fatty acid metabolism (5) |
| kmx00640 | Propanoate metabolism (4) |
| kmx00650 | Butanoate metabolism (4) |
| kmx00250 | Alanine, aspartate and glutamate metabolism (4) |
| kmx00230 | Purine metabolism (4) |
| kmx04141 | Protein processing in endoplasmic reticulum (4) |
| kmx00260 | Glycine, serine and threonine metabolism (4) |
| kmx00900 | Terpenoid backbone biosynthesis (4) |
| kmx00071 | Fatty acid degradation (3) |
| kmx00860 | Porphyrin and chlorophyll metabolism (3) |
| kmx00970 | Aminoacyl-tRNA biosynthesis (3) |
| kmx01040 | Biosynthesis of unsaturated fatty acids (3) |
| kmx04145 | Phagosome (3) |
| kmx04213 | Longevity regulating pathway - multiple species (3) |
| kmx00290 | Valine, leucine and isoleucine biosynthesis (3) |
| kmx00561 | Glycerolipid metabolism (3) |
| kmx04139 | Mitophagy - yeast (3) |
| kmx00600 | Sphingolipid metabolism (3) |

**Table S13** Significantly upregulated genes that are related to mitophagy

| **Mitophagy** (kmx04139) at 30 min $log_2 > 2$ | | | | | |
|---|---|---|---|---|---|
| No. | Protein name | | Function | Query cover (%) | Identity (%) |
| | *S. cerevisiae* | *K. marxianus* | | | |
| 1 | ScATG32 | KmATG32 (KLMA_30710) 2.425406 | Mitochondrial outer membrane protein required to initiate mitophagy; recruits the autophagy adaptor protein Atg11p and the ubiquitin-like protein Atg8p to the mitochondrial surface to initiate mitophagy, the selective vacuolar degradation of mitochondria in response to starvation; can promote pexophagy when placed ectopically in the peroxisomal membrane; regulates mitophagy and ethanol production during alcoholic fermentation | 73 | 29 |
| 2 | ScFIS1 | KmFIS1 (KLMA_70171) 2.36173 | - mitochondria fission 1 protein<br>- Protein involved in mitochondrial fission and peroxisome abundance; may have a distinct role in tethering protein aggregates to mitochondria in order to retain them in the mother cell; required for localization of Dnm1p and Mdv1p during mitochondrial division; mediates ethanol-induced apoptosis and ethanol-induced mitochondrial fragmentation | 99 | 57 |
| Mitophagy (kmx04139) at 2 h $log_2 > 2$ | | | | | |
| No. | Protein name | | Function | Query cover (%) | Identity (%) |
| | *S. cerevisiae* | *K. marxianus* | | | |
| 1 | ScATG32 | KmATG32 (KLMA_30710) 2.081331 | Mitochondrial outer membrane protein required to initiate mitophagy; recruits the autophagy adaptor protein Atg11p and the ubiquitin-like protein Atg8p to the mitochondrial surface to initiate mitophagy, the selective vacuolar degradation of mitochondria in response to starvation; can promote pexophagy when placed ectopically in the peroxisomal membrane; regulates mitophagy and ethanol production during alcoholic fermentation | 73 | 29 |
| 2 | ScFIS1 | KmFIS1 (KLMA_70171) 2.036209 | - mitochondria fission 1 protein<br>- Protein involved in mitochondrial fission and peroxisome abundance; may have a distinct role in tethering protein aggregates to mitochondria in order to retain them in the mother cell; required for localization of Dnm1p and Mdv1p during mitochondrial division; mediates ethanol-induced apoptosis and ethanol-induced mitochondrial fragmentation | 99 | 57 |

**Table S14** Significantly downregulated genes that are related to mitophagy or autophagy

| Mitophagy (kmx04139) at 2 h $log_2$ < -2 | | | | | |
|---|---|---|---|---|---|
| No. | Protein name | | Function | Query cover (%) | Identity (%) |
| | *S. cerevisiae* | *K. marxianus* | | | |
| 1 | ScSSK1 | KmSSK1 (KLMA_80078) -2.07981 | Cytoplasmic phosphorelay intermediate osmosensor and regulator; part of a two-component signal transducer that mediates osmosensing via a phosphorelay mechanism; required for mitophagy; dephosphorylated form is degraded by the ubiquitin-proteasome system; potential Cdc28p substrate | 46 | 52 |
| 2 | ScWsc3 | KLMA_80280 -2.05678 | cell wall integrity and stress response component 3 | 80 | 43 |
| 3 | ScWsc2 | KLMA_50408 -2.03973 | cell wall integrity and stress response component 3 | 40 | 32 |
| Autophagy (kmx04138) at 30 min $log_2$ < -2 | | | | | |
| No. | Protein name | | Function | Query cover (%) | Identity (%) |
| | *S. cerevisiae* | *K. marxianus* | | | |
| 1 | ScRAS2 | KmRAS2 (KLMA_80228) -2.68782 | GTP-binding protein; regulates nitrogen starvation response, sporulation, and filamentous growth; farnesylation and palmitoylation required for activity and localization to plasma membrane; homolog of mammalian Ras proto-oncogenes; RAS2 has a paralog, RAS1, that arose from the whole genome duplication | 79 | 63 |
| 2 | ScGCN4 | KmGCN4 (KLMA_50398) -2.29719 | bZIP transcriptional activator of amino acid biosynthetic genes; activator responds to amino acid starvation; expression is tightly regulated at both the transcriptional and translational levels | 96 | 41 |
| 3 | ScPCL5 | KmPCL5 (KLMA_70375) -3.23831 | Cyclin; interacts with and phosphorylated by Pho85p cyclin-dependent kinase (Cdk), induced by Gcn4p at level of transcription, specifically required for Gcn4p degradation, may be sensor of cellular protein biosynthetic capacity | 76 | 40 |

**Table S15** Primers used in this study.

| No. | Primer name | Nucleotide sequence |
|---|---|---|
| 1 | ACT1-1552906-ins-5'-F | ATCACTCTTTCGGTGTTGCTC |
| 2 | ACT1-1552906-ins-3'-R | GTCATAGACAACGTACATCCTCTG |
| 3 | ACT1-47658-del-5'-F | TTAAGGGCATTAGGTGGCCC |
| 4 | ACT1-47658-del-3'-R | GGGAAGGTGGAATTAGTAACTTG |
| 5 | ACT2-1161817-snv-5'-F | GAAAGCAGTACTTCGTTTGGAC |
| 6 | ACT2-1161817-snv-3'-R | GGTTGGGATCGTATTGACGAAT |
| 7 | ACT2-712698-snv-5'-F | CGGTTATACTCTGGACCAAGC |
| 8 | ACT2-712698-snv-3'-R | CATTCTTGACTGACTCCACGGTG |
| 9 | ACT2-385614-snv-5'-F | GCTTCTTCGGAGGAATACCTTC |
| 10 | ACT2-385614-snv-3'-R | ACCAAGAGAACTAGAGTGTTCGG |
| 11 | ACT2-1269738-snv-5'-F | ACAATTGTGCACCCAAGAGCT |
| 12 | ACT2-1269738-snv-3'-R | GACGGCACTGGGAGCGTA |
| 13 | ACT3-1107715-snv-5'-F | GTCTCCCGTTACCAACAAGTC |
| 14 | ACT3-1107715-snv-3'-R | TCTCCCTTCCTTTCAAACCTG |
| 15 | TML1-613476-snv-5'-F | TACGAGGCTTGCGATCCCT |
| 16 | TML1-613476-snv-3'-R | GATGCACCGAATGATTTCTTGG |
| 17 | TML1-968552-ins-5'-F | CGAAGTTGTCCCAGGTGATATC |
| 18 | TML1-968552-ins-3'-R | CAGCACCGACAGCCATGG |
| 19 | TML1-1010140-snv-5'-F | GGCATCTACGTGAACGCTTC |
| 20 | TML1-1010140-snv-3'-R | CTTCATACCAACCACACAGGG |
| 21 | TML1-1714543-snv-5'-F | GTACTTCCGCCTGCAGTGT |
| 22 | TML1-1714543-snv-3'-R | CCACGCCGGAATTGTCGC |
| 23 | TML1-767036-snv-5'-F | CATGAGGAGACAGCAGTAGCT |
| 24 | TML1-767036-snv-3'-R | TTGAAGGCGCCACCGCCA |
| 25 | TML1-724738-snv-5'-F | GTGCCTCTGGATCGTAATACG |
| 26 | TML1-724738-snv-3'-R | TCGGGCTCGTTGGTTCCAATTA |
| 27 | TML1-815396-snv-5'-F | ACGGCGTTGGTCTGCCTC |
| 28 | TML1-815396-snv-3'-R | GGTGGCCTTTGCACAACGG |

**Table S16** Comparison of evolutionary adaptation in this study with evolutionary adaptations reported previously

| Stress | Condition | Parental strain | Adapted strain | Increased ethanol (%) | Phenotype | Ref |
|---|---|---|---|---|---|---|
| Temperature (In addition, ethanol, acetic acid, other by-products and nutrient starvation) | Repetitive long-term cultivation in YPD medium with a gradual increase of temperature from 40 ˚C to 45 ˚C | *K. marxianus* DMKU 3-1042 | Four mutants (ACT001, ACT002, ACT003 and TML001) | 20 – 40 | - acetate tolerance<br>- formate tolerance<br>- acid tolerance<br>- ethanol tolerance<br>- furfural tolerance<br>- HMF tolerance<br>- vanillin tolerance | This study |
| Inhibitors in acid prehydrolysate of hardwood | Cultivation in acid prehydrolysate of hardwood supplemented with nutrients and minerals at 30˚C for more than 6 weeks. The cultivation was performed with a gradual increase of amount of the acid prehydrolysate. | *P. stipitis* NRRL Y-7124 | One mutant | 48 | - acid tolerance | Nigam 2001 |
| High sugar concentration (22 brix) | Sequential batch fermentation in sugar juice medium, 200 generations at 28 ˚C | *S. cerevisiae* G85 Chinese rice wine yeast | One mutant (G85X-8) | 3 | - ethanol tolerance<br>- osmotic tolerance<br>- temperature tolerance | Bro *et al*. 2006 |
| Ethanol | 266 nm laser radiation and repetitive cultivation in YPD supplemented with 11%-15% ethanol at 34 ˚C | *S. cerevisiae* YE0 | One mutant (SM4) | 29 | - ethanol tolerance | Zhang *et al*. 2014 |
| Acetic acid | Cultivation in YPD supplemented with 0.3%-1.3% acetic acid at 28 ˚C for 33 days. (The cultivation period was short (1-2 days) up to 19 days and increased (3-5 days) after that). | *S. cerevisiae* Y8 industrial osmotolerant strain | One mutant (Y8A) | 26 | - osmotic tolerance<br>- temperature tolerance<br>- saline tolerance<br>- ethanol tolerance<br>- organic acid tolerance | Gurdo *et al*. 2018 |
| Lactose concentration (200 g/L) | Cultivation in whey permeate (150-200 g/L lactose) at 37 °C for 65 days | *K. marxianus* MTCC 1389 | One mutant | 18 | - osmotic tolerance | Saini *et al*. 2017 |
| (Xylose as a carbon source) | Repetitive cultivation in YEP medium supplemented with 2% xylose at 45 ˚C for 24 h, 60 cycles | *K. marxianus* NIRE-K3 | One mutant (K3.1) | 16 | - improved xylose utilization | Sharma *et al*. 2017 |
| (Xylose as carbon source and 2-deoxyglucose) | Repetitive cultivation in YP supplemented with 1.5% 2-deoxyglucose and 4% xylose at 30˚C, 6 times over 50 days | *K. marxianus* 17694-DH1 | One mutant (SBK1) | NR | - improved co-fermentation of glucose and xylose | Kim *et al*. 2019 |
| Ethanol | Ten consecutive rounds of liquid nitrogen freeze–thaw treatment followed by plate screening under osmotic and ethanol stresses | *S. cerevisiae* Y-1 | One mutant (YF10-5) | 16 | - osmotic tolerance<br>- ethanol tolerance | Zhang *et al*. 2019 |